

This PDF was created from the British Library's microfilm copy of the original thesis. As such the images are greyscale and no colour was captured.

Due to the scanning process, an area greater than the page area is recorded and extraneous details can be captured.

This is the best available copy

D 37709'81

Attention is drawn to the fact that the copyright of this thesis rests with its author.

This copy of the thesis has been supplied on condition that anyone who consults it is understood to recognise that its copyright rests with its author and that no quotation from the thesis and no information derived from it may be published without the author's prior written consent.

I

D 37709/81.

CIRANGE J.D.

11

107

Double Paged Insert

Studies of InAs and GaAs layers prepared by molecular beam epitaxy

**A thesis submitted for the degree of Doctor of Philosophy in
partial fulfilment of the requirements of the Council for National
Academic Awards**

by

John David Grange BSc (Wales)

**Department of Physics
Sir John Cass School of Science and Technology
City of London Polytechnic
31 Jewry Street
London EC3N 2EY**

In collaboration with Philips Research Laboratories (Redhill, UK)

September 1980

ABSTRACT

This thesis describes a study of the growth and doping of single crystal thin films of GaAs and InAs by the technique of molecular beam epitaxy (MBE). One micron thick unintentionally doped films of InAs were deposited onto GaAs substrates at the relatively low growth temperature of 370°C and GaAs films were grown over the range 400 - 650°C. A detailed study of the doping properties of silicon in GaAs films was also made. The epilayers were characterized using the van der Pauw technique and Hall measurements, Schottky barrier C-V profiling, photoluminescence analysis, X-ray diffraction, scanning electron microscopy, Rutherford backscattering and in-situ reflection medium energy electron diffraction. The GaAs:Si material was further characterized by the assessment of Mott barrier diodes fabricated from n/n^+ structures. The study has been primarily concerned with investigating the relationships between the MBE growth parameters (e.g. growth rate, growth temperature, group III - group V flux ratio, role of the buffer layer) and the properties of the epilayers. The experimental parameters were found to significantly influence the electrical and optical properties of the layers. An analysis of these effects is presented which shows that the growth parameters determine the extent and nature by which dopant and system derived impurity species as well as defects are incorporated into the layers. The origin and type of some impurities associated with the construction of the MBE system were identified.

Studies of InAs and GaAs Layers Prepared by Molecular
Beam Epitaxy

CONTENTS

	<u>Page</u>
Captions to photographic plates	3
Introduction	4
CHAPTER 1 Experimental	8
CHAPTER 2 An investigation into the low temperature growth of (100) InAs by MBE	26
CHAPTER 3 An investigation into the growth of (100) GaAs by MBE	48
CHAPTER 4 An investigation into the silicon doping of MBE (100) GaAs	60
CHAPTER 5 Fabrication of microwave mixer diodes	78
CONCLUDING REMARKS	81
FURTHER WORK	82
ACKNOWLEDGEMENTS	83
REFERENCES	84
PUBLISHED WORK	

INTRODUCTION

The last decade has seen the development of molecular beam epitaxy (MBE) as a technique for the preparation of semiconductor materials and associated device fabrication. The MBE technique, its technology, growth mechanism and various applications have been discussed in numerous review papers and articles (Chang and Ludeke 1975, Cho and Arthur 1975, Cho 1977, 1979, Farrow 1977a, Foxon 1973, 1978, Grange and Parker 1979, Joyce and Foxon 1977ab, Luscher 1977, Ploog 1979a). Briefly, MBE describes the growth of elemental, compound and alloy films on crystalline surfaces by directing thermal energy molecular beams of the constituent elements under ultrahigh vacuum conditions (pressures $< 10^{-9}$ Torr). In this process the underlying single crystal substrate influences the film growth to produce an "orientated overgrowth" i.e. an epitaxial deposit. This deposited film generally has the same crystallographic orientation as the substrate but not necessarily the same chemical composition. Essentially MBE is a simple UHV evaporation technique, a modification of the high vacuum three-temperature-technique of Günther (1958). The use of a UHV environment not only enables purer films to be deposited due to a reduction in the background impurity incorporation but also allows the use of surface analytical instruments such as Auger electron spectroscopy (AES) (Chang 1974) and secondary ion mass spectrometry (SIMS) (Benninghoven 1975) as well as the various electron diffraction techniques such as RHEED (reflection high energy electron diffraction) (Bauer 1969).

These techniques were of vital importance in the investigations into substrate cleaning and preparation and establishing prerequisite conditions for obtaining epitaxial growth by vacuum deposition (Farnsworth et al. 1958, Jona 1965, Davey and Pankey 1968, Laurence et al. 1979). Indeed most of the earliest MBE experiments were surface physics studies using RHEED (Cho 1969, 1970a, 1971a) leading, only later, to thin film deposition of material for electronic devices. Numerous materials have now been deposited in thin film form by MBE, including: AlAs (Chang et al. 1976); AlGaAs (Cho et al. 1971, Cho and Stokowski 1971); CdS (Tsang et al. 1979); GaAs (Arthur and LePore 1969, Cho 1969, 1970a, 1971a); GaAsP (Arthur and LePore 1969); GaP (Cho 1970b); GaAsSb (Cho et al. 1977); InGaAsP (Cho 1979); GaSb (Yano et al. 1978); InAs (Yano et al. 1977); InGaAs (Chang et al. 1977); InGaP (Scott and Roberts 1979); InP (McFee et al. 1977); PbTe (Parker and Williams 1976); PbSnTe (Holloway and Walpole 1979); ZnSe (Yao et al 1979) and ZnTe

(Smith and Pickhardt 1975). As can be seen the III-V compounds and alloys have received most attention, particularly GaAs. This is because of the commercial advantages of GaAs arising from its superior high frequency properties compared to silicon, coupled with the interest in the Al-Ga-As system for direct bandgap AlGaAs double heterostructure (DH) lasers for optoelectronic communication systems. The growth kinetics of III-V compounds are more fully understood through the work of Arthur and Foxon and Joyce (Arthur 1968, Foxon et al. 1974, Foxon and Joyce 1975, 1977, 1979, 1980, Joyce and Foxon 1975). The formation of films by MBE is not a process that occurs under thermodynamic equilibrium, the growth of layers is controlled by surface kinetics and lifetimes of the molecular species at the growing film interface. However, the interplay of thermodynamics and kinetics in MBE has recently been considered (Heckingbottom et al. 1979, 1980).

For the materials mentioned above the MBE technique offers the ability to produce smooth thin layers ($10\text{\AA} - 10\ \mu\text{m}$) at low growth temperatures ($\sim 500^\circ\text{C}$) over large areas ($\sim 10\ \text{cm}^2$). Furthermore, the slow growth rates employed ($\sim 1\ \mu\text{m}\ \text{hr}^{-1}$) allow complex doping profiles to be incorporated in material over dimensions $\geq 0.1\ \mu\text{m}$. The use of shuttered sources for the molecular beams allows abrupt termination of growth or incorporation of a given species and hence rapid compositional changes. These, coupled with a reduction in diffusion effects due to the low growth temperatures should give rise to very sharp interface profiles (Dingle 1977). The ability of MBE to produce very thin layers ($\sim 20\ \text{\AA}$) has led it to be used in the experimental investigation of superlattices (Chang and Esaki 1979), predominantly alternating thin layers of $\text{Al}_x\text{Ga}_{1-x}\text{As} - \text{GaAs}$. Such structures give rise to quantum electronic effects (Esaki and Tsu 1970) and also offer the possibility of manufacturing semiconductor material with improved electron transport properties (Dingle et al. 1978). The recent innovation of shadow masking (Tsang and Cho 1978) allows different materials or even different structures to be deposited on the same substrate with controlled variations of chemical composition in the lengthwise direction instead of the usual depthwise. This MBE writing technique may be a useful technique for fabricating and integrating various optoelectronic devices.

All the above factors potentially give MBE great advantages over the more well established growth processes such as liquid phase epitaxy (LPE)

(Dawson 1972) and chemical vapour deposition (CVD) (Chopra 1969). An intercomparison of the three techniques has been given by Joyce and Foxon (1977a). However, in spite of these apparent advantages possessed by MBE there remain several problem areas which impede the realization of the full potential of MBE as discussed by Joyce (1979). Since MBE is a new technique it is probable that for it to become an accepted fabrication technology it must be shown either to do certain tasks better than LPE and CVD (e.g. improved device performance or higher yield) or to do certain tasks of which LPE and CVD are incapable of (e.g. 50 Å period superlattices or fully integrated optical circuits). In the past it has been found that, on average, the material and devices produced by MBE were only comparable to (or worse than) those produced by CVD and/or LPE. However, improvements in both MBE material (Morkoc and Cho 1979) and device (Tsang 1979, 1980) production are continually being made.

This situation of steady gradual improvements is mainly due to refinements and improvements in MBE techniques and systems. It would be surprising therefore to find that we have already arrived at the ultimate in MBE material and device performance due to any fundamental limitation of the technique. It is, however, interesting to speculate upon the possible existence of some fundamental limitation on material quality owing to the non-equilibrium kinetic nature of the MBE growth process. At the time of writing majority carrier transport properties of n- and p-type MBE GaAs are frequently 'bulk-like' in the doping range $10^{17} \text{ cm}^{-3} - 10^{19} \text{ cm}^{-3}$ for a variety of dopants (Ploog 1979a), typical system impurity levels being in the $10^{14} \text{ cm}^{-3} - 10^{17} \text{ cm}^{-3}$ range. It is generally acknowledged (though not too frequently) by MBE practitioners that problems do arise from not being able to obtain uncompensated material with regularity. For example, the origin of certain deep levels in MBE GaAs (Lang et al. 1976) and the reason for the abrupt degradation in the electrical properties of MBE GaAs for low growth temperatures (Murotani et al 1978) both remain unknown. Generally there is little quantitative data concerning deviations from ideal electrical, optical, compositional and structural properties. In particular there is little data relating MBE growth parameters to the quality of the epitaxial deposits, the notion of optimum operating conditions is rarely considered.

This thesis contains the results of an experimental investigation into the growth and doping of (100) InAs and (100) GaAs by the technique of molecular beam epitaxy. During this project the prime concern has been to establish the properties of thin films ($d \sim 1 \mu\text{m}$) of InAs and GaAs which can be routinely obtained by MBE and to identify the type and origin of the impurities or defects which influence the transport properties. In so doing the growth parameters have been critically examined and also the MBE system in an attempt to obtain quantitative data for basing decisions on the type of components to be incorporated. Particular interest has been taken in examining how the MBE growth parameters (growth rate and temperature, etc.) influence the electrical and optical properties of the epilayers. A further assessment of the GaAs material has been possible through the fabrication of Mott barrier diodes in a collaborative program with the GEC Hirst Research Centre. Throughout the entire project there has been close collaboration with the MBE group at the Philips Research Laboratories, Redhill (UK).

CHAPTER 1

Experimental

The experimental apparatus used during this project was constructed by a previous researcher and is described in some detail in his thesis (Meggitt 1979). It is necessary, however, to recall some of the details here. Modifications to the apparatus have been made throughout this project and these will be discussed where relevant. In the following general discussion concerning MBE it will be assumed that we are considering the growth of III-V compounds.

1.1 The Basic MBE System

As previously mentioned, MBE is a UHV evaporation technique and as such the main elements of an MBE system are:

- (1) A chamber and suitable pumps to attain UHV conditions.
- (2) Evaporation sources.
- (3) A substrate holder.

A schematic illustration of the MBE system used in this project is shown in Figure 1.

The function of the vacuum pumps is to produce a clean UHV environment within the growth chamber for film deposition. In various laboratories different pumping systems are used including ion pumps (Cho 1971b), liquid nitrogen trapped diffusion pumps (Wood and Joyce 1978), liquid nitrogen trapped turbomolecular pumps (Hirose et al. 1978) and helium cryopumps (Decker 1977). The operation of these pumps is described elsewhere (Redhead et al. 1968). Virtually all MBE chambers are now constructed from stainless steel.

The evaporation sources are generally of the Knudsen type, that is an oven or 'cell' which has a sufficiently small exit orifice so that to a reasonable approximation equilibrium exists between the vapour and solid of the charge within the cell. If true equilibrium does exist then for a given temperature the flux effusing from the cell can be calculated (Ramsey 1956) using saturation vapour pressure data (Honig and Kramer 1969). However, in practice either the cell construction does not permit such equilibrium conditions or the cell temperature monitoring facility is inadequate to allow accurate calibration of the effusing fluxes. Deviations from ideal behaviour have been frequently reported

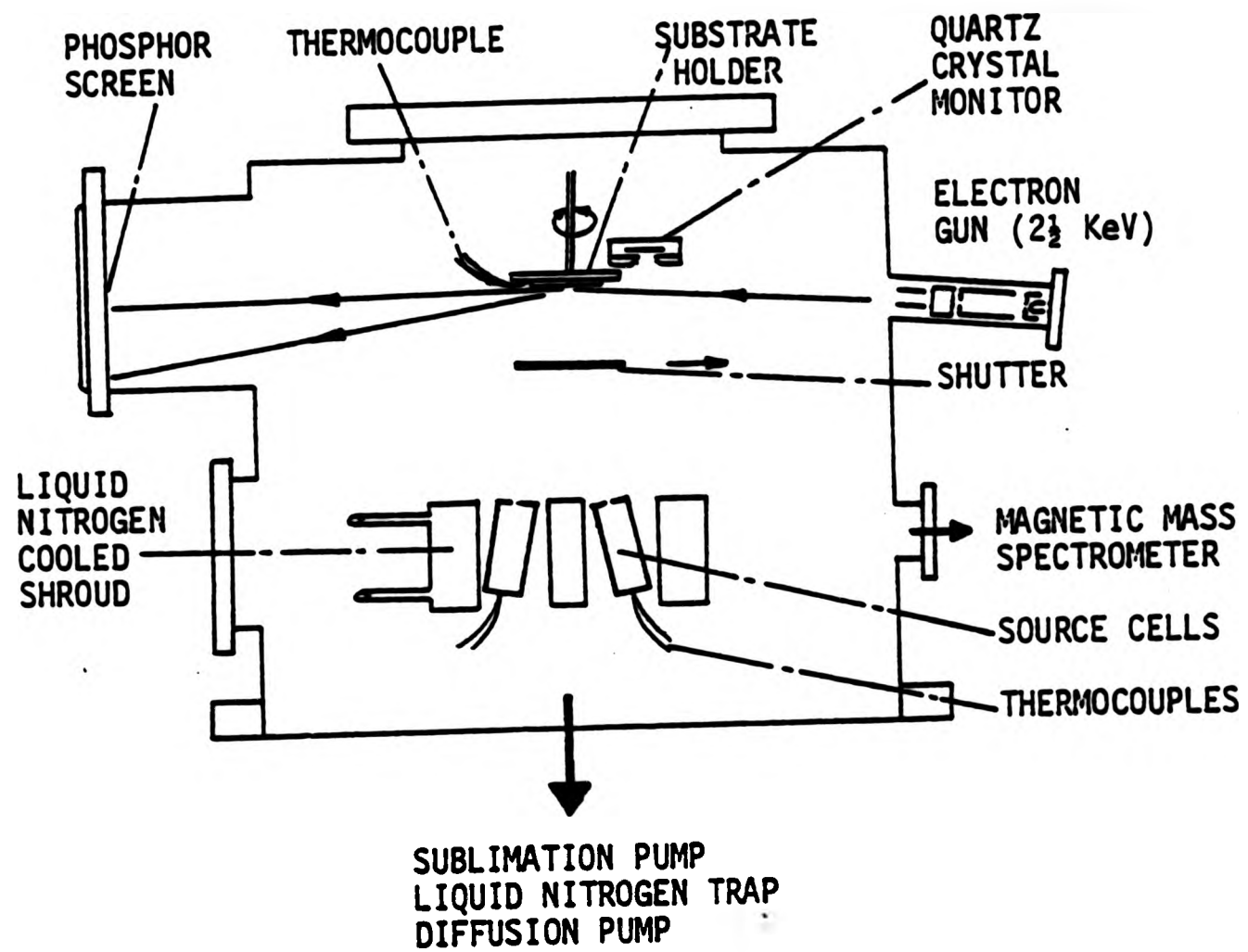


Figure 1 Schematic diagram of the MBE chamber

(Delhomme et al. 1978, Carson et al. 1970, Shen 1978). Consequently in the majority of cases it is necessary to calibrate the fluxes effusing from the individual cells. This is usually achieved by measurement of film thicknesses or from the weight of material deposited in a known time. Two cell materials are in common usage, carbon (high purity graphite) and pyrolytic boron nitride (PBN). The advantages of carbon are its availability, purity, cost and ease of machining, however, PBN is generally considered to give rise to better epitaxial layers. This point will be discussed in more detail later. Carbon is not suitable for the cell material if aluminium is to be evaporated due to an Al-C reaction (Cho and Arthur 1975). The evaporation ovens are generally resistively heated using tantalum (Ta), molybdenum (Mo) or tungsten (W) wire either wound directly on the evaporation cells (as is often the case for PBN) or on some insulator such as alumina (Al_2O_3) which is in good thermal contact with the cell. Radiant heaters are also in use (Cho 1978). The heaters are generally concentric around the evaporation ovens to give uniform heating. The ovens have a facility, either a recess or a drilled hole, for accommodating a thermocouple for monitoring the temperature of the cell. Usually each cell is provided with an individual shutter in order to terminate the deposition of any particular substance at any time without interrupting the evaporation from the other cells.

The substrate holder is a heated platform to hold the substrate during deposition, temperatures of 500°C - 600°C being required for the epitaxial growth of high quality GaAs. Such holders are generally made of molybdenum and heated either using Ta, W or Mo heater wires or thin films of these metals which act as sheet heaters. The GaAs substrate is usually held in place on the block using the surface tension of a thin layer of molten indium residing between the substrate and the block. Loose fitting Ta or Mo clips can also be used for added security, this has the added advantage of producing a step edge suitable for later film thickness measurements. The substrate assembly is normally mounted on a UHV manipulator in order to move the substrate into different positions for possible AES analysis or to present different crystallographic orientations for electron diffraction studies.

While the basic MBE system is quite simple most research facilities do incorporate some surface analytical equipment, most commonly AES and RHEED. A more recent development which will probably become a standard

item on MBE rigs is the load-lock. This is the use of an extra chamber and a valve to enable substrates to be loaded into, and removed from, the growth chamber without having to let the growth chamber up to atmospheric pressure. This innovation should remove any contamination (e.g. dust and water) associated with letting the chamber up to atmospheric pressure and should increase production yields since turnround times should be shortened.

1.2 Experimental Apparatus Used in this Project

1.2.1 Vacuum system

The MBE system used in this project is shown in figure 2 (plate) and has a vertical evaporation configuration. It is a single 12 inch diameter stainless steel chamber composed of two halves, an upper evaporation portion and a lower services well. Both portions of the chamber had a variety of ports welded on to accommodate the effusion cells, substrate heater, view ports, the ionization gauge (Vacuum Generators Ltd - VIG 10) electron gun, fluorescent screen (for diffraction patterns) and mass spectrometer (AEI MS10 or Vacuum Generators Q7B). The system was pumped by an Edwards EO4 oil diffusion pump which had a 600 l sec^{-1} pumping speed and was backed by an Edwards ES200 two stage rotary pump. The diffusion pump contained Santovac 5, a polyphenylether, as the pump fluid. Additional pumping capacity was provided by a three filament titanium sublimation pump which had a maximum pumping speed of 14000 l sec^{-1} . Condensable vapours were also pumped by the Edwards CT100 anti-creep liquid nitrogen trap which, aided by the water cooled baffle (Edwards CB100), reduced oil backstreaming from the diffusion pump. Further pumping capacity was provided by liquid nitrogen cooled cryopaneling within the chamber. The system did not include a high vacuum valve to isolate the MBE chamber from the diffusion pump. The pumping system was capable, after an eight-hour bake-out at 180°C , of routinely obtaining base pressures of 5×10^{-10} Torr. Pressures as low as 5×10^{-11} Torr have been obtained.

1.2.2 Substrate heater

The substrate heater assembly consisted of an $\frac{1}{8}$ inch thick Mo block (99.9%, Nordiko Ltd.) of dimensions 5 cm x 3 cm which was clipped using Ta foil onto a fused quartz plate (99.9%, Thermal Syndicate Ltd.) onto the reverse side of which was sputtered a 1 μm thick Mo film. Heating of the block was effected by the passage of a current through the Mo film. Under UHV conditions a temperature of $\sim 500^{\circ}\text{C}$ was obtained for a

Figure 2

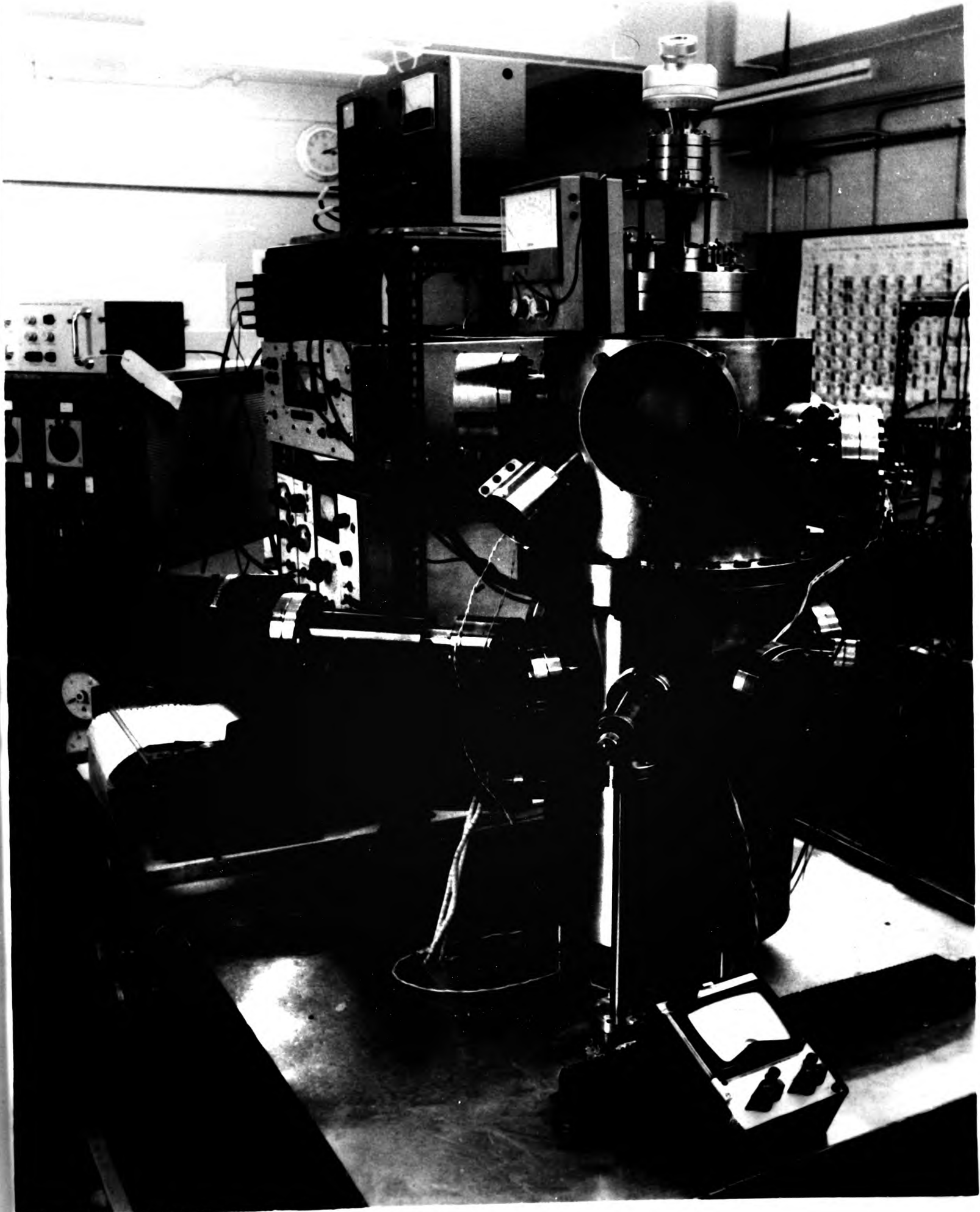
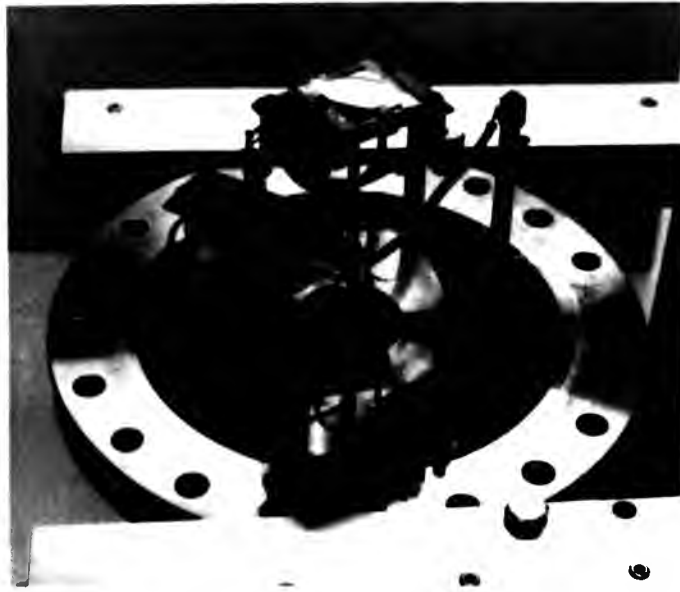


Figure 3



TOP PLATE



ELECTRON GUN



KNUDSEN CELLS

SOURCE SHROUD



current of 6 amps at 12 volts. A 1 mm diameter hole drilled into the centre of the Mo block allowed the insertion of a chromel-alumel thermocouple which was used to monitor the substrate (i.e. growth) temperature. The whole assembly was attached to a rotary feedthrough (Vacuum Generators Ltd., RD2) which had a 3 cm extension bellows incorporated into it. This arrangement gave the substrate rotation and vertical elevation, primarily of use for the electron diffraction studies. The bellows allowed some variation in the source to substrate distance though throughout this work a distance of 10 cm has been used.

1.2.3 Effusion cells

Two types of effusion cell (graphite and PBN) have been used in this project though for most of the work the cells were constructed out of spectroscopically pure graphite (Ringsdorff, grade RWO - total impurity level <3 ppm, MCP Ltd.). The graphite cells consisted of a hollow cylindrical body closed at one end and with a small removable plug fitting into the other. In this plug was drilled a 3.5 mm diameter hole which constituted the source aperture. Removal of this plug allowed access to the cell body to replenish the evaporant. The cells were 3 cm in length and 1 cm in diameter, however, for the growth of the GaAs samples a larger 4 cm x 2 cm cell for the arsenic was used. In the base of each cell was a hollowed enclosure in which was fitted a chromel-alumel thermocouple spot welded to a Ta disc which acted as a radiation collector. The thermocouple was used to monitor the cell temperature. The MBE system accommodated three effusion cells.

Heating of the cells was effected by fitting a cylindrical alumina (Degussit Al23, Friedrichsfeld GmbH) sheath over each graphite cell and winding 0.025 mm diameter Ta wire into a machined screw thread on the outside of the sheath. A second alumina sheath was then fitted over the first to constrain the windings and to provide an insulating surface on which to wrap three layers of Ta foil radiation shielding. Each cell was mounted in an individual opening in a water cooled shroud. The purpose of the shroud was, as well as providing a mounting for the cells, to act as a heat sink for reflected radiation and also to thermally isolate the cells i.e. reduce thermal cross-talk. The cells were individually shuttered or totally shuttered (i.e. one large shutter) using Ta foil as required for different experiments.

Figure 3 (plate) shows photographs of the substrate heater assembly on the flange which attached it to the top of the system. Also shown is

the graphite/alumina effusion cell assembly used in the initial part of this project, the shroud into which the cells fitted and the electron gun used for the electron diffraction studies.

The BN cells used later in the project were purchased from the Fulmer Research Institute Ltd. and were a more simple design being approximately concentric, slightly tapered cylinders closed at one end. The approximate dimensions being 1.5 cm x 6.5 cm and 2 cm x 7 cm for the inner and outer pieces respectively. No defining aperture was used with these cells. A self-supporting heater wire (0.5 mm diameter Ta wire) was wound directly on the inner smaller cylinder which was then placed inside the larger one and radiation shielding was wound directly around the whole structure. A chromel-alumel thermocouple was fitted between the inner and outer BN pieces to give a measure of the cell temperature.

The source materials (elemental indium, gallium, arsenic and silicon) evaporated from the cells were all of 99.9999% purity as supplied by Koch Light Laboratories. The substrates used in this work were usually Cr-doped semi-insulating GaAs cut on the (100) plane, however, some of the later substrates were cut misoriented 1° - 3° off (100) in the $\langle 110 \rangle$ direction. The semi-insulating substrates had a resistivity $> 10^7 \Omega\text{cm}$. Tellurium doped n^+ ($n > 1 \times 10^{18} \text{ cm}^{-3}$) (100) GaAs substrates were used for the preparation of GaAs n/n^+ structures for the fabrication of the Mott barrier diodes. All the substrates used had a nominal thickness of 0.5 mm and pieces of area 1 cm^2 to 8 cm^2 have been used. The semi-insulating substrates were obtained from three sources: RSRE (Malvern), MCP Ltd. (Wembley) and Monsanto (USA). The n^+ substrates were supplied by MCP Ltd. The electrical properties of the epilayers did not appear to be a function of the substrate supplier.

The epitaxial layers of InAs and GaAs grown on the semi-insulating substrates were electrically characterized using a Hall apparatus and the method of van der Pauw (1958). The GaAs samples on both n^+ and n^- substrates were also examined using a Hg probe C-V depth profiling apparatus (Binet 1975) in collaboration with both PRL (Redhill) and GEC Hirst (Wembley). Film thickness measurements have been obtained with a variety of techniques including scanning electron microscope measurements on step and cleaved edges of films, Talystep measurements and interference fringes. The existence of energy levels within the

forbidden gap (and consequently impurities within the layers) has been confirmed using the photoluminescence technique at PRL (Redhill). Structural properties, mainly confirmation of the samples single crystal nature, have been examined using in-situ reflection medium energy electron diffraction (RMEED), Rutherford backscattering, inclined beam Laue and back reflection X-ray diffraction.

1.3 The Experimental Growth Procedure

A typical MBE growth procedure may be summarized:

- (1) Clean a new substrate.
- (2) Let the MBE system up to atmospheric pressure using oxygen free nitrogen and keep the nitrogen flowing all the time the system is open to the air.
- (3) Remove the top flange securing the substrate heater assembly, place in a dust free environment and remove the previously deposited layer for later electrical characterization.
- (4) Load the new substrate, fixing it to the Mo block with molten indium.
- (5) Replace the top flange and pump the system so as to attain UHV.
- (6) Outgas the source cells at $\sim 50^{\circ}\text{C}$ above their operating temperature for the required time (typically ~ 1 hour).
- (7) Set up the evaporation fluxes as required for growth.
- (8) Thermally anneal the substrate.
- (9) Set the substrate at the required growth temperature.
- (10) Open the shutter(s) and grow the film using monitoring facilities as required.
- (11) Close the shutter(s) at the end of the required growth time and switch off the source and substrate heaters.
- (12) When sources etc. are cool switch off the vacuum pumps closing the appropriate valves.
- (13) Let the system up to atmospheric pressure using oxygen free dry nitrogen.

Some of the earlier procedures were carried out concurrently so as to minimise the time for which the system was exposed to the laboratory environment, which was typically $\frac{1}{2}$ hour. Of the above points (1), (8) and (5) need further discussion here.

1.3.1 Substrate cleaning - ex situ

A clean substrate is required for epitaxial film growth and to obtain epilayers of high optical and electrical quality. The pregrowth cleaning technique will determine which impurities are present on the substrate which in turn affect resulting film growth and electrical properties (Otsubo et al. 1977, Ploog 1979b, Laurence et al. 1979).

The as supplied substrates had been saw cut into nominally 0.5 mm thick slices diamond paste polished and then pad polished using, for example, a weak (~2%) solution of bromine in methanol (Fuller and Allison, 1962). It is unfortunately not possible to obtain from certain suppliers details of their cleaning methods. The substrate cleaning technique used in this project consisted of an initial degrease in propan-2-ol in a reflux apparatus followed by a wash in deionized distilled water, after which the substrate was allowed to dry. This was then followed by etching the slice in a solution of $\text{H}_2\text{SO}_4:\text{H}_2\text{O}_2:\text{H}_2\text{O}$ at room temperature for 2 minutes. The beaker containing the substrate in the solution was agitated with a circular motion throughout the procedure. After the 2 minutes the acid solution was diluted down to water and the substrate given a final wash in deionized distilled water. Immediately prior to mounting on the substrate heater block the excess surface water was blown off the substrate using oxygen free dry nitrogen passed through a millipore filter. Mixtures of 15:1:1 and 15:2:2 of $\text{H}_2\text{SO}_4:\text{H}_2\text{O}_2:\text{H}_2\text{O}$ have been used with equal success. A successfully etched substrate would appear mirror-like with no surface blemishes. The polishing of compound semiconductors has been discussed by Jensen (1973) and Tuck (1975). The etching of GaAs in $\text{H}_2\text{SO}_4\text{-H}_2\text{O}_2\text{-H}_2\text{O}$ solutions has been investigated by Iida and Ito (1971), Shiota et al. (1977) and Laurence et al. (1979). Briefly, this etchant produces oxides of GaAs on the surface, H_2O_2 being the oxidising agent. These oxides are then soluble in the general ambient of the etch solution, thus GaAs is removed or etched away and fresh material exposed to form the surface of the substrate. For example, using the data of Iida and Ito (1971) we can estimate that using the 15:2:2 solution our etch procedure removes 2-4 μm of GaAs off the substrate. The composition of the remaining surface oxide will depend upon the method of terminating the etch, for example certain gallium oxides (Ga_2O_3) are more soluble in water than their arsenic equivalents (As_2O_3) (Schwartz 1975). As such one might expect the above procedure of terminating the etch in water to produce a surface oxide layer richer in arsenic oxides than gallium

oxides. This surface oxide layer is considered to be only several monolayers thick (Laurence et al. 1979).

1.3.2 Substrate cleaning - in situ

In order to generate a clean (as judged by AES) surface it is necessary to thermally anneal the substrate in the MBE system immediately prior to film deposition. The heating is normally carried out with an incident arsenic flux. This process is considered to desorb the etch related oxide and reconstruct the surface crystallinity leaving a surface clean enough for epitaxial growth (Cho and Arthur 1975). The appearance of surface crystallinity is evident from the RMEED patterns. The as loaded chemically etched surface gives a diffuse dull RMEED pattern indicative of an amorphous surface oxide. However, on heating a bulk spot pattern appears quite suddenly at a substrate temperature of $\sim 530^\circ\text{C}$ which has been taken to imply that the surface oxide has desorbed (Cho and Arthur 1975, Cho and Hayashi 1971a). The GaAs substrates used in this project were all heated to 580°C for 20 minutes in an arsenic flux of $10^{14} - 10^{15}$ molecules $\text{cm}^{-2} \text{sec}^{-1}$. This procedure has been found to routinely give a suitable starting surface for both the growth of homoepitaxial GaAs and heteroepitaxial InAs.

AES examination (Ploog and Fischer 1977) of GaAs substrates etched in an $\text{H}_2\text{SO}_4:\text{H}_2\text{O}_2:\text{H}_2\text{O}$ solution showed two major contamination peaks at 510 eV (oxygen) and 272 eV (carbon) on heating the substrates in an arsenic flux to 550°C the oxygen peak disappeared supporting the earlier conjecture of oxide desorption occurring near this temperature. The carbon peak remained although it could be removed by argon ion sputtering. Ion sputter cleaning has not been used in this project. The minimum acceptable level of carbon contamination is in some doubt, Cho and Arthur (1975) state that 20% of a monolayer will influence subsequent film growth yet Laurence et al. (1979) put a much lower figure of 6×10^{-2} monolayer.

SIMS analysis (Boyle et al. 1977) of semi-insulating (100) GaAs substrates etched in a $15\text{H}_2\text{SO}_4:1\text{H}_2\text{O}_2:1\text{H}_2\text{O}$ solution and thermally annealed in UHV also indicated that contamination levels do decrease in the annealing process (580°C for 10 minutes). However, residual coverage of As_2O_5 , As_2O_3 , Ga_2O_3 and Ga_3AsO_4 were observed in the SIMS spectra from the annealed surfaces and although below the detection limit of AES the concentrations of which are easily sufficient to severely influence the electrical properties of thin layers deposited on this surface.

1.3.3 Attaining UHV conditions

Some care must be taken in the pumpdown cycle to avoid oil contamination (i.e. backstreaming) of the MBE system or damage to the vacuum pumps. The following sequence was generally used during this project:

- (1) Evacuate the system using the rotary pump only to a pressure of 0.1-0.075 Torr. The rotary pump being trapped using a foreline trap filled with activated alumina.
- (2) Isolate the rotary pump from the system.
- (3) Switch on the diffusion pump.
- (4) Fill the liquid nitrogen trap.
- (5) When the diffusion pump has fired reconnect the rotary pump while ensuring that the critical backing pressure (0.5 Torr) is not exceeded.
- (6) Switch on the ion gauge and when the system pressure is $\sim 10^{-6}$ Torr bake the system at 180°C for 8 hours.
- (7) Outgas the titanium sublimation pumps during bake out.
- (8) Switch off the bake out heaters and fire the titanium sublimation pumps.
- (9) Outgas the gauge when the system temperature is 100°C.
- (10) Allow the system to cool and reach 10^{-10} Torr

This procedure has the disadvantage in that although the filling of the liquid nitrogen trap (4) before the diffusion pump has fired may reduce pump oil backstreaming into the MBE system it can lead to a lot of water vapour collecting on the trap and entering the system when the trap later warms up.

1.4 Electron Diffraction Studies

Although not an extensive part of these studies, it is necessary to discuss the use of electron diffraction in relation to MBE associated surface studies. As previously mentioned, RHEED studies played an integral part in the development of MBE (Cho 1969, 1970a, 1971a) and are still of considerable interest (Neave and Joyce 1978ab). The major attractions of a reflection electron diffraction technique being that it is an inexpensive surface analytical tool which can be used to examine the epilayer surface during deposition. In the RMEED system used in

this project 1-3 keV electrons were incident upon the substrate or growing film surface at a grazing angle of 1° - 2° . At these energies and with such a shallow incident angle the primary electrons penetrate only the outermost 1-2 atomic layers of the crystal. The single crystal substrate or epilayer acts as a two dimensional grating which diffracts the incident electrons onto a fluorescent screen placed perpendicular to the substrate and the incident beam azimuth. A diffraction pattern of spots or streaks was seen on the screen. The general theory of this form of electron diffraction is well documented (Bauer 1969, Prutton 1975), and it is sufficient to note here that the symmetry and spacing of the reciprocal lattice can be obtained directly from examining the resultant diffraction patterns from two or more different azimuths and from a knowledge of the electron energies and diffraction geometry. From the reciprocal lattice a picture of the surface in real space can be built up.

It is generally found that the RMEED patterns from GaAs and related compounds give rise to a series of well defined streaks and it has been assumed that such patterns alone are indicative of a well ordered, flat, single crystal surface (Cho and Arthur 1975). However this assertion is no longer satisfactory (Neave and Joyce 1978b) and it must be accepted that no adequate explanation of the origin of the streaks in RMEED is available although several suggestions have been put forward (Menudue 1972, Masud and Pendry 1976, Holloway and Beebey 1978). The RMEED technique is frequently employed during investigations into surface reconstruction. The perfect (100) surface of the III-V compounds contains atoms each of which has two spare or "dangling" bonds giving rise to a large surface energy. It is found that the (100) surface has a tendency to lower the free energy by forming a different or "reconstructed surface". Reconstruction is a re-ordering of the outermost layer of atoms at the surface. Various surface reconstructions have been reported for both (100) InAs (Meggitt et al. 1978, 1980) and (100) GaAs (Cho and Arthur 1975). The two most frequently observed reconstructions being the (2 x 4) and (4 x 2) structures (the notation following Wood 1964). However, it should be added that a totally unambiguous identification of these structures has not been obtained by RMEED (Neave and Joyce 1978b). In both these reconstructions the surface atoms all have some (unspecified) displacements with respect to their bulk positions and these different displacements occur with a definite periodicity of two and four times the bulk atomic spacing (i.e. every two or four surface atoms have a

↑
↓
2x4
4x2

particular displacement). For example, a (100) InAs or GaAs (2 x 4) reconstruction implies that alternate atoms along the $[1\bar{1}0]$ direction have the same displacement whilst along the $[110]$ direction the repeat spacing is equal to four times the bulk spacing. This in turn will give an extra three diffraction lines in between each adjacent pair of bulk lines in the diffraction pattern viewed in the $[1\bar{1}0]$ azimuth and an extra one line between adjacent bulk lines in the $[110]$ azimuth. This is frequently referred to as $\frac{1}{2}$ - and $\frac{1}{4}$ -order streaking. The (2 x 4) and (4 x 2) structures are simply related by a rotation of the surface atoms of 90° about the direction of the growth plane i.e. $[100]$. Photographs of these reconstructions are shown in the experimental chapters.

The (100) GaAs (2 x 4) structure is generally known as the arsenic-stabilized structure since it is formed when growth takes place under conditions of excess arsenic flux. The (4 x 2) structure on the other hand is generally known as the gallium-stabilized structure since it is formed under conditions of no excess arsenic or slight gallium excess. No detailed mechanism for reconstruction in III-V materials exists although recent work (Neave and Joyce 1978b) indicates that a vacancy model (Phillips 1973) may be an area of fruitful investigation. Van Vechten (1977) has discussed the possibility of reconstruction occurring in other growth techniques where techniques such as RMEED cannot be used for direct observation of the reconstruction.

1.5 The MBE Growth Process

The growth of (100) InAs and (100) GaAs by MBE has been investigated by Foxon and Joyce (1975, 1977, 1978) in modulated molecular beam mass spectrometric studies. In these experiments both the incident and desorbed fluxes were examined and sticking coefficients and surface lifetimes of the different species obtained. Furthermore, the careful design of the experimental apparatus (Foxon et al. 1974) enabled a clear distinction to be made between a molecular species in the vacuum ambient and the same species as part of an incident or desorbed flux, a point which invalidated earlier experiments by other workers.

In considering the MBE growth process there are three distinct areas, viz:

- (1) The substrate or film may be in the MBE system at some elevated temperature and it is necessary to know what changes, if any, will take place in the layer's composition.
- (2) It needs to be known what species are effusing from the Knudsen cells for a given source material.
- (3) Having established (1) and (2) it is then necessary to allow an interaction of the effusing species on the substrate surface by directing the molecular beams to impinge upon the substrate at the growth temperature and thereby to establish which interactions take place in the formation of the epilayer.

Foxon et al. (1973) have examined the non-equilibrium (i.e. Langmuir or free) evaporation of GaAs which in effect represents the situation of a hot substrate in the MBE chamber. They found that the gross evaporation of GaAs was congruent below 657°C but above this temperature arsenic is lost preferentially in the form of As_2 molecules. This loss of As_2 occurs at this temperature irrespective of whether we are considering an as loaded GaAs substrate, a deposited film or a growing film. This non-congruent evaporation of As_2 above 657°C can lead to gallium droplet formation on the GaAs surface though this loss can be counter-balanced by the use of an incident arsenic flux. In practice GaAs MBE film growth is usually performed at temperatures below this congruent evaporation point so as to reduce the risk of gallium droplet formation and associated non stoichiometric growth. Although the congruent evaporation temperature is 657°C a small excess gallium surface population is established in the absence of an incident arsenic flux for temperatures above $\sim 480^{\circ}\text{C}$ due to the evaporation of As_2 from the surface (Foxon and Joyce 1975), producing a Ga-stabilized surface.

The situation for a heated InAs substrate or epilayer is qualitatively very similar to GaAs but quantitative differences exist due to the lesser thermal stability of InAs, the congruent evaporation temperature being $\sim 500^{\circ}\text{C}$ (C.T. Foxon, private communication 1977). Also the (100) InAs surface produces some free surface indium for temperatures $\geq 330^{\circ}\text{C}$, giving rise to an In-stabilized surface i.e. As_2 is lost much more rapidly from InAs than GaAs as the temperature is increased from 300°C . In general this has led to the deposition temperatures for InAs being lower than those for GaAs. However, InAs epilayers have been deposited at growth temperatures of 530°C (e.g. Meggit et al. 1978) by supplying sufficient arsenic to satisfy both the incident indium flux and that

free surface indium caused by the non-congruent evaporation of the InAs epilayer already deposited.

The evaporation cells used in this project for the growth of InAs and GaAs contained elemental indium, gallium and arsenic. The metals evaporate as atomic species of indium and gallium whilst elemental arsenic evaporates as As_4 molecules. Thus the growth systems of interest in this project can be described as In- As_4 -(100) InAs and Ga- As_4 -(100) GaAs. The other growth system of current interest is the Ga- As_2 -(100) GaAs system (Foxon and Joyce 1977), the As_2 being obtained from either the thermal cracking of As_4 or by using GaAs as the arsenic source.

Figure 4 is a schematic diagram (after Foxon 1978) illustrating the growth of GaAs from the constituents of As_4 and Ga beam impinging upon a GaAs substrate. The diagram is equally applicable to the growth of InAs from In and As_4 beams. The model based on modulated molecular beam mass spectrometric studies is due to the following experimental observations: (i) To a good approximation all the incident gallium will stick to the GaAs substrate at practical growth temperatures; there is some measurable re-evaporation of indium for growth temperatures $> 430^\circ C$ - however this is slight and will only cause the deposited InAs layers to be slightly thinner than expected; (ii) the As_4 molecules were found to stick only if free Ga (or In) was present on the surface. This free surface metal arises from two sources, namely the incident group III flux and by thermal dissociation of the deposited epilayer. In all the cases discussed in this project the group III atomic arrival rate in the incident flux is several orders of magnitude greater than the surface concentration produced by thermal decomposition of the compound. The model requires that the incident As_4 molecules are first bound to the surface in some weak precursor state and are free to migrate about the GaAs surface. By migrating across the surface the As_4 molecules become involved in either film growth (i.e. condensation) or As_4 desorption can take place. In the former case the results suggest that an interaction between two As_4 molecules occurs prior to GaAs condensation. In the model proposed a pairwise dissociation of these two As_4 molecules takes place with four As atoms taking part in the film growth via interactions with surface gallium atoms to make GaAs. The remaining four arsenic atoms then reform an As_4 molecule and desorb from the surface. This quite complex model is based on the experimental observation that the maximum sticking coefficient of As_4 upon a GaAs (or

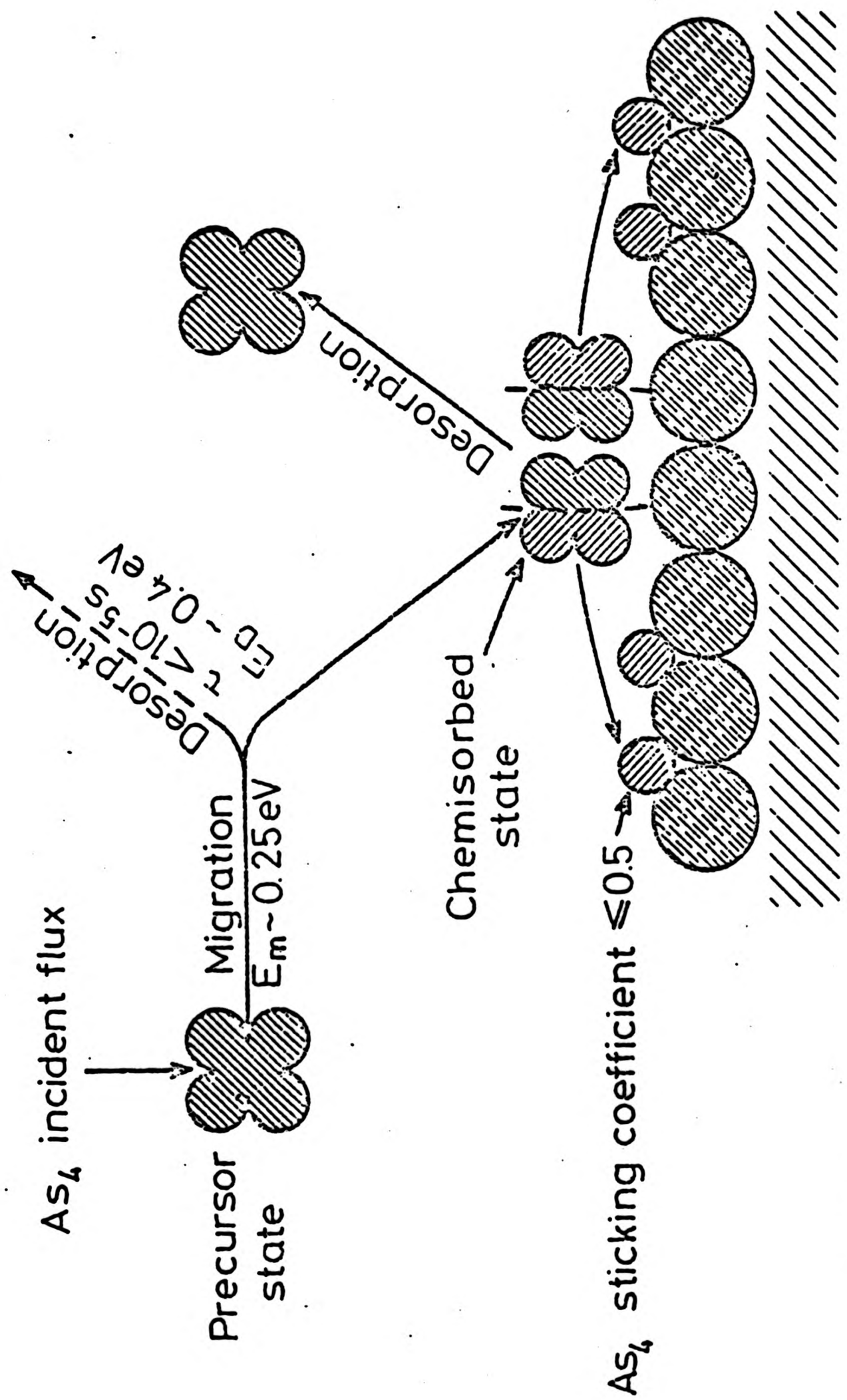


Figure 4 Ga stabilized GaAs surface

Figure 4

Diagram illustrating the Ga-As₄-(100) GaAs growth kinetics (after Foxon 1978)

InAs) surface is $\frac{1}{2}$ i.e. there is always some desorbed As_4 even when the incident As_4 flux is insufficient to satisfy all the gallium atoms on the surface. This maximum sticking coefficient arises for a Ga-stabilized surface (i.e. the (4×2) reconstruction). Should the incident As_4 flux exceed the concentration of free gallium on the surface then the excess As_4 molecules will be desorbed.

Neave and Joyce (1978a) have reported the growth of MBE (100) GaAs over a wide temperature range. The kinetic model implies that the upper limit is governed by the thermal instability of the compound and the lower limit by the non-dissociative absorption of the As_4 molecules which occurs at $\sim 180^\circ C$. They obtained results which are in good agreement with the kinetic model above.

This model says nothing of defect incorporation or how different reconstructions might affect the mechanism of condensation. Both of these processes may greatly influence the electrical properties of the deposited material.

CHAPTER 2

An investigation into the low temperature growth of (100) InAs by MBE2.1 Introduction

The binary semiconductor InAs has itself found limited application in electronic devices (Wieder 1970, Kunig 1970), but is of considerable interest in the alloy form $\text{Ga}_x\text{In}_{1-x}\text{As}_y\text{P}_{1-y}$. The quaternary alloys have opto-electronic applications when lattice matched to InP covering the spectral range 0.93 μm to 1.68 μm (Nogai and Noguchi 1978). $(\text{Al}_x\text{Ga}_{1-x})_y\text{In}_{1-y}\text{As}/\text{InP}$ heterostructures are also of interest for use in the 1.3 μm region (Miller et al. 1978). Furthermore $\text{Ga}_x\text{In}_{1-x}\text{As}$ may be of use in MESFET devices (Wood 1976) and $\text{InAs}_y\text{Sb}_{1-y}$ is of interest for use in the 3-9 μm spectral range (Cheung et al. 1977). The InAs-GaSb superlattice is also attracting considerable interest (Chang et al. 1979ab). A comprehensive understanding of the growth and properties of the binary III-V compounds is required prior to undertaking a study of the ternary and quaternary alloys by MBE.

This chapter contains the results of a systematic investigation into the relationship of MBE growth parameters to the electrical properties of heteroepitaxial (100) InAs layers grown at 370°C. It is of interest to investigate the origin of the degradation of the electrical properties of MBE layers that occurs for low growth temperatures and for this reason a relatively low deposition temperature was chosen for this study. Kinetic studies (Foxon and Joyce 1978) and RMEED studies (Meggitt 1979) indicate that stoichiometric single crystal InAs is obtained down to growth temperatures of at least 200°C. The benefits to be obtained from using the lowest possible growth temperature include a reduction in interlayer diffusion and facilitating the incorporation of elements with high vapour pressures. A study of low temperature growth would also help to define the fundamental limits to MBE growth. Previous work on the growth of InAs by MBE (Yano et al. 1977, Meggitt et al. 1978) showed that improved electrical properties were obtained with thicker layers ($\sim 3 \mu\text{m}$) and layers grown at higher temperatures ($\sim 500^\circ\text{C}$).

2.2 Experimental Details

The MBE system incorporating the graphite effusion cells, as described in Chapter 1, was used throughout this work. Layers of InAs 1 μm thick were deposited at 370°C onto high resistivity GaAs buffer layers which had been predeposited at 530°C to a thickness of 0.1 μm onto Cr-doped semi-insulating (100) GaAs substrates. The buffer layers were sufficiently resistive ($\sim 1 \Omega\text{cm}$) not to influence subsequent electrical measurements on the InAs layers. Semi-insulating or high resistivity InAs is not available and consequently GaAs substrates were used which meant a 7% lattice mismatch existed between epilayer and substrate. Better lattice matching would have been achieved by using semi-insulating (Fe-doped) InP substrates, but the cleaning of such substrates is far more complex (Farrow 1977). The β form, air stable, arsenic was used throughout these experiments since it has been found to give layers with improved electrical properties. The effusion rates from the group III cells were determined absolutely to $\pm 10\%$ by depositing indium and gallium onto thin aluminium foils, the fluxes being determined from the change in weight of the foils. Repeated calibration depositions, SEM measurements on both step and cleaved edges of layers and quartz crystal monitoring showed that the effusion rates were reproducible to $\pm 5\%$. The As_4 flux was monitored using the ionization gauge reading from within the growth chamber and calibrated from the onset of indium rich (i.e. non stoichiometric) growth which was readily established from a series of depositions. Using the kinetic approach (Foxon and Joyce 1978) we have that the minimum arsenic flux required for stoichiometric growth is given by:

$$F_{\text{As}_4} = \frac{1}{2} F_{\text{In}}$$

The above expression is only approximate since at 370°C an InAs layer is losing $\sim 3 \times 10^{12}$ molecules $\text{cm}^{-2} \text{sec}^{-1}$ of As_2 due to thermal decomposition. However, this loss is very small compared with the incident growth fluxes of $10^{14} - 10^{15}$ atoms $\text{cm}^{-2} \text{sec}^{-1}$ and hence the error in assuming an equality in the above equation is negligible.

The substrates were all etched in $15\text{H}_2\text{SO}_4 : 1\text{H}_2\text{O}_2 : 1\text{H}_2\text{O}$ solution and heated in the vacuum system for 20 minutes at 580°C under an arsenic flux immediately prior to epilayer deposition. The electrical properties of the layers were examined using the van der Pauw technique. The reproducibility of the measured properties from run to run was in general better than $\pm 10\%$ and samples showed a variation of electrical

properties of <10% across a 4 cm long substrate.

In this study InAs layers were grown with As_4 :In flux ratios varying from <0.5:1 to >50:1 using In fluxes of 5.6×10^{14} atoms cm^{-2} sec^{-1} and 1.0×10^{14} atoms cm^{-2} sec^{-1} . These fluxes correspond to growth rates of $1.1 \mu\text{m hr}^{-1}$ and $0.2 \mu\text{m hr}^{-1}$. A gas leak in facility on the MBE system enabled the effects of oxygen and hydrogen gaseous ambients to be studied.

2.3 Results

2.3.1 Structural Properties

A variety of techniques have been used to confirm the single crystal nature of these samples. Figure 5 (plates) shows two photographs of X-ray diffraction patterns. The upper one is a back reflection X-ray diffraction pattern from a $5 \mu\text{m}$ InAs epilayer which indicates that the sample is a single crystal, other $1 \mu\text{m}$ samples have given identical patterns. The lower photograph is of an inclined beam Laué X-ray diffraction pattern from a $1 \mu\text{m}$ thick InAs layer obtained using a texture camera (Wallace and Ward 1975). The pattern implies a single crystal nature with a (100) orientation with the absence of low angle grain boundaries.

The Rutherford backscattering technique (Chu et al. 1973) has been used on some samples and has indicated that there was a good degree of crystallographic order within the samples as judged by the ratio of the random to the channelled signals. Typical ratios of 0.2-0.1 were obtained (S.R.L. McGlashan, private communication 1979) whilst the best quality bulk crystals give ratios of 0.1 or less. The technique revealed no gross contaminants or major deviations from stoichiometry within the samples.

The RMEED patterns also support, albeit tentatively, the case for hetero-epitaxial growth. Figure 6 (plates) shows the $\frac{1}{2}$ and $\frac{1}{2}$ order lines of the (2 x 4) arsenic-stabilized reconstruction on (100) InAs taken along the $[0\bar{1}1]$ and $[0\bar{1}\bar{1}]$ azimuths respectively. The (4 x 2) indium-stabilized structure has been observed at higher temperatures ($>400^\circ\text{C}$). This structure appears with the $\frac{1}{2}$ and $\frac{1}{2}$ order lines in the $[0\bar{1}1]$ and $[0\bar{1}\bar{1}]$ azimuths i.e. as Figure 6 but with the azimuthal directions interchanged. The starting (i.e. post annealed) GaAs surface generally showed the (100)

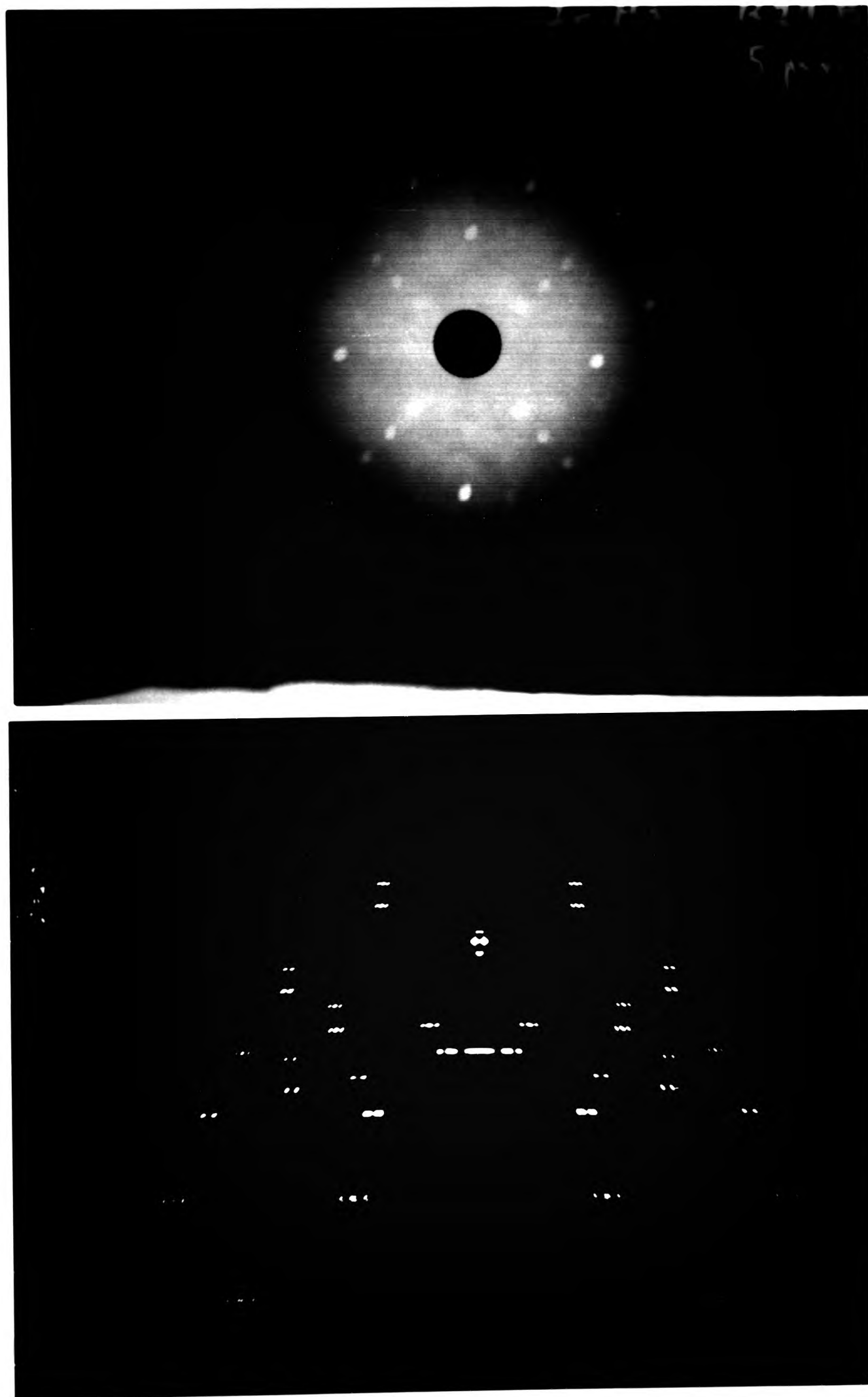
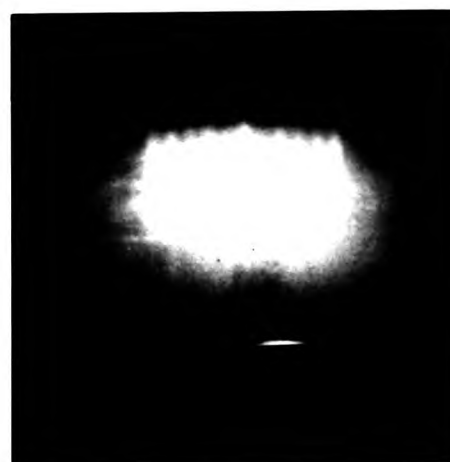


Figure 5 X-ray diffraction photographs

Figure 6 RMEED patterns from an InAs layer illustrating the arsenic-stabilized (2 x 4) reconstruction



$[0\bar{1}\bar{1}]$



$[0\bar{1}1]$

(azimuthal directions)

GaAs (2 x 4) arsenic-stabilized reconstruction. A detailed investigation of the reconstructions of heteroepitaxial InAs is given elsewhere (Meggitt et al. 1980).

2.3.2 Electrical Properties

For a given indium flux the measured carrier concentration $n (= 1/R_H e)$ of the epilayers was found to depend upon the arsenic flux used during each growth. As shown in Figure 7 the layers produced with a high arsenic flux were found to have a higher measured free carrier concentration. This dependence of epilayer free carrier concentration on the arsenic flux used during deposition is shown in Figure 7 for the two indium fluxes used. The point labelled A was obtained with an increased arsenic background to beam pressure by not using any liquid nitrogen trapping in the system. The plotting point was then obtained by filling the shrouds at the termination of growth. The mobility-carrier concentration plot of Figure 8 shows the reduction in Hall mobility associated with this arsenic induced increase in free carrier concentration. This figure also suggests the existence of an independent source of doping and scattering which is associated with the indium arrival rate (i.e. the growth rate). The data of Rode (1971) implies that all the epilayers were compensated with $N_A + N_D/n \sim 4-7$. The layers deposited at the slower growth rate appear to be less compensated since they have a higher Hall mobility for a given free carrier concentration. The scatter in the experimental data coupled with the absence of detailed theoretical results precludes an accurate assessment of the effect of the arsenic flux on the level of compensation in the layers though it appears to remain approximately constant.

The variation of Hall mobility with inverse temperature for two epilayers is shown in Figure 9. The form of these curves is similar to those of intentionally compensated bulk InAs (Balagurov et al. 1976) and have been interpreted in terms of phonon and ionized impurity scattering (Meggitt et al. 1980, Mizuno et al. 1975). No carrier freeze out has been observed even down to liquid helium temperatures (Meggitt et al. 1978). Electrical characterization of an epilayer every working day for 33 days showed no systematic variations in the electrical properties with time.

Further experiments were done using the minimum arsenic flux with an indium flux of 5.6×10^{14} atoms $\text{cm}^{-2} \text{sec}^{-1}$ with growth taking place in

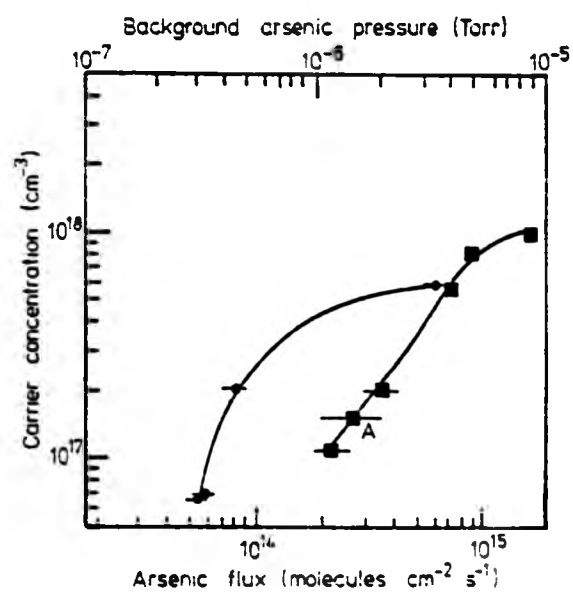


Figure 7 The room temperature carrier concentration of InAs epilayers plotted against arsenic flux used during deposition. ■ $F_{In} = 5.6 \times 10^{14}$ atoms $\text{cm}^{-2} \text{s}^{-1}$; ● $F_{In} = 1.0 \times 10^{14}$ atoms $\text{cm}^{-2} \text{s}^{-1}$.

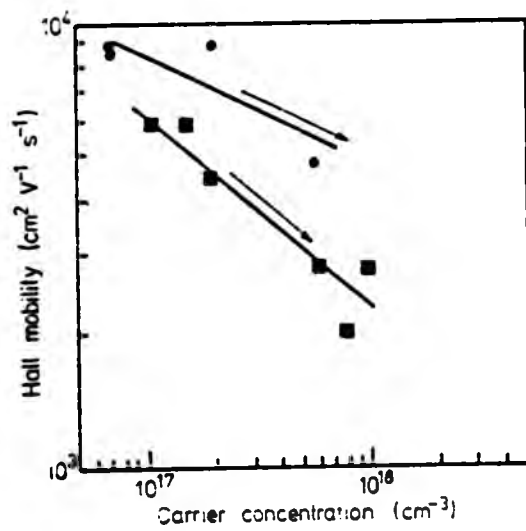


Figure 8. Room temperature carrier concentration/Hall mobility plot for the epilayers deposited using the two different indium fluxes. Arrows indicate directions of increasing As_4 flux: symbols as in figure 7

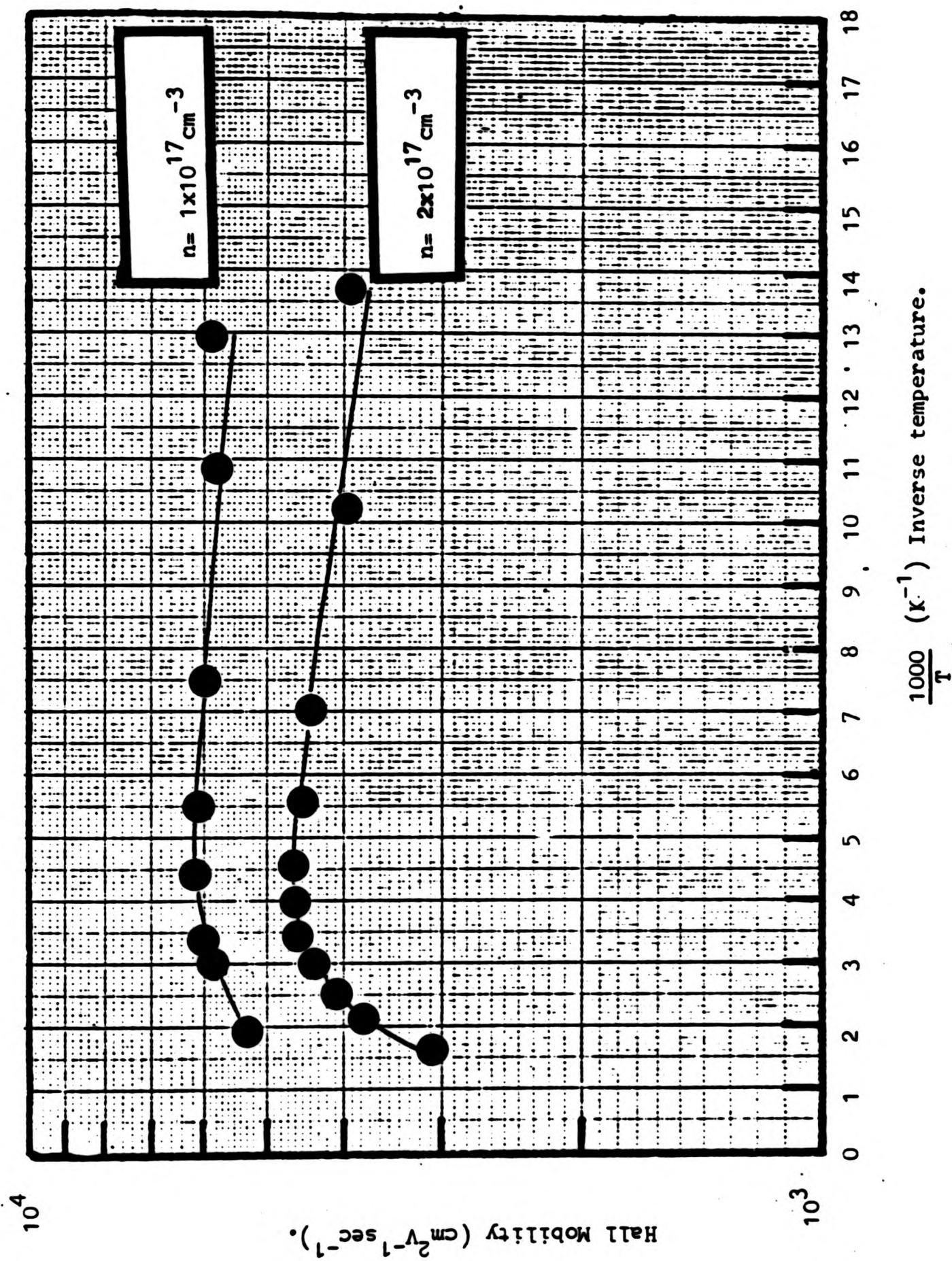


Figure 9. Variation of Hall mobility with inverse temperature for two typical InAs epilayers.

oxygen and hydrogen ambients of 5×10^{-7} Torr. The effect of oxygen was to severely degrade the film properties ($n = 2 \times 10^{18} \text{ cm}^{-3}$; $\mu = 700 \text{ cm}^2 \text{ V}^{-1} \text{ sec}^{-1}$). No effect was observed using a hydrogen ambient.

Figure 10 is a depth profile of two epilayers deposited using the minimum arsenic flux for an indium flux of $1.0 \times 10^{14} \text{ atoms cm}^{-2} \text{ sec}^{-1}$. These two InAs epilayers were deposited simultaneously, one on a $0.1 \mu\text{m}$ GaAs buffer layer, the other directly onto the substrate. This was effected on the same substrate by employing a Mo mask to shield half the substrate from the impinging Ga beam. The depth profile was then obtained by step etching in $1\text{H}_2\text{SO}_4:1\text{H}_2\text{O}_2:100\text{H}_2\text{O}$ and taking sequential van der Pauw measurements.

2.3.3 Surface Morphology

Most of the layers were mirror-like in appearance but for an $\text{As}_4:\text{In}$ flux ratio >4 many layers took on a milky appearance. For an $\text{As}_4:\text{In}$ flux ratio >75 epitaxial InAs was not obtained at this growth temperature. Any further reduction in the arsenic flux from the minimum values shown resulted in In-rich growth and an obvious degradation of electrical properties as well as surface morphology. SEM micrographs of InAs layers grown under indium rich, optimum and arsenic rich conditions are shown in Figure 11 (plate).

2.4 Discussion

2.4.1 Structural Properties

Good evidence has been obtained to support the notion that single crystal heteroepitaxial InAs layers are being obtained by MBE. The reconstruction behaviour observed for (100) InAs is very similar to that of (100) GaAs implying that the mechanisms of reconstruction are similar.

2.4.2 Electrical Properties

(a) Effect of arsenic flux

Figures 7, 8 and 11 clearly show an effect on the electrical properties and surface morphology due to increasing the arsenic flux for a given indium flux. Kinetic studies of the Ga- As_4 -GaAs (100) and In- As_4 -InAs (100) systems have been reported (Foxon and Joyce 1975, 1978). The interpretation of these studies has been that for arsenic incorporation

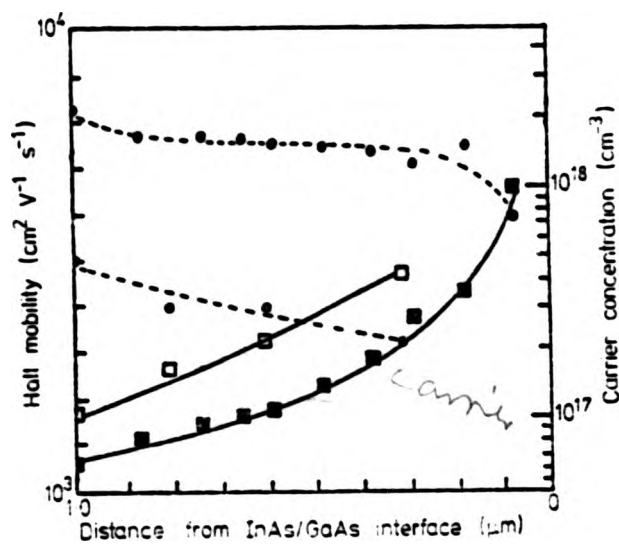


Figure 10 Variation of carrier concentration and mobility with depth for two of the epilayers deposited under optimum conditions at the lower indium flux. ●, mobility of buffered layer; ○, mobility of unbuffered layer; ■, carrier concentration of buffered layer; □, carrier concentration of unbuffered layer. Broken (for the mobilities) and solid (for the carrier concentrations) curves are best fits to the experimental data.

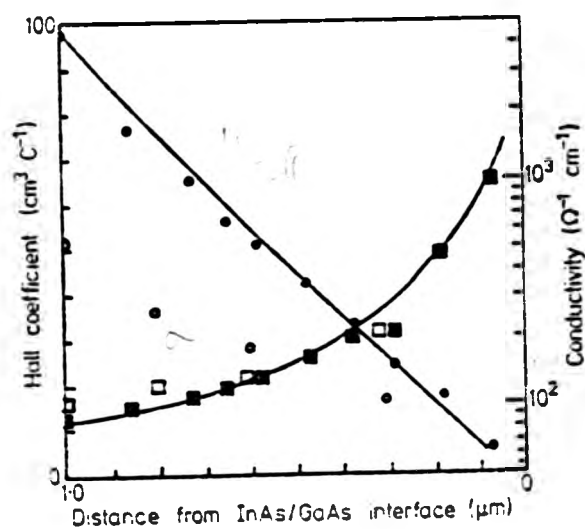


Figure 13 Variation of the measured Hall coefficient and conductivity with depth for the epilayers of figure 10 ■, conductivity of buffered layer; □, conductivity of unbuffered layer; ●, Hall coefficient of buffered layer; ○, Hall coefficient of unbuffered layer. Solid curves are calculated variations with the parameters given in the text and using equation (1) and (2).

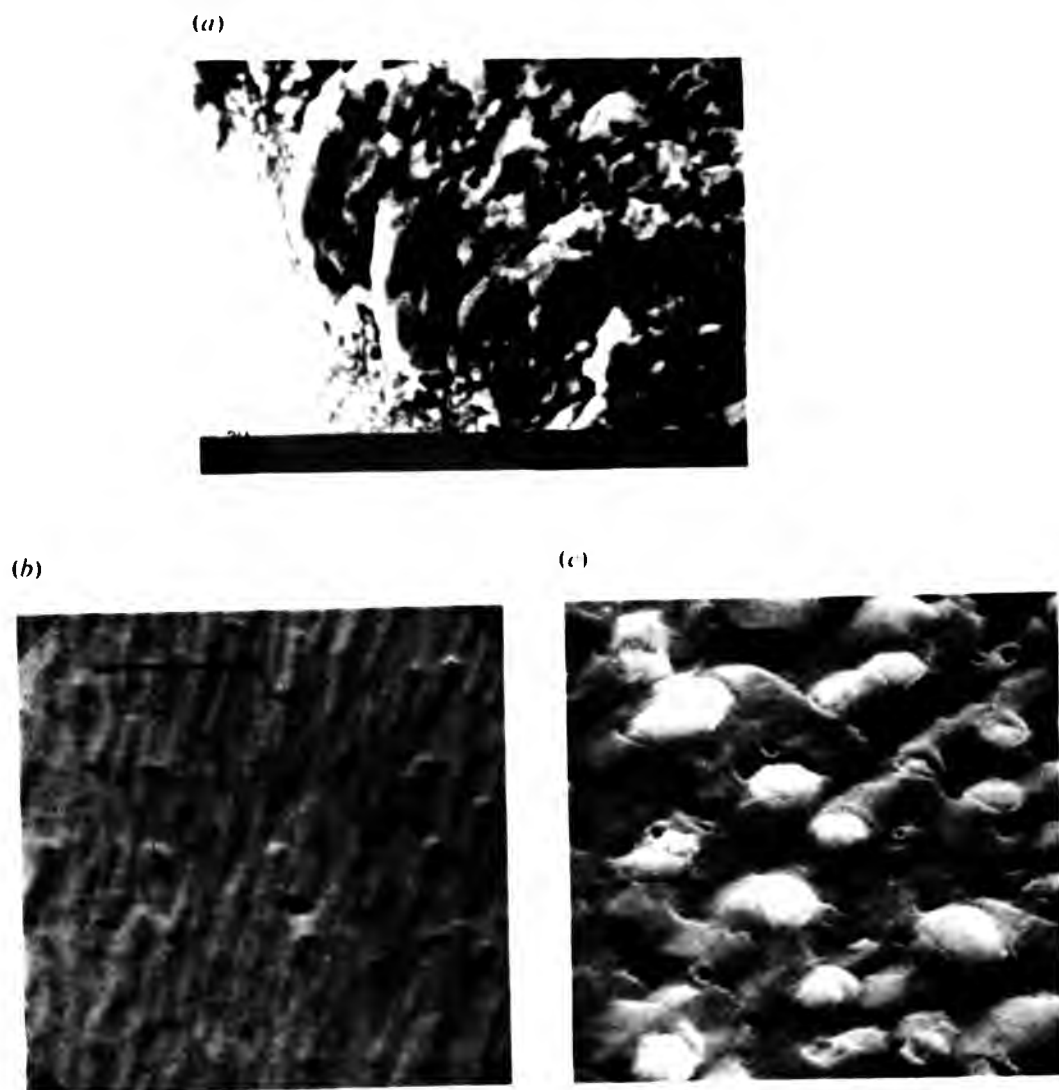
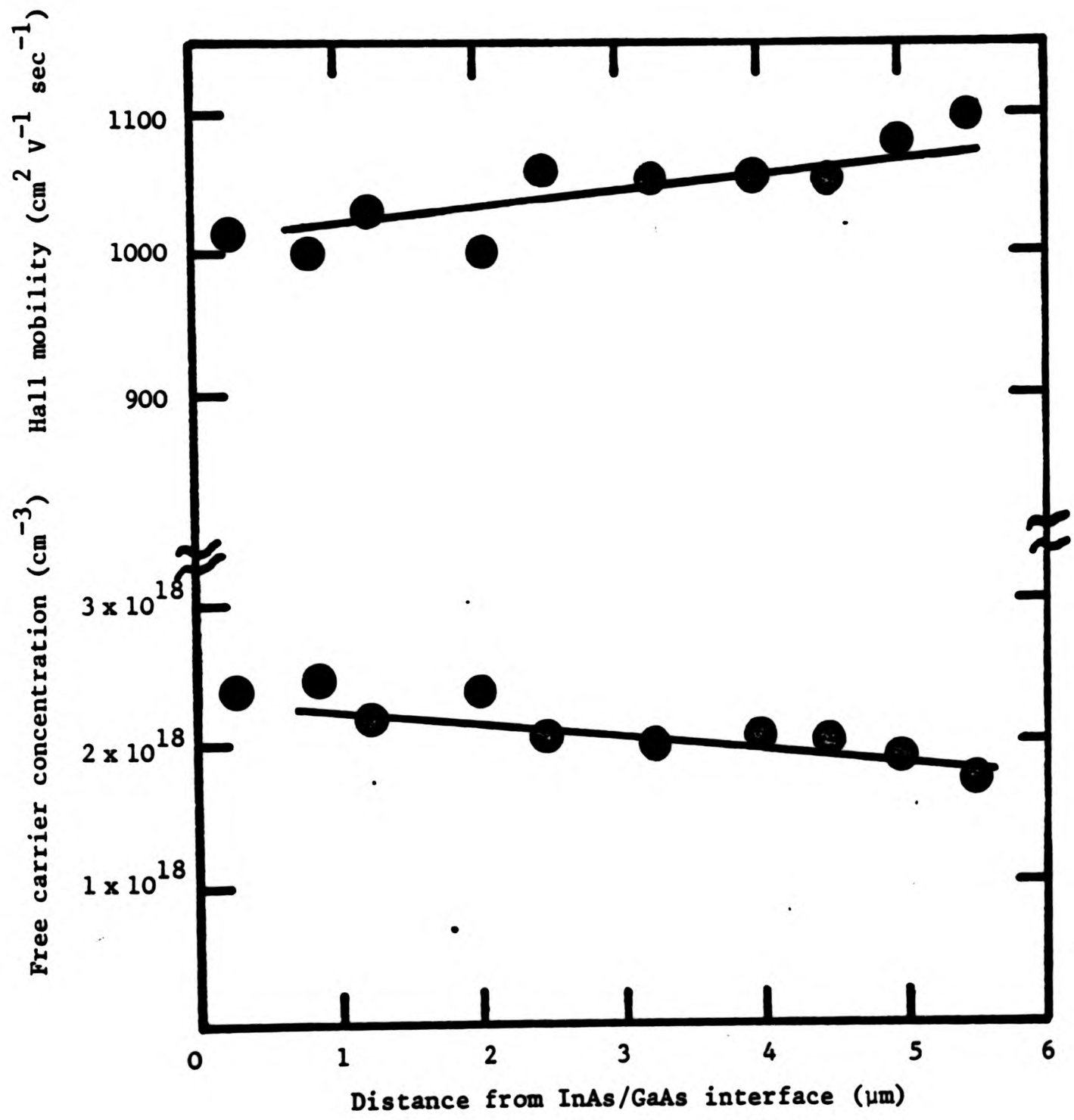


Figure 11 SEM micrographs of $1\ \mu\text{m}$ InAs epilayers deposited with different $\text{As}_4:\text{In}$ flux ratios. Marker length is $2\ \mu\text{m}$ in all cases. (a) Edge region of an indium precipitated surface, $\text{As}_4:\text{In}$ flux ratio $< 0.5:1$. (b) Surface of an epilayer deposited under optimum conditions, $\text{As}_4:\text{In}$ flux ratio $0.5:1$. (c) Surface of an epilayer deposited under arsenic-rich conditions, $\text{As}_4:\text{In}$ flux ratio $25:1$.

Figure 12 Variation of carrier concentration and mobility with depth for an epilayer with $n \sim 10^{18} \text{ cm}^{-3}$



into GaAs or InAs epilayers there must be free gallium or indium at the growing surface otherwise arsenic desorption occurs. The kinetic studies are not, however, sufficiently accurate to preclude a non zero sticking coefficient for As_4 on GaAs and InAs stoichiometric layers. In situ MEED examination on separate layers has shown that all the layers reported here were grown under As-stabilized conditions. Arsenic-stabilized conditions were maintained right up to the onset of indium precipitation which may be indicative that at the initial stages of indium rich growth the surface coverage of indium is not sufficient to generate an indium-stabilized reconstruction over the whole surface. None of the epilayers used for electrical analysis were examined by electron diffraction prior to electrical characterisation. The possibility of electron beam induced effects has previously been conjectured (Joyce and Foxon 1977a) and it is known that local electron beam irradiation of PbTe thin films can modify the transport properties of the whole film (McGlashan et al. 1979).

One concludes therefore that optimum electrical properties (i.e. low free carrier concentration and high mobility) are obtained with the smallest arsenic flux consistent with the deposition of stoichiometric layers. Once this critical flux is exceeded the electrical properties are degraded. The experimental point labelled A (Figure 7) was obtained with an artificially high background arsenic pressure of 6×10^{-6} Torr produced by not using liquid nitrogen trapping in the system. The arsenic flux used during deposition was then obtained by filling the trapping at the termination of growth, whereupon the system pressure fell to $\sim 1.5 \times 10^{-6}$ Torr. The electrical properties of this sample are commensurate with those expected if an arsenic background pressure of 1.5×10^{-6} Torr had been used throughout the deposition. This result is rather surprising since the kinetic theory of gases shows that a background pressure of 6×10^{-6} Torr corresponds to an As_4 flux at the substrate of 7×10^{14} molecules $cm^{-2} sec^{-1}$. This is nearly three times the estimated beam flux. This large background As_4 flux, apparently, does not influence the growing InAs film in the same manner as does the incident As_4 beam flux. The most likely explanation is that the ionization gauge, which is calibrated for nitrogen, gave an artificially high arsenic pressure reading and the background As_4 arrival rate was really small compared to the beam flux. The author is not aware of any work which has obtained an ionization gauge sensitivity factor for As_4 pressure measurements, but a factor of 10

variation in this parameter has been reported for different gases (AEI publication 2032-69).

If the background pressure readings were indeed correct then it seems that there is something in the mechanism of InAs film growth by MBE which enables a differentiation between the As_4 molecules arriving direct from the source and those which arrive after one or more collisions with the chamber walls. As_4 molecules coming from the background would presumably be thermally equilibrated with the walls of the chamber ($\sim 20^\circ C$) and also have a different distribution of incident directions to those arriving at nearly normal incidence directly from the arsenic source at $260^\circ C$. It is far from clear how either of these properties could affect the incorporation of arsenic into the growing film.

The mechanism by which donor and acceptor centres are incorporated due to the use of an excessive arsenic flux is as yet unknown though several possibilities do exist. The results could be interpreted as the incorporation of some impurities from the MBE system in general or the arsenic cell in particular. The two major system impurities present during this work were later identified (Chapter 3) as manganese and carbon. Mn is a p-type dopant in GaAs (Ilegems and Dingle 1975) and InSb (Dashevskii et al. 1971) and as such may be expected to be a p-type dopant in InAs. Carbon, present in the residual gas primarily as CO, CO₂ and CH₄, is normally associated with the acceptor site in III-V materials (Brozel et al. 1978; Ashen et al. 1975). However a carbon atom substitutionally on an indium site may give rise to donor properties. The required indium vacancies being generated by the As_4 flux. There are no obvious impurities present in the arsenic which could give rise to the observed doping. Any impurities would have to be present not only in sufficient quantities but also have suitable vapour pressures to be effusing from the arsenic cell (at $\sim 300^\circ C$) at a rate of $10^9 - 10^{10}$ atoms $cm^{-2} sec^{-1}$. Silicon was the major impurity in the indium source material (2ppm, Koch Light Laboratories, private communication 1977) and its incorporation as an n-type dopant may be a function of the arsenic flux.

Alternatively the incorporation of excess arsenic may be giving rise to the doping. Excess arsenic could be incorporated on the indium sublattice or as interstitials. The low growth temperature may lead to As_4 inclusions within the layers due to the non-dissociative adsorption

of As_4 molecules. Indium vacancies can be considered as another form of excess arsenic and it would seem probable that the generation of V_{In} would be increased as the $As_4:In$ flux ratio is increased. From purely thermodynamic arguments Van Vechten (1975) has postulated that antisite defects (As_{In}^{2+} ; In_{As}^{2-}) and antisite pairs ($As_{In}^{2+} In_{As}^{2-}$) should be the most common defects in stoichiometric material. It could be that for low temperature MBE growth under arsenic rich conditions that the double donor defect As_{In}^{2+} will predominate over the compensating In_{As}^{2-} defect. One could envisage an increase in the number of As_{In}^{2+} defects, and hence an increase in the n-type carrier concentration, as the arsenic flux increased for a given indium flux. It should be noted that quite small deviations from stoichiometry could give rise to the observed increases in carrier concentration. For example, if we consider As_4 inclusions are the donors then a sticking coefficient for As_4 on InAs of $\sim 10^{-5} - 10^{-6}$ would suffice and this is assuming that each As_4 molecule produces only one donor electron. Such a low sticking coefficient would not have been measurable in the experiments of Foxon and Joyce (1978).

A final mechanism which should be mentioned is the possibility of interstitial indium atoms giving rise to donor properties (Kroger 1974). It is possible that the indium atoms which arrive at the surface have to diffuse around in order to find the correct lattice sites (i.e. unoccupied In-sites). This diffusion process may be inhibited by the use of an excessive As_4 flux and lead to incorrectly sited indium atoms. The variation of surface morphology with arsenic flux (Figure 11 - plate) indicates that there are associated structural imperfections. The surface diffusion length of free Ga on GaAs is known to depend upon the As_4 arrival rate (Nogata and Tanaka 1977).

The growth of heteroepitaxial InAs by VPE under high $AsCl_3$ mole fractions has been observed (Cronin et al. 1966) to lead to compensated material. However, a recent examination of the effect (Trifonova and Hitova 1980) showed that the quality of the InAs material was improved by the use of a higher $AsCl_3$ mole fraction. They interpreted this effect as the suppression of the incorporation of group IV impurity elements (particularly silicon) by their removal from the system as stable chlorides.

Depth profiling data (to be discussed shortly) indicates that these MBE layers deposited under very high As_4 fluxes are uniformly doped throughout

the epilayer, and hence that the observed dependence of the carrier concentration on the As_4 flux is a bulk phenomenon and not a problem related to the initial vacuum cleaning or nucleation stage of the film growth. Annealing the InAs samples either in sealed ampoules or in the UHV chamber at $530^\circ C$ did not produce any improvements in the electrical properties.

An important remaining consideration is whether the observed increase in epilayer carrier concentration associated with the arsenic flux is connected with a fundamental MBE defect or merely an impurity problem. The magnitude of the effect coupled with the later identification of system impurities perhaps favours an impurity incorporation effect despite the fact that the origin of the impurity donor in both the InAs and GaAs remains unknown. Little is known about the effects of low temperature MBE growth except that the electrical properties are eventually severely degraded. For example even doped ($[Si] \geq 10^{17} \text{ cm}^{-3}$) MBE GaAs samples are insulating when grown below $\sim 450^\circ C$ (Murotani et al. 1978). A detailed examination of structural defects in MBE material would be extremely useful. However, it does appear that some fundamental defect is associated with the As_4 flux as revealed by deep level transient spectroscopy (Lang 1974) on MBE GaAs (Wood et al. 1979, Neave et al. 1980). For MBE GaAs material the As_4 flux appears to have a prominent role in the formation of deep electron traps although such traps are generally only in the $10^{12} - 10^{15} \text{ cm}^{-3}$ range. Whether the arsenic associated deep levels in MBE GaAs have any relation to the donor level(s) observed here in InAs is a matter only for speculation.

(b) Effect of indium arrival rate

The indium arrival rate controls the growth rate of the sample and it can be seen from figure 8 that the layers deposited at the slower rate have, for a given $As_4:In$ flux ratio, lower carrier concentrations and higher mobilities. The layers deposited with the lower In flux are also less compensated i.e. the growth rate either introduces or influences the incorporation of both donor and acceptor centres into these layers. Since all samples were $1 \mu\text{m}$ thick, the films with the best electrical properties were exposed to the background ambient for over five times as long and although the measured background pressure was lower for the slower growth rate the concentration of impurity species (CO and H_2O predominantly) were roughly equal in all cases. We

thus conclude that the residual doping in these epilayers was not due to the background UHV ambient. The fact that the lowest growth rate gave samples with the best electrical properties indicates that the nucleation/condensation rate of InAs was influencing film properties. The use of too high a growth rate could introduce point defects, stacking faults and dislocations originating at the film-substrate interface. Application of the theory of heterogeneous nucleation to epitaxy (Moazed 1966) implies that at low flux rates preferred epitaxial sites will act as nucleation centres whereas for higher fluxes random nucleation may occur. The increase of epitaxial temperature with increased growth rate has been observed by Cho (1970b) in the MBE growth of GaP on (111) CaF₂. The electrical properties of InP have been noted (McFee et al. 1977) to be affected by the growth rate. The effect of the growth rate on the properties of vacuum deposited Ge is well documented (Sloope and Tiller 1965, 1966, 1967).

The growth rate is often fixed by the thickness of the layer(s) required and the time available for deposition, and as such is not always an arbitrary parameter.

(c) Gaseous Effects

The improvement in electrical properties found by using the β -arsenic was considered to be due to inadequate outgassing of the α -arsenic source which oxidises on air exposure. Some supportive evidence for this has been obtained from the growth of layers under artificially high oxygen levels (5×10^{-7} Torr). The observed degradation in film properties presumably resulted from oxygen incorporation in the InAs lattice. There has, however, been no correlation between carrier concentrations and base pressure (in the limits 2×10^{-10} Torr to 2×10^{-9} Torr). Using an ambient hydrogen has been reported to improve the electrical properties of MBE GaAs (Calawa 1978) but no evidence was obtained for an effect on the electrical properties of the InAs when deposition took place with a hydrogen ambient of 5×10^{-7} Torr.

(d) Buffer Layer

It has been reported (Meggitt et al. 1978) that the surface morphology of the InAs epilayers was improved if deposited on a $0.1 \mu\text{m} - 0.5 \mu\text{m}$ high resistivity GaAs buffer layer. This observation has been

confirmed on many layers though occasionally the buffered and unbuffered layers had comparable smoothness.

Over twenty layers were deposited, at 370°C, with different As₄:In ratios in the manner described earlier using a buffer layer of 0.1 μm on only half of the substrate. For most of the layers there was little or no appreciable difference in the electrical properties of the buffered and unbuffered layers. But for the layers grown at the slower rate under optimum conditions (i.e. $n < 1 \times 10^{17} \text{ cm}^{-3}$) a reproducible difference did exist. We believe that the effect is present on all the epilayers but is only observed when the effective bulk doping is reduced below $\sim 1 \times 10^{17} \text{ cm}^{-3}$.

Table I shows that the best layers were deposited on a GaAs buffer layer:

TABLE I

Film No.		Room temperature	
		$n(\text{cm}^{-3})$	$\mu(\text{cm}^2 \text{V}^{-1} \text{sec}^{-1})$
42	buffered	6.4×10^{16}	8300
	unbuffered	9.7×10^{16}	5000
40	buffered	6.2×10^{16}	8600
	unbuffered	1.2×10^{17}	4900

The implication of this is that the buffer layer is responsible for isolating the InAs epilayer from a source of donor centres on the GaAs substrate which could originate from impurities present on the annealed substrate or diffuse out from the substrate bulk.

(e) Depth Profile Data

Depth profiles have been obtained for high ($n \sim 10^{18} \text{ cm}^{-3}$) and low doped ($n \leq 10^{17} \text{ cm}^{-3}$) InAs epilayers. These profiles indicate that two separate doping processes are occurring in these samples. One is a bulk effect, the other associated with the film-substrate interface. The increase in doping observed due to high impinging arsenic and indium fluxes is considered to lead to bulk doping of the epilayers. A 5.5 μm epilayer deposited under a high arsenic flux, at the faster growth rate was measured as having a room temperature carrier concentration of $2 \times 10^{18} \text{ cm}^{-3}$ and a mobility of $1000 \text{ cm}^2 \text{ V}^{-1} \text{ sec}^{-1}$. Depth profiling of this sample indicated uniform transport properties

(Figure 12), though no measurements were obtained on a layer thinner than 0.3 μm . Such a profile is indicative of uniform bulk doping. Completely different carrier concentration profiles are obtained on the lowest doped samples. There is an approximately constant mobility up to within $\sim 0.1 \mu\text{m}$ of the interface yet at the same time the carrier concentration varies by over an order of magnitude (Figure 10). Such a profile does, however, imply that the number of charge centres per unit area was independent of the remaining epilayer thickness. It is the profile obtained from a low doped sample which will now be considered in more detail.

The depth profiles obtained are striking since they can be accurately fitted to the equations (Zemel 1975) relating surface or interface band bending to the measured transport properties of the layer.

The Hall coefficient, R_H , and conductivity, σ can be expressed:

$$\sigma d = \sigma_o d + e\Delta N \mu_{NS} + e\Delta P \mu_{PS} \quad (1)$$

$$R_H \sigma^2 d = R_{Ho} \sigma_o^2 d - e\Delta N \mu_{NS}^2 + e\Delta P \mu_{PS}^2 \quad (2)$$

where

- R_{Ho} = Hall coefficient at flat band conditions
- σ_o = conductivity at flat band conditions
- ΔN = surface charge density (electrons)
- ΔP = surface charge density (holes)
- μ_{PS} = surface mobility (holes)
- μ_{NS} = surface mobility (electrons)
- d = layer thickness

An equally good fit can be obtained using the two layer model (Petritz 1958) as applied by Wieder (1974, 1977) and Sites and Wieder (1975) to thicker heteroepitaxial InAs samples. The variation of carrier concentration and mobility with depth (Figure 10) has been replotted (Figure 13) as the variation of Hall coefficient and conductivity with depth. This is because it is more convenient to treat these quantities in a theoretical analysis. The fit of experimental points to the theoretical curve (Figure 13) was made by using the experimental data

with equations (1) and (2) to obtain the unknown quantities ΔN , μ_{NS} , σ_o and R_{Ho} , (it was assumed $\Delta N \mu_{NS} \gg \Delta P \mu_{PS}$). This gives:

$$\begin{aligned}\sigma_o &= 10 (\Omega\text{cm})^{-1} \\ R_{Ho} &= 2988 \text{ cm}^3 \text{ C}^{-1} \\ \Delta N &= 8.7 \times 10^{12} \text{ cm}^{-2} \\ \mu_{NS} &= 5342 \text{ cm}^2 \text{ V}^{-1} \text{ sec}^{-1}\end{aligned}$$

From which we obtain:

$$\begin{aligned}n_{\text{bulk}} &= 2.1 \pm 0.7 \times 10^{15} \text{ cm}^{-3} \\ \mu_{\text{bulk}} &= 3.0 \pm 0.5 \times 10^4 \text{ cm}^2 \text{ V}^{-1} \text{ sec}^{-1}\end{aligned}$$

for the material remote from the space charge region.

this compares with the directly measured values of $n = 6.4 \times 10^{16} \text{ cm}^{-3}$ and $\mu = 8300 \text{ cm}^2 \text{ V}^{-1} \text{ sec}^{-1}$. The implication of the analysis is that the measured electrical properties of the epilayer were dominated by a strong accumulation region at the film-substrate interface and that the material remote from the interfacial space charge region is comparable to the best obtained by any method of preparation. Using the expressions of Many et al. (1971) the derived value of ΔN implies band bending of ≈ 11 kT units ($T = 300\text{K}$), assuming that the bulk Fermi level is near its intrinsic position. The band gap of InAs = 14 kT units so that the Fermi level at this interface is well into the conduction band. The free surface and interface (InAs-GaAs) of VPE InAs samples are generally accumulated (Wieder 1974, 1977). The existence of a positive interface charge density in $p(\text{GaAs})-N(\text{Al}_x\text{Ga}_{1-x}\text{As})$ heterojunctions produced by MBE also has been recently proposed (Kroemer et al. 1978).

The two layer model used by Wieder (1974) was supported by data obtained by an examination of the variation of R_H and ρ with magnetic field. The presence of a non-uniform doping profile is expected to give rise to circulating Hall currents (Petritz 1958) and be evident in the dependence of the Hall coefficient and the resistivity on the applied magnetic field. The variation of $(\Delta\rho/\rho_o)$, viz the magnetoresistance effect, observed with these thin MBE samples is consistent with the application of the two layer model. However, little variation of R_H with field ($B < 0.5\text{T}$) was observed.

Baliga and Ghandi (1974) reported that the carrier concentration of various thin InAs layers (0.2 - 1.0 μm) produced by VPE was inversely proportional to the layer thickness. They interpreted their results in terms of a continuously varying defect density in the epilayers, decreasing away from the film-substrate interface. In isolation, the results on the variation of measured carrier concentration with depth support this theory. However, we note that the mobility (especially on the buffered layer) is constant up to 0.1 μm of the epilayer-substrate interface, yet the carrier concentration has apparently increased by over an order of magnitude. By itself the n vs. d profile is not open to unambiguous interpretation. It is possible that the lattice mismatch at the interface is responsible for generating defects in the InAs layer but an interface space charge model finds more experimental support than a theory based on the variation of defect density with epitaxial layer thickness.

The interface between VPE InAs and the GaAs substrate has been examined using AES and EDAX (energy dispersive X-ray analysis) by Wagner (1976). He found that for samples grown at 700 $^{\circ}\text{C}$ there was a graded compositional ($\text{In}_x\text{Ga}_{1-x}\text{As}$) region of $\sim 1500 \text{ \AA}$. This graded layer was considered to play a major role in strain relief. MBE interfaces are generally considered to be sharper than those prepared by VPE. The reduction, or absence, of this grading layer in these low temperature samples may lead to an InAs-GaAs interface which is electrically more active.

The author has reservations arising from the use of the acid etch to thin down layers. The etch rate has been observed to vary from 0.03 $\mu\text{m min}^{-1}$ to 0.1 $\mu\text{m min}^{-1}$ on different samples. Samples grown on buffer layers have always etched slower than those deposited directly onto the substrate. This may be due to more structural defects present in the unbuffered layers. It is possible that the etch rate did increase towards the interface because of an increasing defect density caused by the large lattice mismatch between InAs and GaAs. The effects of the relief, or non relief, of lattice mismatch has been discussed by Olsen (1975). Attempts have been made using SEM measurements and X-ray analysis to ascertain whether the etch rate is uniform both over the whole sample area and with depth. Measurements obtained have not been conclusive regarding the variation of etch rate with depth throughout the entire film although they did indicate that the etch rate is constant to at least within 0.2 μm of the interface. Also

it has been established that the etch rate is the same over the sample area (16 mm^2) with too few etch pits or hillocks to affect the measurements. C-V profiling of samples was not possible due to a very large leakage current across the diode.

2.5 Conclusions

The As_4 :In flux ratio and the value of the indium flux are important parameters influencing the electrical properties of the heteroepitaxial (100) InAs layers grown by MBE at 370°C . The use of an excessive As_4 flux produced residual n-type carrier concentrations above 10^{18} cm^{-3} and high indium flux rates gave additional doping and mobility degradations. The electrical data obtained can be interpreted in terms of the incorporation of excess arsenic into the bulk of the epilayers. Depth profile measurements on the lowest doped epilayers indicate a strong accumulation region ($\Delta N \sim 8 \times 10^{12} \text{ cm}^{-2}$) at the epilayer-substrate interface which dominated the measured electrical properties of these $1 \mu\text{m}$ thick films. Analysis using a space charge model indicated that the deposited material remote from this interface had near bulk mobility ($\sim 3 \times 10^4 \text{ cm}^2 \text{ V}^{-1} \text{ sec}^{-1}$) and low residual carrier concentration ($\sim 2 \times 10^{15} \text{ cm}^{-3}$). However the results on the growth of (100) GaAs in this same MBE system (to be discussed in the next chapter) clearly show the presence of system impurities in the 10^{16} cm^{-3} range. As a consequence the conclusion regarding the quality of the InAs material remote from the InAs - GaAs interface must remain tentative.

CHAPTER 3

An Investigation into the Growth of (100) GaAs by MBE3.1 Introduction

The binary compound semiconductor GaAs is certainly the most frequently prepared material by MBE. Primary interest has centred on the preparation of doped (n and $p \sim 10^{16} - 10^{18} \text{ cm}^{-3}$) layers for various devices such as FETs (Wood 1976), lasers (Tsang 1979), varactors (Covington and Hicklin 1978) and LEDs (Lee et al. 1978). However the undoped GaAs layers are of considerable interest, the production of which is an integral part of producing good quality doped material. Furthermore, studies of the undoped GaAs offers another means of comparing different MBE systems and MBE with other growth techniques. Undoped GaAs layers have been deposited for kinetic studies into MBE growth (Foxon and Joyce 1975, 1977) and surface studies (Cho 1969, 1970ab, Neave and Joyce 1978ab). The electrical properties of the undoped, or more correctly unintentionally doped, MBE GaAs layers will depend on which impurities or electrically active defects are incorporated into the epilayers. For example, silicon is a major impurity in melt grown single crystal GaAs and consequently MBE GaAs layers deposited using GaAs as the arsenic (As_2) source were found to be n -type with $n \sim 10^{16} \text{ cm}^{-3}$ (Cho and Reinhardt 1974).

Many MBE systems produce GaAs with a residual p -type conductivity due to the incorporation of carbon (Scott and Roberts 1979) the origin of which is uncertain. Improvements in the MBE system design have led to a reduction in system associated impurities and residual impurity levels of $\sim 10^{14} \text{ cm}^{-3}$ for MBE GaAs have been achieved (Morkoc and Cho 1979).

This chapter contains the results of an investigation into the growth of unintentionally doped (100) GaAs epilayers by MBE. The experiments were of a similar type to those carried out on InAs (Chapter 2) but on the technologically more important material, GaAs. Furthermore the investigation prepared the way for a study of the silicon doping of MBE GaAs (Chapter 4).

3.2 Experimental

The experimental apparatus as described in Chapter 1 was used. The only initial modification being the introduction of a large capacity (30 gms) graphite effusion cell for the arsenic. This cell enabled the arsenic charge to be outgassed without the risk of exhausting the cell charge. Consequently the more usual α -arsenic was used throughout, though tests did indicate that both the α and β forms produced GaAs with similar properties. During the previous InAs work the cell had barely contained enough material to fully outgas the arsenic charge and to complete the growth of 1 μm layers using large As_4 fluxes.

For this study 1 μm GaAs layers were deposited onto (100) Cr-doped semi-insulating GaAs substrates at growth temperatures of 500 - 570°C using As_4 :Ga flux ratios of 0.5:1 to 5:1 for growth rates of 0.3 $\mu\text{m hr}^{-1}$ and 1.0 $\mu\text{m hr}^{-1}$. Electrical characterization of the epilayers was undertaken using the van der Pauw technique and this was supported by the use of the photoluminescence (PL) technique. The PL spectra were taken by Dr. G.B. Scott at PRL (Redhill, UK).

3.3 Results

3.3.1 Electrical Properties

Figures 14 and 15 are 300K and 77K free carrier concentration - Hall mobility plots for the unintentionally doped 1 μm thick GaAs epilayers deposited in this study. The epilayer reference numbers are quoted for easier comparison of the two graphs. Figure 14 also includes the bulk plot taken from Sze (1969). All the layers were p-type. No effect attributable to the growth rate was observed. Investigations showed, however, that the p-type doping of the epilayers was associated with:

- (i) the presence of hot stainless steel in the vacuum chamber,
- and (ii) the As_4 surface coverage during the deposition.

The later point is connected with both the As_4 flux and the substrate temperature, high As_4 fluxes and low substrate temperatures tending to increase the As_4 coverage. Both of the above points are illustrated in Figure 16 which shows the variation in p-type carrier concentration with inverse temperature (a "freeze-out plot") for four epilayers deposited at 570°C and one (dotted curve) deposited at 500°C. The upper two solid curves are from epilayers (R51 and R52) which were

Figure 14 Free carrier concentration-Hall mobility plot for the GaAs epilayers at 300K

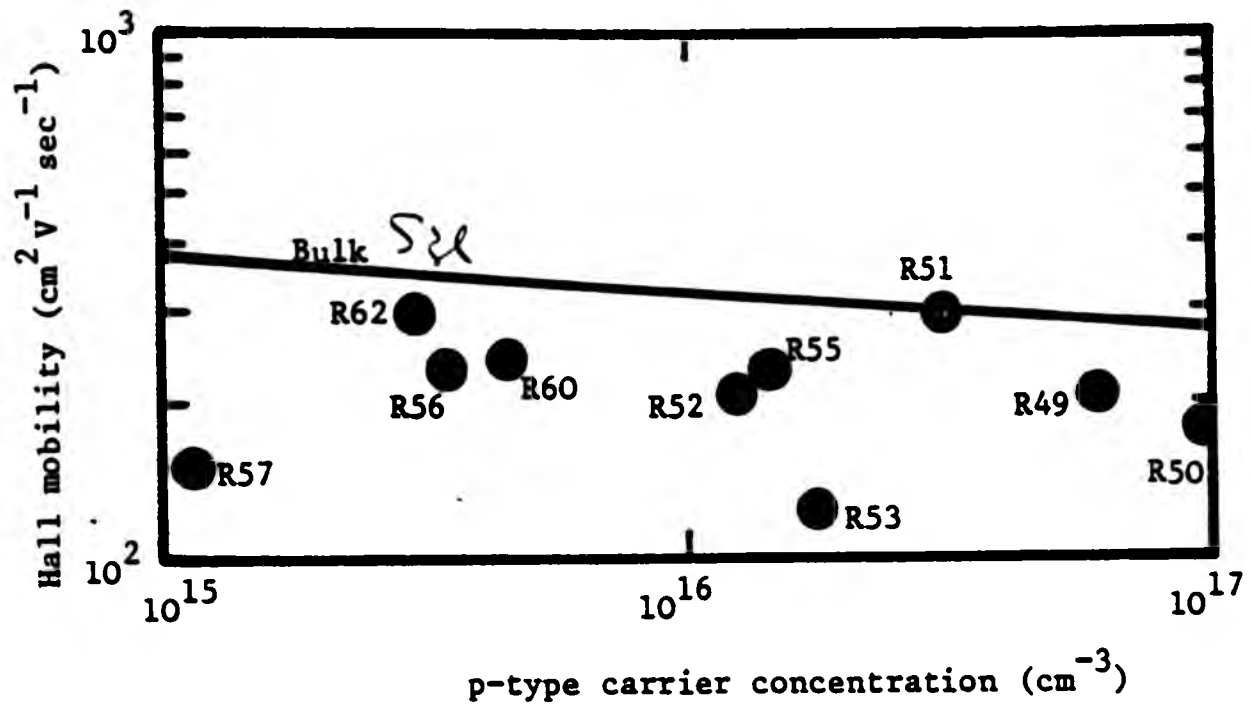


Figure 15 Free carrier concentration-Hall mobility plot for the GaAs epilayers at 77K

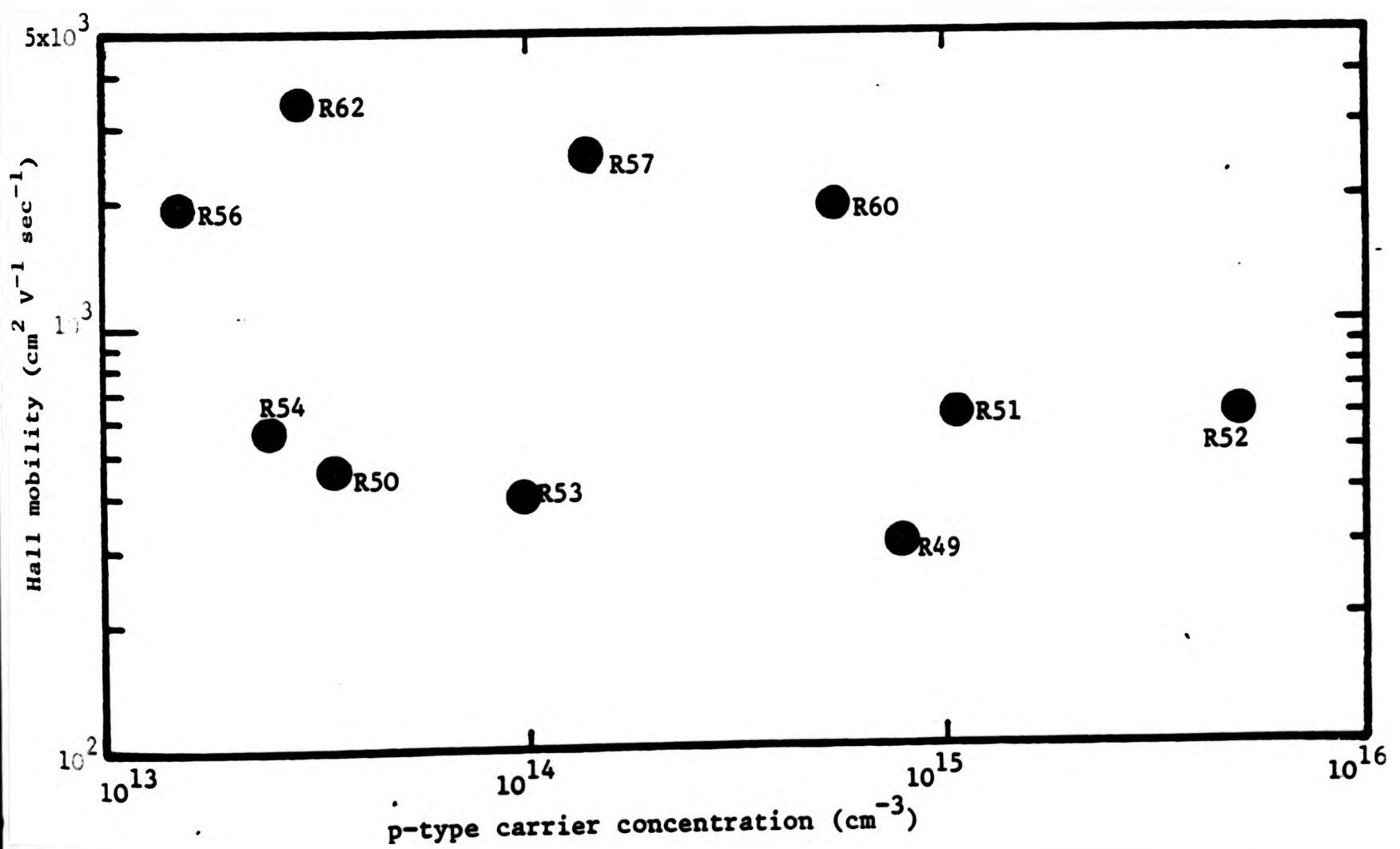
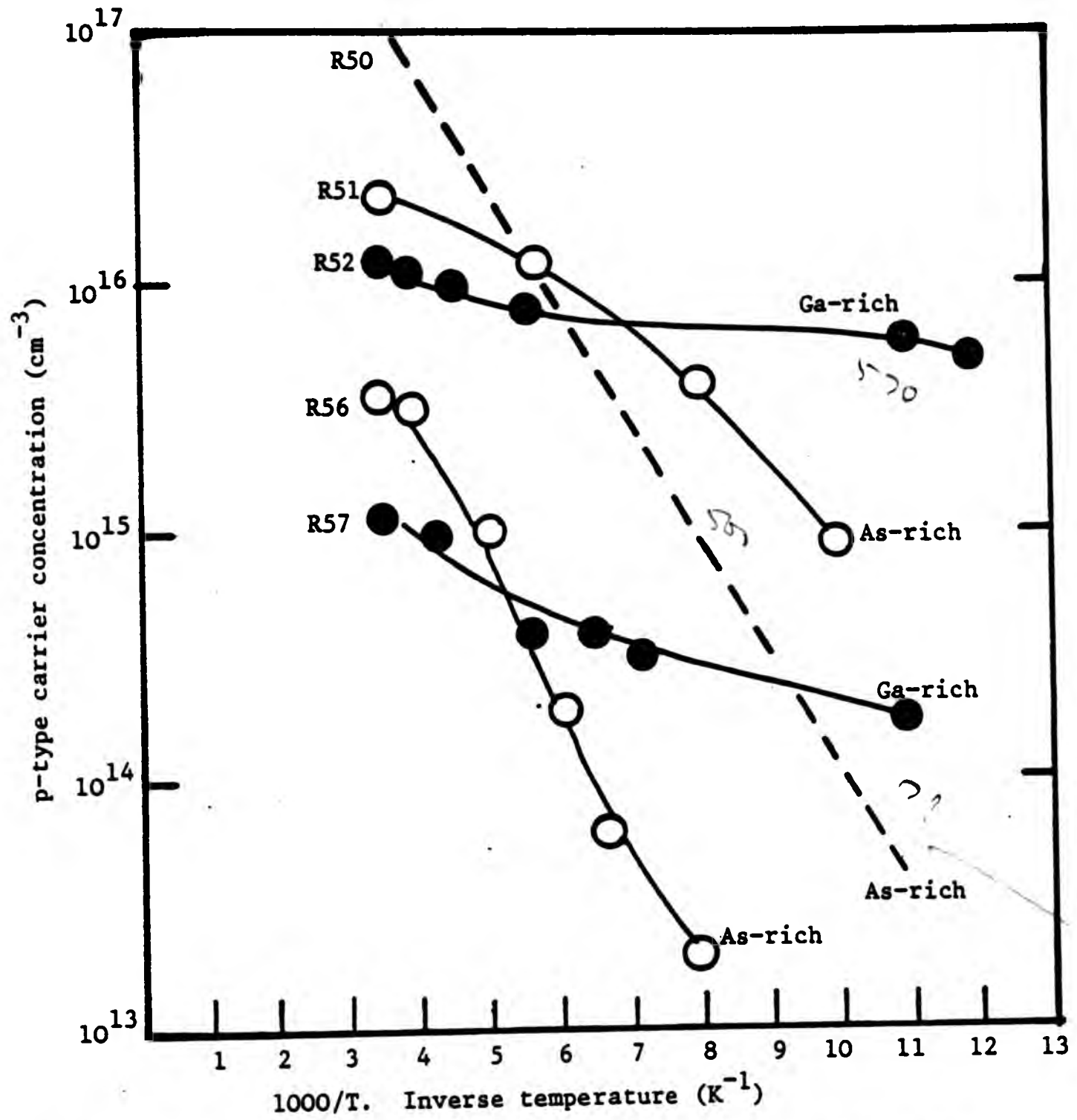
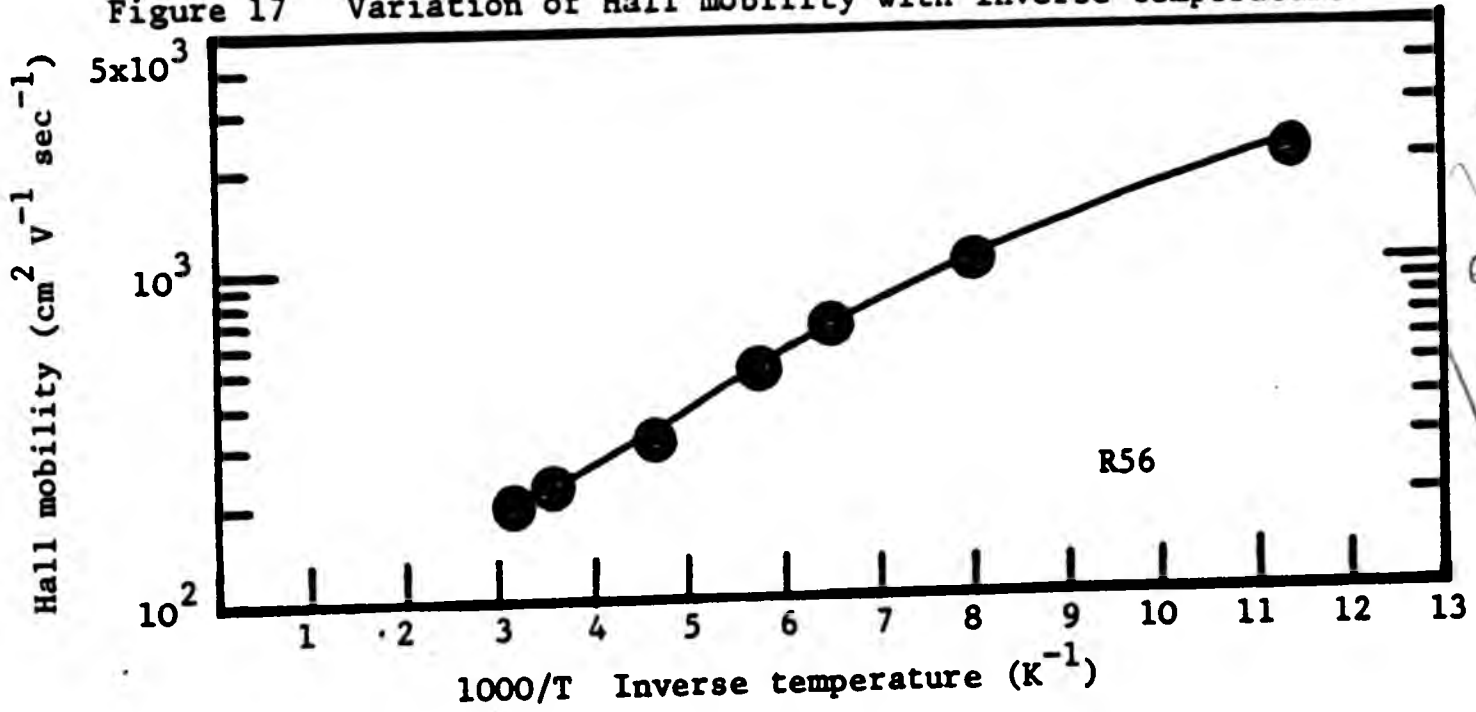


Figure 16 Freeze-out plots for undoped GaAs epilayers deposited under As- and Ga-rich conditions at 570°C (solid lines) and under As-rich conditions at 500°C (dotted line)



Handwritten note: Line blank and one point

Figure 17 Variation of Hall mobility with inverse temperature



Handwritten note: very low carrier density

deposited at 570°C using the evaporation cells mounting as shown in Figure 3 (plate of Chapter 1). For the epilayers (also deposited at 570°C) giving the lower two solid curves (R56 and R57) this mounting was modified by replacing the stainless steel support rods and base plate with a Mo plate and Mo foil supports. This data and that contained in figures 14 and 15, where layers R49 - R55 were those deposited using the stainless steel mounting, clearly identifies stainless steel as a major source of some p-type impurity dopant. The two curves in each set show the effect of varying the As₄ flux for a fixed gallium flux, the growth rate being 0.3 μm hr⁻¹. The shallower freeze-out behaviour and the lower 300K carrier concentrations arise for layers deposited under Ga-rich growth conditions (As₄:Ga flux ratio ~0.5:1) whilst the stronger freeze-out behaviour and higher 300K carrier concentrations arise for layers deposited under As-rich growth conditions (As₄:Ga flux ratio ~2:1). Lowering the substrate temperature to 530°C and 500°C for As-rich growth conditions increased the 300K p-type carrier concentration to ~1 x 10¹⁷ cm⁻³ in both cases, the form of the freeze out curves remaining approximately as for As-rich growth at 570°C as can be seen from Figure 16.

Figure 17 shows the variation of Hall mobility with inverse temperature for one layer. Depth profile data obtained using the C-V Hg probe method indicated that the p-type carrier concentration was uniform with depth. Attempts to deposit GaAs layers using only a GaAs source in the manner as described by Cho and Chen (1970) were not successful. Gallium precipitation and non-stoichiometric growth resulted.

3.3.2 Structural Properties

Back reflection X-ray diffraction patterns from these samples indicated that they were single crystals. RMEED patterns showed the (2 x 4) and (4 x 2) reconstructions.

3.3.3 Optical Properties

Figure 18 is a PL spectra from an epilayer deposited at 570°C under As-rich conditions. It shows the presence of manganese and carbon impurities with acceptor activation energies of ~112 meV and 26 meV respectively. The manganese peak shows two longitudinal optical phonon sidebands. Figure 19 shows how the PL spectra changed as the As₄ surface coverage used during deposition was increased. The Mn

Figure 18
Detail of photoluminescence spectra of an unintentionally doped GaAs layer deposited at a growth rate of $1 \mu\text{m hr}^{-1}$.
TS = 570°C; $P_{\text{As}_4} = 2 \times 10^{-6}$ Torr; $\text{NA-MD}_{300\text{K}} = 2 \times 10^{16} \text{ cm}^{-3}$

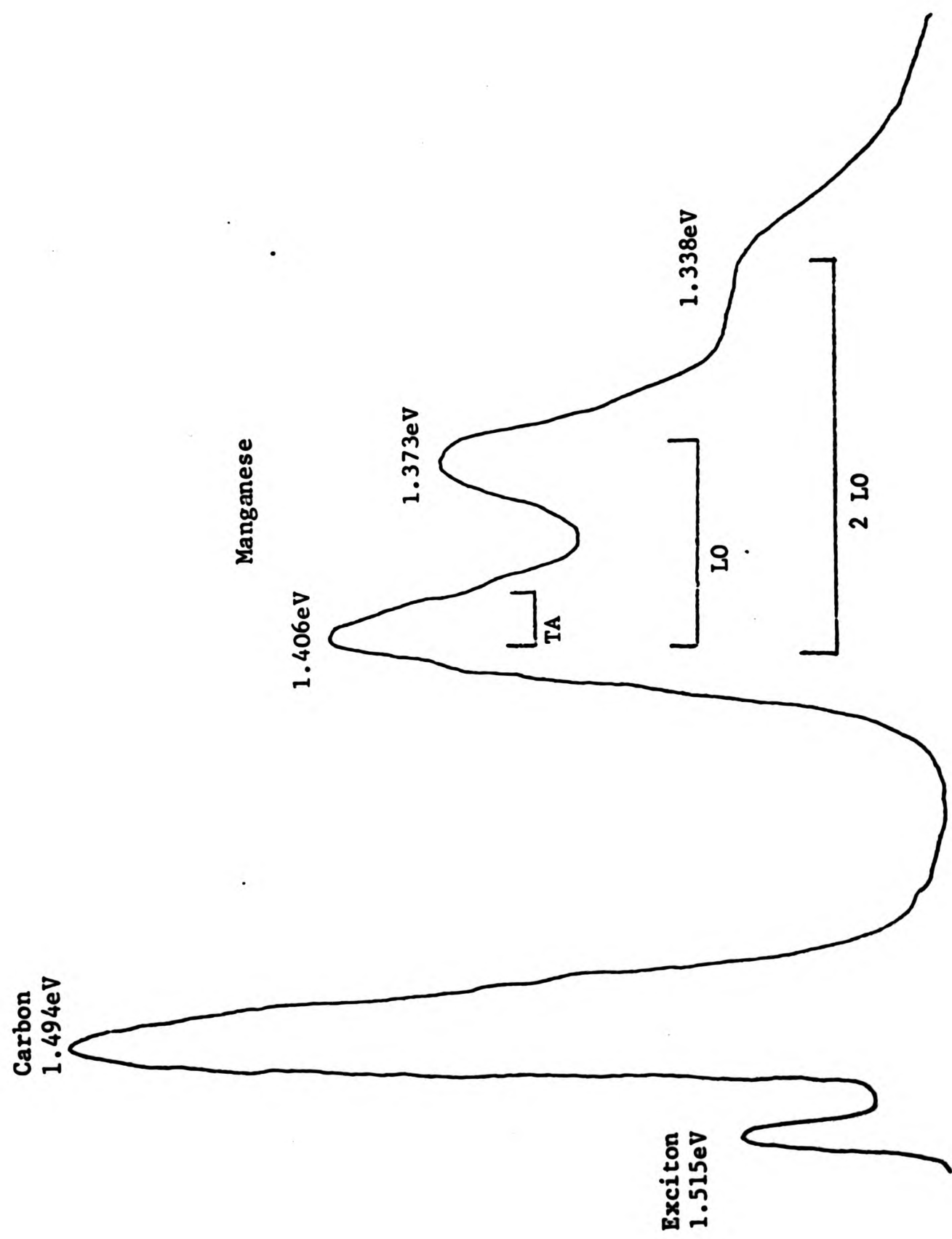
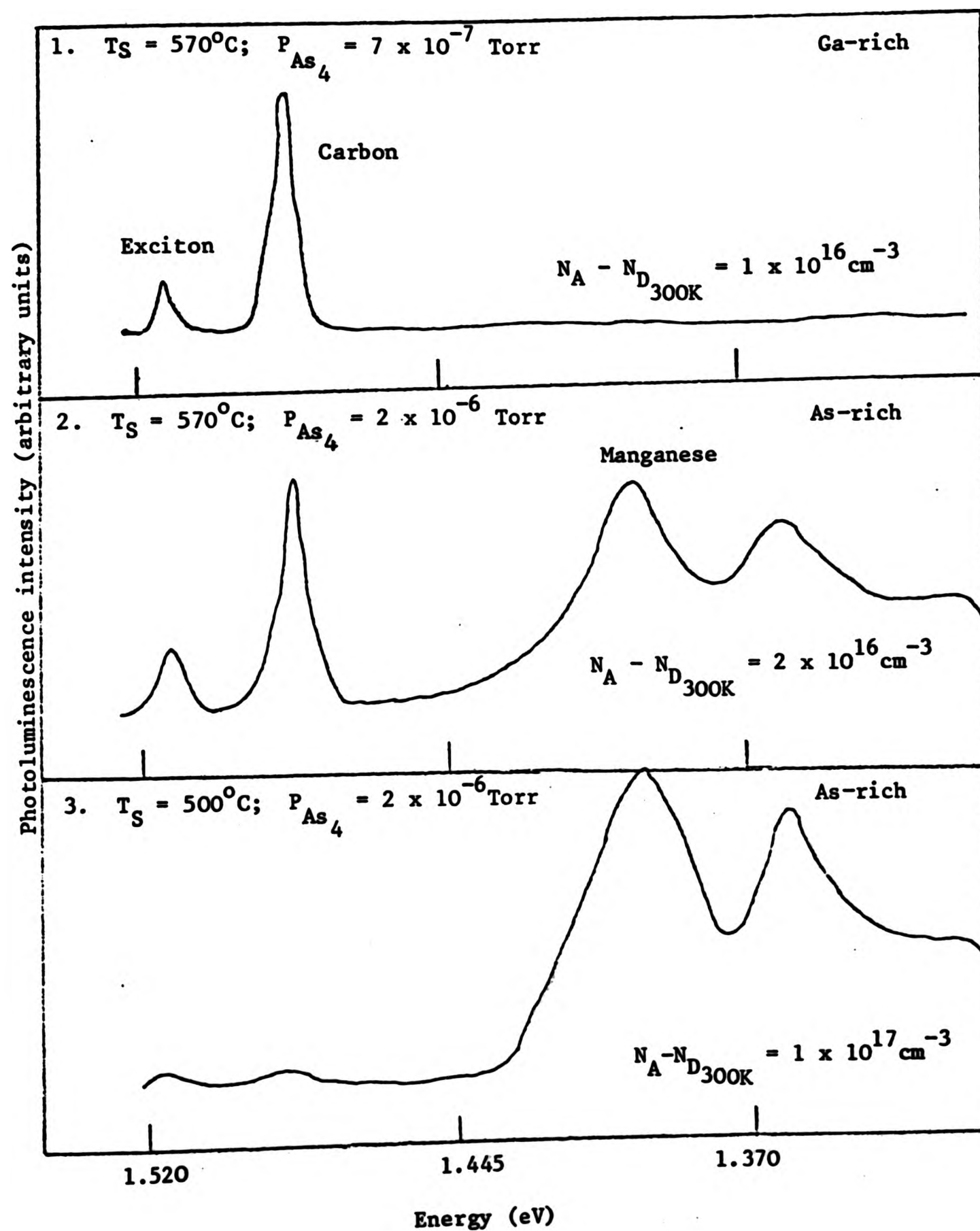


Figure 19

Photoluminescence spectra of three unintentionally doped GaAs layers deposited under different As_4 fluxes and substrate temperatures (T_S) for a growth rate of $1 \mu\text{m hr}^{-1}$.



associated luminescence band increases with the As_4 surface coverage. Also shown are the measured p-type carrier concentrations of the layers. All these layers (Figure 19) were deposited prior to removing the stainless steel from the evaporation cell assembly. There is clearly some correlation also between the intensity of the Mn associated luminescence band and the p-type carrier concentration.

*What is
the explanation*

3.4 Discussion

The electrical properties (Figures 14 and 15) of these p-type layers indicate that the layers are compensated. Although the PL technique has been able to identify some of the acceptor centres, the type and origin of the compensating donor centres remains the subject of some speculation. The identification of the donor impurity would also be beneficial to the interpretation of the results on the growth of InAs (Chapter 2). PL spectra such as Figure 18 are now generally accepted as being indicative of the presence of the two impurity species carbon and manganese (Ilegems and Dingle 1975, Ilegems et al. 1975). Earlier work attributed the ~ 100 meV deep luminescence band to centres associated with Ga vacancies (Cho and Hayashi 1971b). The more recent proposal (Lum et al. 1977) that this feature involves a $C-V_{As}$ complex has yet to find experimental support (Scott and Roberts 1979). Optically detected electron spin resonance studies on the highest doped p-type samples were unable to provide conclusive identification of Mn due to the technique's limited sensitivity when applied to thin films (G.B. Scott, private communication 1979). The PL spectra of Figure 18 implies that Mn is a p-type dopant in MBE GaAs with an acceptor activation energy ~ 112 meV. Estimates of the activation energy from the freeze-out plots (Figure 16) and other data, yield a figure of 60 - 120 meV. Differences in freeze-out behaviour are frequently observed due to inaccuracies and fluctuations associated with the temperature measurements from within the cryostat. An activation energy of ~ 100 meV is rather large for a dopant and this has partly limited the use of Mn as a dopant in MBE GaAs. Also, manganese dopant levels in excess of 10^{18} cm^{-3} are difficult to achieve without deterioration of the surface morphology (Joyce and Foxon 1977a). Beryllium is probably the best p-type dopant for MBE GaAs (Ilegems 1977), although the use of Zn^+ ion beams shows promising results (Bean and Dingle 1979).

*53
20*

*What is
the explanation*

Figures 16 and 19 show that the incorporation of Mn as an optically and electrically active impurity is dependant on the As_4 surface coverage present during growth. The incorporation of the impurity is least for Ga-rich growth where the PL spectra and the freeze-out behaviour show the dominant acceptor to be a shallower centre (~ 30 meV) identified as carbon. For some intermediate growth conditions the concentration of ionized Mn and C acceptor centres could be roughly equal and a more complex two level analysis of the freeze-out plots would be required. Even in the Mn dominated cases the presence of the compensating donors further complicates the freeze-out mechanism. The relative heights of the peaks in the PL spectra cannot be taken as the relative concentrations of the different impurities (G.B. Scott, private communication 1978).

The variation of the epilayer carrier concentrations and the Mn-associated luminescence as the As_4 flux and substrate temperature changed to produce either As- or Ga-rich growth indicates that Mn is incorporated primarily as a substitutional acceptor on Ga sites, where the concentration of gallium vacancies is some function of the As_4 flux and the growth temperature. It seems probable that the gallium vacancy concentration would increase if the As_4 flux or the substrate temperature were increased or decreased respectively. It is possible that even under Ga-rich conditions the Mn is still incorporated into the epilayers but on some electrically and optically inactive site. As appears to be the case with magnesium (Mg) (Joyce and Foxon 1977a), the impurity is incorporated yet only a very low level of electrical activity is obtained ($\sim 10^{-5}$, Cho and Panish 1972). It was considered that this could be due to Mg occupying mainly interstitial sites. By analogy, the observed behaviour of Mn could be due to Mn occupying interstitial sites under Ga-rich growth conditions. Thermodynamic considerations argue against simple re-evaporation of the Mn. From the above discussion it would seem preferable to deposit the epilayers under Ga-rich growth conditions. To do so however requires fine control over the incident fluxes so as not to produce either gallium precipitation or a drift into As-rich growth.

In common with other researchers (Ilegems and Dingle 1975) hot stainless steel has been identified as the source of the Mn impurity and as such should not be used in those parts of the MBE system which are hot during the growth procedure. Unfortunately practical and financial

considerations sometimes lead to stainless steel being used in situations where Ta or Mo would be preferable. The removal of the stainless steel from the source cell assembly led to an immediate and reproducible reduction in the 300K p-type carrier concentration by about an order of magnitude (Figure 16). Even after the introduction of the Mo plate some Mn remained in the system and was incorporated into the layers as is illustrated by the freeze-out behaviour of the lower doped As-rich layer (R56) of Figure 16. Furthermore, Mn continued to be present as judged by the PL spectra. However, after four further depositions the Mn signal in the PL spectra suddenly disappeared. This is shown in Figure 20 which shows the spectra of two consecutively deposited layers grown under similar As-rich conditions. Mn is a good luminescer (G.B. Scott, private communication 1979) and consequently the differences in the amount of Mn in the two layers may have been quite small despite the dramatic differences in PL spectra. No further depositions of undoped material took place and so this point could not be further investigated. Indeed in the later work, on Si doped GaAs, the Mn peak was again observed. It is interesting to note that in the Mn free spectrum (Figure 20) there is evidence for a much deeper acceptor level (~ 0.2 eV) which may be silicon. Silicon is generally considered as an amphoteric dopant in GaAs (Kressel 1974) although only n-type MBE GaAs:Si has been obtained. Other workers have obtained MBE GaAs:Si material which showed no silicon acceptor levels in PL (K. Ploog, private communication 1979). The presence of the silicon acceptor levels in the present work would therefore strongly suggest the presence of compensating silicon donor levels. The origin of the silicon could be the gallium charge (~ 1 ppm Si, Koch Light Laboratories, private communication 1977), the quartz tubing which was used to electrically isolate various wires or the Mo/fused quartz plate heater assembly. Covington and Meeks (1979) have found that a fused quartz/Ta resistive film heater can lead to residual n-type doping levels of $2 \times 10^{15} \text{ cm}^{-3}$ and they suggested that silicon was the donor.

Three samples were found to have a semi-insulating nature (resistivity $> 10^5 \Omega \text{cm}$) and the reasons for this are unknown. The chances of achieving such perfect compensation for three layers in a batch of fifteen would seem remote. The PL spectra showed no extra features except to note that the individual peaks were somewhat broadened.

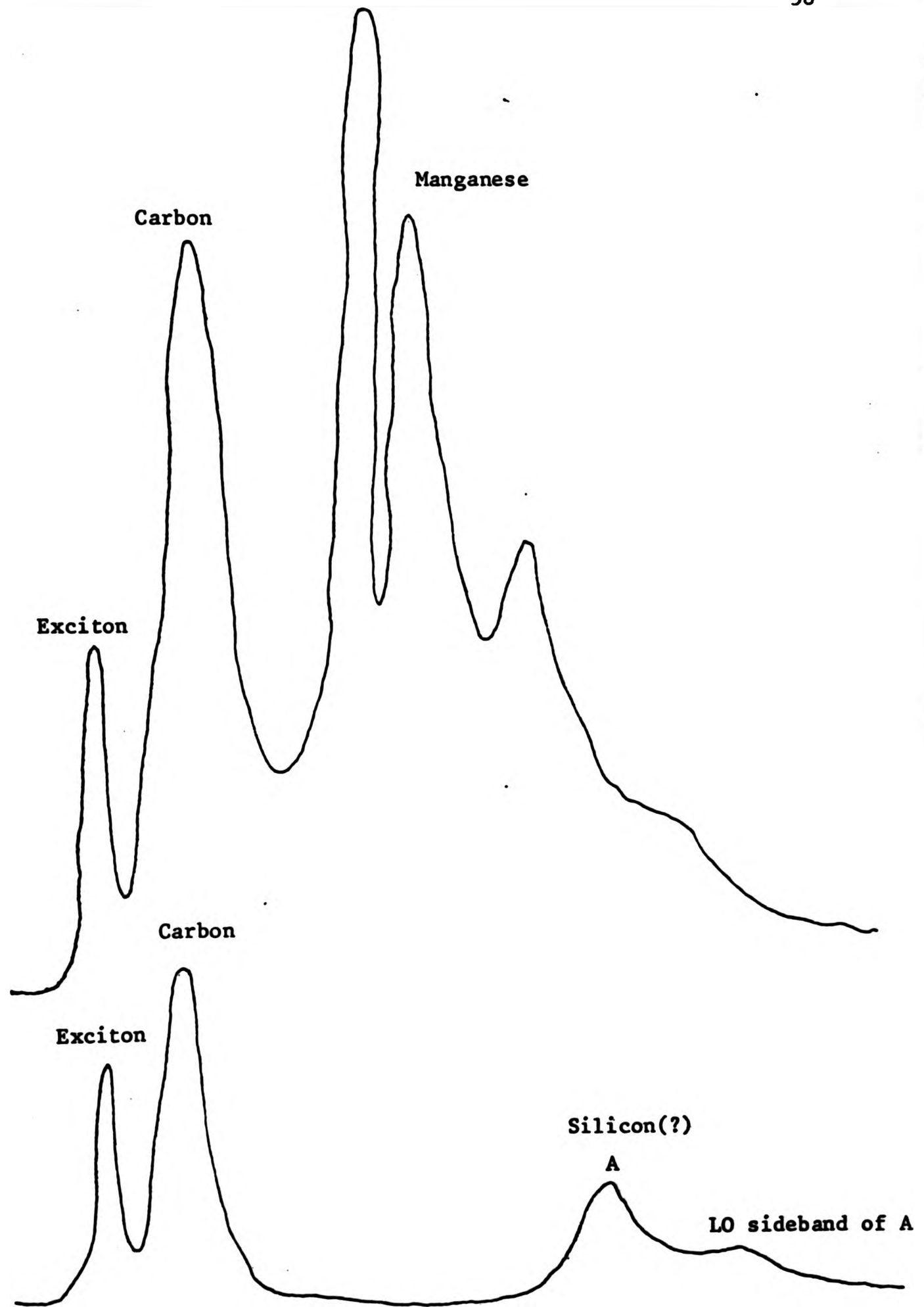


Figure 20

Photoluminescence spectra of two unintentionally doped GaAs layers deposited under similar conditions.
 $N_A - N_D = 300K = 4 \times 10^{15} \text{ cm}^{-3}$ in both cases.

3.5 Conclusions

The MBE system used in this project produced compensated p-type GaAs layers when not intentionally doped. The system impurities carbon and manganese have been identified as the sources of acceptor centres and some evidence has been found for silicon being a compensating donor impurity. Hot stainless steel in the vacuum system has been shown to be a source of the p-type dopant manganese. The incorporation mechanism of the manganese impurity can be described as a simple substitutional process, the Mn being incorporated into the GaAs lattice on Ga sites. The GaAs material ultimately produced was p-type with $N_A - N_D \sim 10^{15} \text{ cm}^{-3}$ and $\mu \lesssim 300 \text{ cm}^2 \text{ V}^{-1} \text{ sec}^{-1}$, such a mobility is typical of bulk material with $p \sim 5 \times 10^{16} \text{ cm}^{-3}$. Nevertheless one cannot discount a priori the possibility of producing bulk-like material for dopant levels $> 10^{17} \text{ cm}^{-3}$.

CHAPTER 4

An Investigation into the Silicon Doping of MBE (100) GaAs4.1 Introduction

Despite the rapid development of the MBE technique it is interesting to note that the fundamental requirement of n-type doping MBE GaAs still remains an impediment to its progression into an established material and device fabrication technology. A number of donor impurities have been used with varying degrees of success, these include: Si (Cho and Hayashi 1971c, Calawa 1978); Ge (Cho and Hayashi 1971a, Cho 1975, Wood et al. 1979); Sn (Ploog and Fischer 1978, Wood and Joyce 1978); PbS and PbSe (Wood 1978) and SnTe (Collins 1979). Tin (Sn) is the most widely used n-type dopant giving a very low level of compensation when compared with both theoretical calculations of electron transport properties and bulk material. However, the presence of a rate limited incorporation mechanism (Wood and Joyce 1978) can give rise to non-uniform doping profiles at the commencement and termination of growth and difficulty in producing abrupt changes in doping levels. Germanium is an amphoteric dopant for MBE GaAs and as such frequently gives rise to compensated material. The lead and tin chalcogenides have been examined in much less detail though initial results suggest that they may be extremely useful n-type dopants. It would appear from the literature that Si has been somewhat neglected as a dopant especially in view of the excellent electrical data for GaAs:Si reported in Cho and Arthur (1975). Recently the research group at the Mitsubishi Semiconductor Laboratory (Murotani et al. 1978, Wataze et al. 1978, Shimano et al. 1979) have published results which show that Si should be considered as the best elemental n-type dopant, giving rise to near bulk electrical properties without the interface complications associated with Sn. Although these reports do not represent an in-depth examination of Si incorporation into MBE GaAs, they do clearly identify the production of a pure Si dopant beam as a vital factor in the production of low compensation ($N_D + N_A/n \sim 1.5$) GaAs:Si. However, in spite of these published results it is interesting to note that the worker producing the best MBE opto-electronic devices still uses Sn as the n-type dopant (Tsang 1979, 1980). Furthermore other researchers have experienced considerable difficulty in obtaining only fair quality GaAs:Si (J.S. Roberts, private communication 1979, G. Laurence, private

communication 1979).

This chapter contains the results of an investigation into the growth of (100) GaAs:Si. The object of the study being to establish the properties of the silicon doped material which could be routinely produced and to identify the experimental parameters and/or system impurities which influence and give rise to these properties. Furthermore, the use of the GaAs:Si material as a standard has enabled a critical evaluation of the MBE system to be made. Particular attention has centred upon the relative merits of graphite and BN effusion cells and assessing if the rotary/oil diffusion pumping system is a limiting factor in the production of high quality MBE epilayers. Such considerations are important for the future development of the MBE systems within the research group.

4.2 Experimental

1 μm thick Si doped GaAs layers were grown by MBE onto Cr- and Te-doped ($n \sim 2 \times 10^{18} \text{ cm}^{-3}$) (100) GaAs substrates. The substrates were etched in a $15\text{H}_2\text{SO}_4:2\text{H}_2\text{O}_2:2\text{H}_2\text{O}$ solution prior to being loaded into the vacuum system. For the initial experiments the graphite-alumina assembly was used for all the cells, though later a BN cell was used for the Si evaporation. Deposition temperatures of $400^\circ\text{C} - 650^\circ\text{C}$, growth rates of 0.4, 0.5, 1.3, 1.8 and $4.0 \mu\text{m hr}^{-1}$ and $\text{As}_4:\text{Ga}$ flux ratios in the range $<0.5:1$ to $30:1$ have been used for the growth of the layers. Silicon source temperatures of $800^\circ\text{C} - 1200^\circ\text{C}$ have been used to obtain layers with free carrier concentrations in the range $1 \times 10^{16} - 7 \times 10^{18} \text{ cm}^{-3}$. Hall mobilities and free carrier concentrations have been determined by the van der Pauw technique and additionally the double probe Hg-Schottky barrier C-V technique has been used to examine various free carrier concentration profiles. Compensation ratios have been estimated from the theoretical data of Rode and Knight (1971) and Rode (1975).

4.3 Results

4.3.1 General Electrical Properties

Figures 21 and 22 are free carrier concentration-Hall mobility plots at 300K and 77K respectively for the $1 \mu\text{m}$ MBE (100) GaAs:Si layers. Also shown are the relevant compensation curves from Rode (1975), the curve

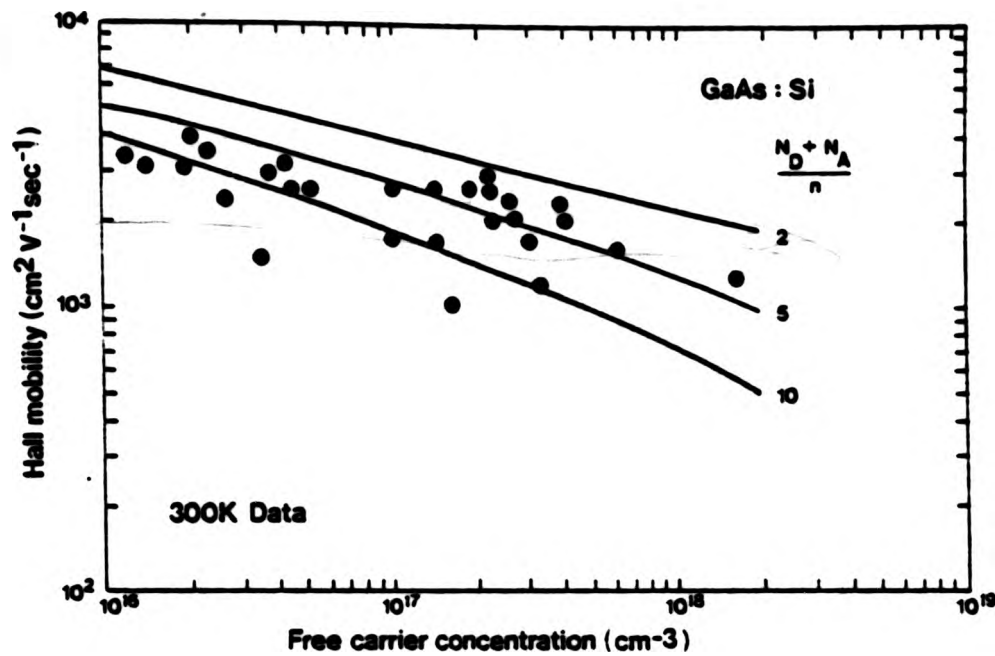


Figure 21

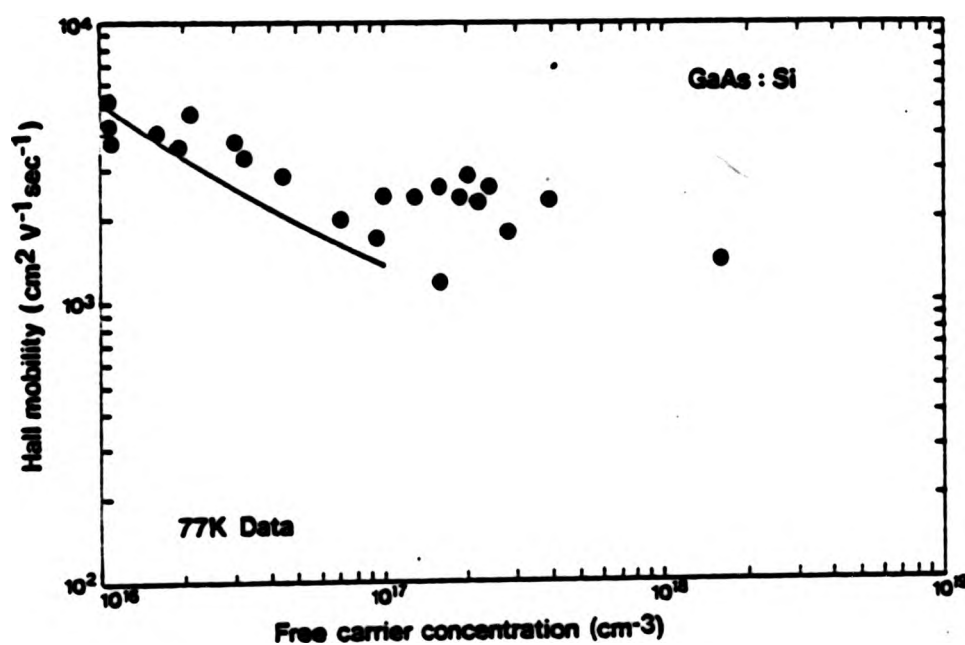


Figure 22

Free carrier concentration-Hall mobility plots at 300K and 77K for the initial layers deposited using a graphite effusion cell for the silicon evaporation. The theoretical compensation curves are taken from Rode (1975). The one curve on the 77K plot is for a compensation ratio of 10.

shown with the 77K data being that for a compensation ratio of 10. These layers were deposited under widely different growth conditions as mentioned in 4.2 and the effects of which will be discussed shortly. Only n-type conduction has been observed. Figure 23 is a plot of the Hall mobility against inverse temperature for two layers of different doping levels. C-V depth profiling has indicated that uniform free carrier profiles are readily obtainable. No evidence for a strong accumulation or depletion region at the n/n^+ or n/n^- interfaces has been obtained. Figure 24 is part of a C-V profile illustrating the variation of free carrier concentration across an n/n^+ epilayer-substrate interface.

4.3.2 Effects of Growth Parameters

(1) Deposition temperature. The substrate temperature has not been found to be a critical experimental parameter. Layers have been deposited at growth temperatures of 400°C, 450°C, 530°C, 580°C and 650°C. The layers deposited at 400°C were high resistivity ($\rho > 10^4 \Omega\text{cm}$) though showed no sign of any degradation in surface morphology. Those deposited at 650°C had Ga inclusions, exhibited three dimensional growth features and were highly n-type ($n \sim 10^{19} \text{cm}^{-3}$). Between these extremes the growth temperature appeared to have no effect upon the majority carrier transport properties for layers with $n \sim 10^{17} \text{cm}^{-3}$.

(2) Growth rate. The growth rate has not been observed to be an important experimental parameter within the range 0.4 - 1.8 $\mu\text{m hr}^{-1}$. The one layer deposited at a growth rate of 4.0 $\mu\text{m hr}^{-1}$ was found to have inferior electrical properties compared to the rest.

(3) As₄:Ga flux ratio. The As₄:Ga flux ratio is an interesting parameter since it affords a means of examining the Si incorporation mechanism (in a similar manner to the work of Chapter 3 on the Mn incorporation). The initial investigation consisted of depositing a GaAs:Si layer and varying the As₄:Ga flux ratio during the growth whilst keeping the Ga and Si fluxes constant. The free carrier concentration through the epilayer was then profiled using the double probe Hg-Schottky barrier C-V technique. The results of this experiment are shown in Figure 25 along with the form of the variation in As₄:Ga flux ratio used. There is clearly some correlation between the two. However, such a profile cannot be unambiguously interpreted and in order to obtain a more detailed understanding of the effect of the

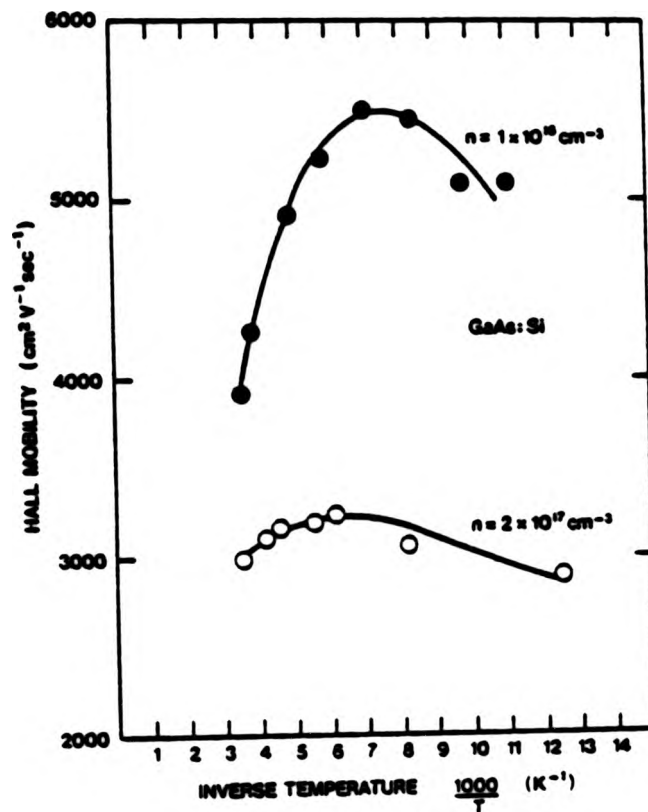


Figure 23 Hall mobility-inverse temperature plot for two epilayers of different doping levels

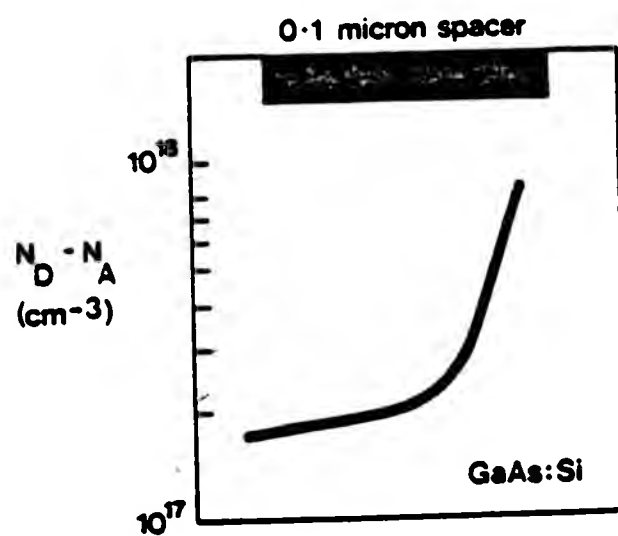


Figure 24 C-V derived variation of the free carrier concentration across an n/n^+ interface

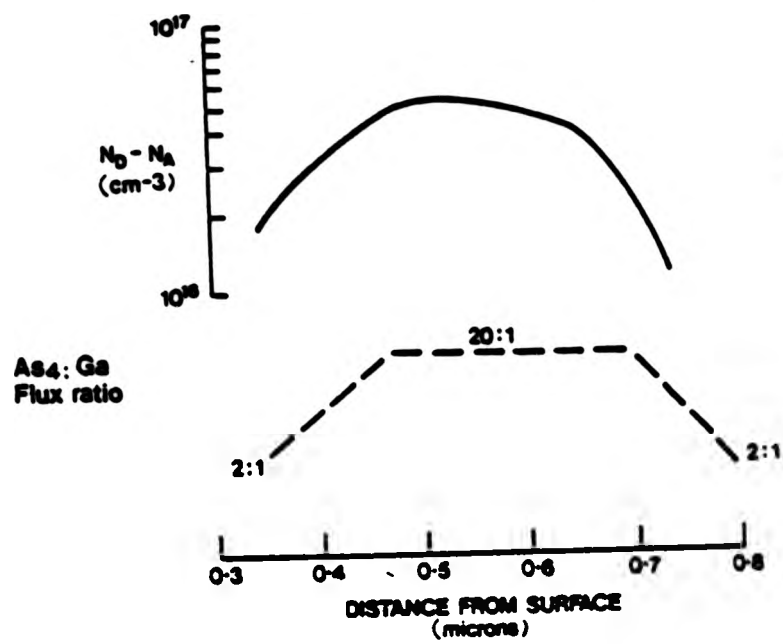


Figure 25 Variation of free carrier concentration through an epilayer deposited with a varying As₄:Ga flux ratio. The form of the variation in flux ratio used is also shown.

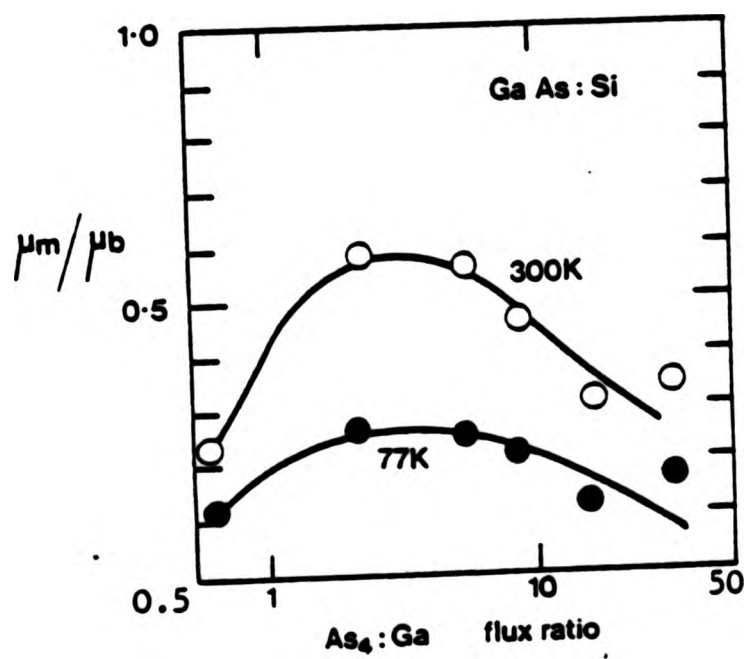


Figure 26 Effect of the As₄:Ga flux ratio used during deposition upon the μ_m/μ_b parameters

As₄:Ga flux ratio a number of separate layers were deposited so that both the free carrier concentration and Hall mobility could be determined. Several layers were deposited under nominally identical conditions except for variations in the As₄:Ga flux ratio. These layers either had free carrier concentrations in the range $2.5 - 4.5 \times 10^{16} \text{ cm}^{-3}$ or $1.5 - 3.5 \times 10^{17} \text{ cm}^{-3}$. It was not possible to establish individual changes in N_A and N_D since theoretical results based on 77K Hall mobility data are not available for layers of such high impurity content where the Brooks-Herring theory fails. Consequently the results are presented in an illustrative manner. The ratio μ_m/μ_b (at 300 and 77K) has been examined for various As₄:Ga flux ratios, where μ_m is the measured Hall mobility and μ_b is the bulk mobility i.e. the mobility expected for uncompensated material with that carrier concentration at that same temperature. Clearly μ_m/μ_b gives a qualitative measure of the compensation and can be used to illustrate changes in the amount of compensation within a group of epilayers. Figure 26 shows the variation in μ_m/μ_b for the higher doped group of epilayers ($n \sim 2 \times 10^{17} \text{ cm}^{-3}$) as the As₄:Ga flux ratio used during each deposition was changed. Estimates from Rode's 300K data would imply that the layers of Figure 26 cover the range of compensation given by $8 \geq N_D + N_A/n \geq 3$. An identical type of investigation was carried out on the layers having $n \sim 3 \times 10^{16} \text{ cm}^{-3}$ and a similar behaviour was observed, quantitative differences existed due to the more compensated nature of the lower doped layers (Section 4.4) owing to the influence of the background impurities.

(4) Buffer layer. It was suggested (C.T. Foxon, private communication 1978) that the out-diffusion of impurities or arsenic-vacancies from the substrate may be the origin of, or associated with, compensating centres. If this were the case then the use of a buffer layer might lessen any effects. However the GaAs:Si material deposited either upon high resistivity (i.e. low growth temperature) or undoped GaAs 1 μm buffer layers did not show any improvements in electrical properties when compared to epilayers deposited directly on the GaAs:Cr substrates.

4.3.3 System Considerations

Additional experiments were performed to assess whether the oil diffusion/rotary pump combination was a source of contamination. Care was always taken during the initial evacuation from atmospheric pressure using the rotary pump and a vacuum of only $1 \times 10^{-1} - 7.5 \times 10^{-2}$ Torr

obtained prior to firing the diffusion pump. Even this procedure does represent a possible source of contamination through rotary pump oil entering the MBE chamber. However the use of an oil-free sorption pump to initially evacuate the system to 10^{-2} Torr did not lead to an improvement in the GaAs:Si material. Although the system was baked into a full liquid nitrogen trap, no evidence was obtained for a deterioration in the electrical properties on the few occasions this was not done. The use of a dummy-run was also employed i.e. the substrate was loaded and normal growth procedures were executed with the exception that a shutter was kept in front of the substrate. Then UHV was re-attained and a normal growth run initiated. In effect this constituted the simulation of an air lock system. This procedure did not lead to any improvement in the GaAs:Si material.

4.3.4 Effect of a long outgas of the graphite effusion cell containing the Si charge

A 4 hour outgas of the Si cell at 1300°C ($\sim 400^{\circ}\text{C}$ above the operating temperature) did lead to a consistent improvement in the material as can be seen in figures 27 and 28. These figures are free carrier concentration-Hall mobility plots of the initial data plus the extra data (larger plotting points) corresponding to the layers deposited using this long pre-growth outgas. These newer layers exhibited a much lower level of compensation for $n > 1 \times 10^{17} \text{ cm}^{-3}$ ($N_A + N_D/n = 2$) and far more consistent results were obtained. Attempts to further improve the quality of the material by heating the dopant cell to 1500°C were not successful as the cell was destroyed through cracking.

4.3.5 The use of a BN cell for Si dopant evaporation

Figures 29 and 30 are free carrier concentration-Hall mobility plots obtained using a BN cell for the dopant evaporation. As above, this new data is presented alongside the initial data. This material obtained using the BN cell also had a compensation ratio of 2 i.e. as good as, though not better than, the layers produced using the graphite cell and the long outgas. No improvement in the material could be obtained by the use of a long, high temperature, outgas of the BN cell containing the Si charge.

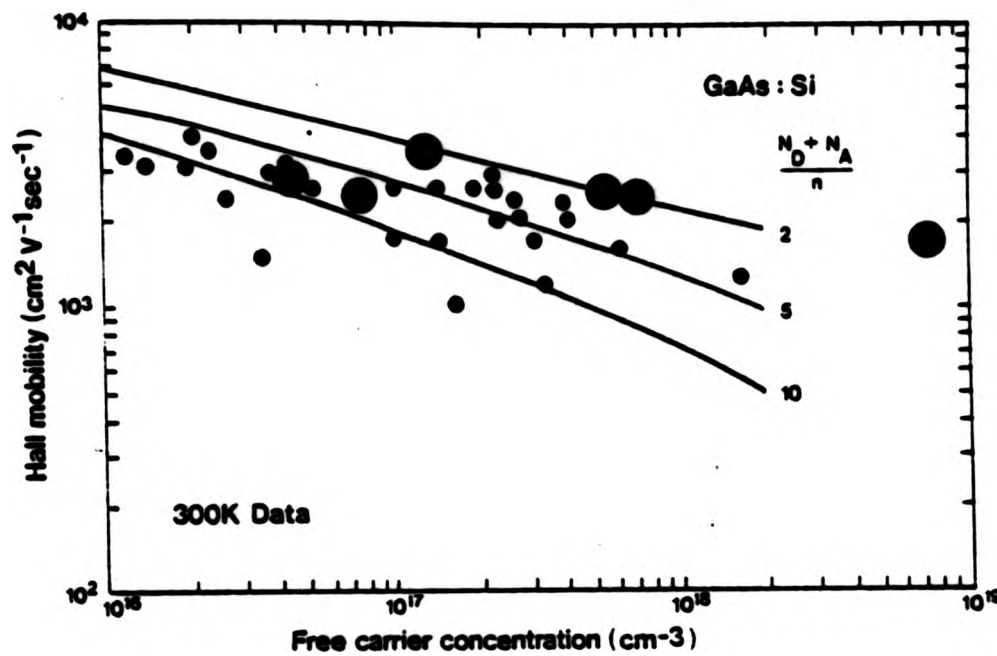


Figure 27

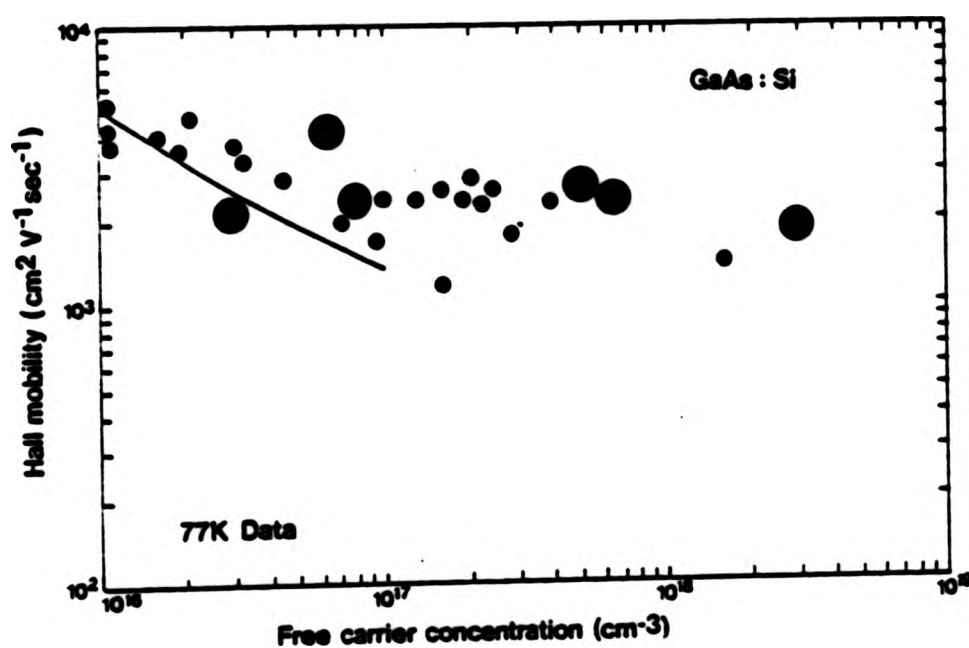


Figure 28

Free carrier concentration-Hall mobility plots at 300K and 77K for the layers deposited with a high temperature pregrowth outgas of the graphite cell containing the silicon dopant. This data (larger plotting points) is shown along with the initial data (figures 21 and 22).

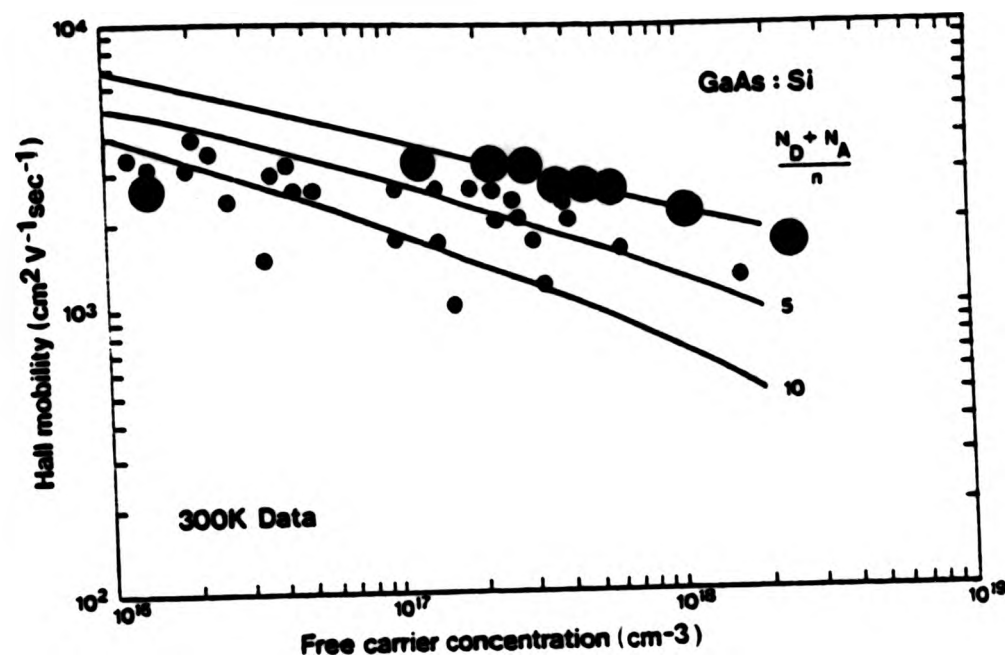


Figure 29

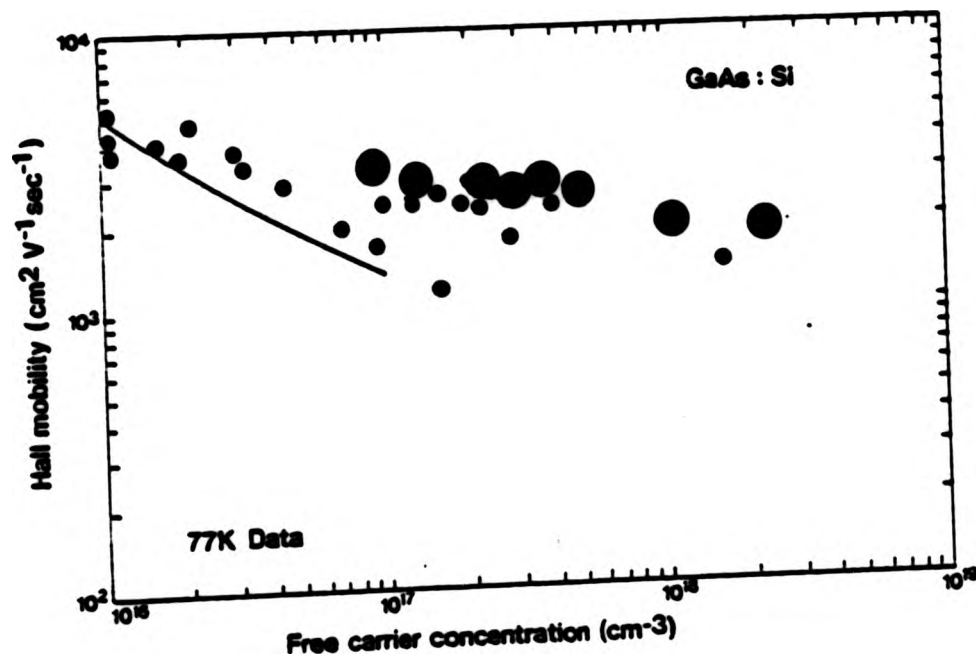


Figure 30

Free carrier concentration-Hall mobility plots at 300K and 77K for the layers deposited using a BN cell for the silicon evaporation. This data (larger plotting points) is shown along with the initial data (figures 21 and 22).

4.3.6 Effects of various gaseous ambients

The effect of various gases in the UHV ambient has been examined to assess whether certain major species in the residual gas were limiting the electrical properties of the GaAs:Si material. Depositions took place with 5×10^{-7} Torr of H_2 , H_2O , CO_2 and CO and 1×10^{-8} Torr of O_2 deliberately introduced into the system. These pressures represent an increase in concentration of the particular gas by approximately a factor of ten. In all cases the epilayers were deliberately doped with Si to give $n \sim 3 \times 10^{17} \text{ cm}^{-3}$. No effects attributable to the introduction of the gases could be discerned from an examination of the electrical properties or surface morphologies of the epilayers. Furthermore, no difference in the electrical properties or surface morphologies of the epilayers has been observed for layers deposited under normal UHV conditions with, or without, the ion gauge on during deposition. All these experiments were undertaken whilst using the BN cell for the Si evaporation.

4.4 Discussion

All the GaAs:Si material produced during this project was compensated with $N_A + N_D/n \geq 2$. The contention that the reduced mobilities were due to compensation effects is supported by the Hall mobility-inverse temperature curves of figure 23, the form of which is typical of a phonon-ionized impurity scattering limited mobility. For a given carrier concentration the 77K mobilities are well below that expected and indicate the presence of extra ionized impurity scattering associated with compensating centres. This is further supported by the direct observation in PL spectra of extra acceptor levels in this and other MBE GaAs:Si (G.B. Scott, private communication 1979). However, the physical incorporation mechanism of the Si impurity seems not to be complicated by any surface phenomenon as is the case with Sn (Wood and Joyce 1978).

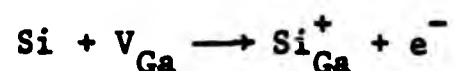
With reference to figures 21 and 22 (the initial layers produced using the graphite cells) the observed compensation is due to at least two different sources. One of these is the system impurity background level which is in the range $10^{16} - 10^{17} \text{ cm}^{-3}$ and consequently dominates the electrical properties of the layers which are deliberately doped with Si in this range. However the degradation in the electrical properties, when compared to bulk material, throughout the entire

doping range covered is not consistent with the notion that the observed compensation is solely due to the system impurities. If this were the case then the material with $n > 10^{17} \text{ cm}^{-3}$ would be much more bulk-like. It is therefore necessary to postulate the existence of another source of the compensation. The results of 4.3.4 and 4.3.5 point to the evaporation cells as being the source of at least some of the problem. However, it was initially considered that the compensation may be due solely to the dopant occupying both donor and acceptor sites. Consequently the initial investigations centred on examining the effect of the growth parameters to see if conditions more favourable for the production of n-type material could be obtained. LPE GaAs:Si can be n- or p-type depending on the growth conditions (Kressel 1974), this has been interpreted by postulating that the Si occupies either Ga sites (as a donor) or As sites (as an acceptor). A similar situation exists for MBE GaAs:Ge (Cho and Hayashi 1971a, Wood et al. 1979) where p-type material is produced under Ga-rich conditions and n-type material under As-rich conditions. In spite of any analogy with Ge which may tend us to expect p-type material to be obtainable, there are thermodynamic arguments which indicate that p-type GaAs:Si cannot be produced under typical MBE growth conditions (R. Heckingbottom, private communication 1979). However, figures 25 and 26 suggest that the As_4 :Ga flux ratio (unlike the other growth parameters) does influence the incorporation of the Si as an electrically active impurity and consequently the level of compensation. It should be noted that since only compensated material has been obtained these results may appertain to the incorporation of Si in association with some other impurity.

Figure 25 shows that the free carrier concentration of the epilayers is roughly proportional to the As_4 :Ga flux ratio used during the deposition. The origin of the extra carriers cannot be inferred from this figure, though we can note that it must be associated with the silicon doping since the effect would otherwise be equally evident in the undoped layers and it is not. It is interesting to note that the free carrier concentration seems to be very closely linked to the variation in As_4 flux with no indication of saturation in the range studied. GaAs:Si produced by the alkyl technique (Bass 1979) showed exactly the opposite behaviour, the measured carrier concentration being reduced by an increase in the AsH_3 mole fraction. This effect was considered to be due to the arsenic blocking the silicon from the growing surface and the Si incorporation being controlled by kinetics and not thermodynamic factors. Figure 26 implies that the level of compensation decreases

as the $\text{As}_4:\text{Ga}$ flux ratio is increased up to a maximum plateau region. This plateau region was for $\text{As}_4:\text{Ga}$ flux ratios of 2-6 and gave material with $N_A + N_D/n \sim 3$. Any further increase in the $\text{As}_4:\text{Ga}$ flux ratio increased the level of compensation. This behaviour is not consistent with a simple model based on the variation of Si site occupancy, as the level of compensation is the same for widely different $\text{As}_4:\text{Ga}$ flux ratios (0.5:1 and 30:1). If one were to attempt to explain these results merely in terms of the Si incorporation and defects then an explanation based on two competing processes may be invoked. For example, it is possible that the Si does behave in a similar manner to Ge in MBE GaAs except that the donor site is always more populated than the acceptor. As the $\text{As}_4:\text{Ga}$ flux ratio is increased from Ga-rich conditions the donor site is increasingly preferred over the acceptor and eventually uncompensated material obtained. A further increase in the $\text{As}_4:\text{Ga}$ flux ratio results in a degradation of the electrical properties due to an increase in compensation effects associated with As-induced defects. These may be of the form of antisite defects or pairs (Van Vechten 1975) as considered in Chapter 2 when discussing InAs, or possibly As induced defect-Si impurity complexes. For example $(\text{Si}_{\text{Ga}} + \text{V}_{\text{Ga}})$ complexes form deep acceptor levels in LPE GaAs:Si (Spitzer and Allred 1968) and certain dislocations are known to have acceptor like behaviour (Read 1954, Schröter 1979). These defects (or whatever) must not only give rise to the observed compensation effects but also the observed variation in free carrier concentration (figure 25). No published results are available from any of the research groups which have obtained near uncompensated material on the effects of the $\text{As}_4:\text{Ga}$ flux ratio on Si incorporation. However, it is interesting to note that the Japanese group used a flux ratio of ~ 6 which is in the plateau region of least compensated material obtained here. If we consider that some impurity is limiting the quality of the material of figures 21 and 22 then we have a third factor to consider. If this impurity is also subject to an incorporation mechanism which is dependant upon the $\text{As}_4:\text{Ga}$ flux ratio then the situation becomes too complex to analyse with any degree of certainty. It should be noted, however, that the dopant incorporation behaviour implied in figures 25 and 26 cannot be analysed only in terms of any known acceptor incorporation mechanism coupled with a constant Si donor activity. Furthermore, the concentrations of C and Mn acceptors (as discussed in Chapter 3) are insufficient to explain the observed levels of compensation throughout the entire doping range $10^{16} - 7 \times 10^{18} \text{ cm}^{-3}$.

If we, tentatively, assume that the compensating impurity has a level of activity independent of the As_4 flux then we can postulate a modified model to account for the observed impurity/dopant incorporation behaviour: As the $As_4:Ga$ flux ratio is increased from 0.5:1 to 2:1 the Si atoms increasingly occupy V_{Ga} sites and act as n-type dopants, viz.



as this occurs $N_A + N_D/n \rightarrow 1$ but is limited by the compensating impurity to $N_A + N_D/n \sim 3$. This situation is arrived at when the $As_4:Ga$ flux ratio is ~ 2 . Increasing the $As_4:Ga$ flux ratio above $\sim 6:1$ results in the electrical properties of the layers being degraded due to some As-induced defect/Si-impurity complex. The plateau region of best material which occurs for $As_4:Ga$ flux ratios of 2:1 - 6:1 is due to this being the region where these compensating impurities limit the electrical properties of the material. The origin of the compensating impurities has been at least partially identified as the Si cell (4.3.4, 4.3.5) and as such explains how the concentration of these impurities increases as the doping level increases. The investigations into the possible contamination associated with the pumping system were rather inconclusive, being one-off experiments. Any oil contamination present in the system may be expected to linger for several runs prior to eradication. However, it is known that bulk-like GaAs:Sn can be produced in an oil diffusion/rotary pump system using graphite effusion cells (Wood and Joyce 1978). The results in figures 27, 28 and 29, 30 show that less compensated material ($N_A + N_D/n = 2$) can be obtained by either: (i) the use of a 4 hr $1300^{\circ}C$ outgas of the graphite cell containing the Si dopant or (ii) the use of a BN cell for the Si evaporation. The fact that this better material can be obtained from the use of a BN cell with less effort (no high temperature long outgas needed) indicates that the graphite cells themselves are a source of contamination. It has been found that CO evolves from graphite cells at much higher rates than for BN cells (H. Kunzel, private communication 1979). However, it appears that if adequately outgassed the graphite effusion cells are as good as the BN cells. Yet once again a qualifying remark concerning the inability to produce uncompensated material must be made. Perhaps for better quality material some advantages of BN over graphite (or vice versa) would become evident.

Even the material with $N_D + N_A/n = 2$ is not quite "state of the art" material. The best MBE GaAs:Si has a compensation ratio of 1.5 - 1.4

(Ploog 1979a, Shimano et al. 1979). This represents quite a small difference in the measured electrical properties and consequently any inaccuracies associated with the measuring techniques are important. A shortcoming of the present study is that no Sn doped material was grown, as it is generally acknowledged that MBE GaAs:Sn of bulk-like quality can be obtained for a doping level of $\sim 10^{17} \text{ cm}^{-3}$. Sn doping would thus have been a good test of both the MBE system and the measuring techniques. It should be noted that a compensation ratio of 1.5 implies that $N_D:N_A = 5:1$ (i.e. 16.7% acceptors) compared to 25% acceptors ($N_D:N_A = 3:1$) for a compensation ratio of 2. For example, the best material produced in this study with $n = 1 \times 10^{17} \text{ cm}^{-3}$ had $N_A = 5 \times 10^{16} \text{ cm}^{-3}$, $n = 5 \times 10^{17} \text{ cm}^{-3}$ had $N_A = 2.5 \times 10^{17} \text{ cm}^{-3}$ and $n = 1 \times 10^{18} \text{ cm}^{-3}$ had $N_A = 5 \times 10^{17} \text{ cm}^{-3}$. Clearly the material is not limited by some constant background acceptor impurity concentration, nor is it likely that the concentration of C and/or Mn impurities would vary so precisely with the doping level as to keep the level of compensation constant. Indeed it is rather remarkable that such a close level of compensation can be maintained over such a wide variation in carrier concentration. However, in view of the published results of other researchers it is not valid to ascribe the effect to some fundamental limitation of the use of Si as a dopant. A constant level of compensation for layers with $n = 1 \times 10^{17} - 1 \times 10^{18} \text{ cm}^{-3}$ for a variety of growth rates and two different types of evaporation cell suggests that the compensating acceptors are closely linked with the Si dopant flux. An alternative explanation is that there is some impurity flux associated with the cell assembly which increases with the dopant cell temperature, the net effect being to keep the level of compensation constant. It is also possible that the Si dopant is dragging some impurity with it from the evaporation cell. Oxygen is known to give rise to compensation effects in VPE and LPE GaAs:Si (Bass 1979, Palm et al. 1979, Mil'vidiskii and Solv'eva 1979) through an O-Si impurity. The concentration and level of electrical activity of any impurity, relative to the Si dopant, must be such as to give the observed level of compensation ($N_D:N_A = 3:1$). Spark source mass spectrometry detected only carbon and oxygen as impurities in sufficient concentrations in these epilayers to influence the electrical properties. The bulk concentrations of these impurities could only be estimated as ≤ 30 ppma owing to their large surface concentrations due to handling and storage (J.A. Roberts and D. Hilton, private communication 1980). It is intended that secondary ion mass spectrometry will be shortly used in an attempt to identify the

impurities in these epilayers and particularly those which increase in concentration with the Si doping level or are closely associated with the Si dopant. The exposure of the MBE chamber to the laboratory environment during substrate loading and the actual UHV ambient both represent possible sources of gaseous contamination of the Si charge. However, the deliberate introduction of the major carbon and oxygen containing gaseous species into the MBE chamber was observed to have no effect nor was a prolonged outgas of the Si cell found to produce material with a compensation level less than two. The natural oxide on Si (air exposed) is known to be SiO_2 with a thickness $\sim 30 \text{ \AA}$ (Zehner et al. 1980) and amorphous material such as that used in this work can contain voids which allow gases to penetrate to depths greater than 1000 \AA (Bean and Poate 1980). Natural oxidation could therefore represent a considerable source of impurity on the surface and possibly in the bulk of the Si charge which may require many hours outgassing to eliminate (the vapour pressure of SiO_2 being similar to that of Si). Consequently this would in practice represent a constant impurity source. Both Ploog and Shimano et al. use air-locked systems.

Despite the failure of the gaseous experiments to produce a degradation in the electrical properties of the epilayers (i.e. an increase in the concentration of acceptor centres) this does not eliminate the residual UHV ambient as the possible source of the compensation. Indeed it can be argued that the compensation arises from an interaction between some species in the residual gas and the surface of the hot Si charge to produce an impurity compound which is then incorporated into the epilayer through evaporation. The experiments using various gases may have failed to further increase the concentration of this impurity if: (i) the correct gas (or gaseous mixture) was not used or (ii) some form of saturation in the production of the impurity had already occurred through residual gaseous interactions.

To achieve the doping range $10^{17} - 10^{18} \text{ cm}^{-3}$ Si dopant fluxes at the substrate of $\sim 3 \times 10^9 - 3 \times 10^{10} \text{ atoms cm}^{-2} \text{ sec}^{-1}$ are required for a growth rate of 1 \mu m hr^{-1} this corresponds to an evaporation rate of $\sim 10^9 - 10^{10} \text{ atoms sec}^{-1}$ per cm^2 of source material area. This has to be compared with a total background impurity pressure (mainly CO, CO_2 and H_2O) during deposition of $10^{-8} - 10^{-9}$ Torr which corresponds to an impurity arrival rate throughout the system of $10^{12} - 10^{11} \text{ molecules cm}^{-2} \text{ sec}^{-1}$. These figures show that the Si flux per cm^2 of source material leaving the Knudsen cell is smaller than the impurity flux

impinging from the residual gas. As a consequence it is possible that a monolayer equilibrium is established in the production of some impurity compound from a hot silicon-gas interaction. If some form of saturation is already attained for the concentration of impurity species in the UHV ambient then the deliberate addition of extra gas would have no effect until the partial pressures were sufficient to promote gaseous-Ga/As interactions at the epilayer surface. These effects would only become observable when the electrical effects were comparable to those of the dopant (i.e. $\sim 10^{17} \text{ cm}^{-3}$).

One way to test this hypothesis, which was not available, would be to improve the pumping and cryopanelling and hence the partial pressures of the residual gases in the MBE system. An alternative approach would be to increase the rate of effusion of the Si (and impurity) flux so as to exceed the rate of formation of the impurity from the residual gas. The simplest method being to increase the growth rate so that a corresponding increase in the Si flux is required to produce material with the same doping level. No improvement in doping properties was observed for growth rates in the range $0.4 - 1.8 \text{ } \mu\text{m hr}^{-1}$ and $4 \text{ } \mu\text{m hr}^{-1}$, when tried, seemed to be too fast and the deposited material was electrically inferior possibly due to the introduction of structural defects. Although extrapolation of the curves of Rode and Knight (1971) shows that the highest doped epilayer ($n = 7 \times 10^{18} \text{ cm}^{-3}$) had a compensation ratio of 2, this is probably an overestimate since their analysis did not include a correction for degeneracy (Ploog 1979a). It appears therefore that the best GaAs:Si produced in this study was that obtained using the maximum silicon dopant flux. This indicates that Si is a better dopant than Ge for use in n^+ buffer layers. ??
??

4.5 Conclusion

An investigation of the silicon doping of MBE (100) GaAs has shown that Si is a useful n-type dopant especially for highly doped layers. The GaAs:Si layers deposited during this project were compensated with $N_A + N_D/n \geq 2$. The Si dopant source cell has been shown to be a potential source of major contamination if not outgassed thoroughly. Adequate outgassing of a BN cell was easier than a graphite cell, though for both types of cell material a compensation ratio of two could be routinely obtained for the doping range $n = 1 \times 10^{17} - 7 \times 10^{18} \text{ cm}^{-3}$. It is considered that the residual compensating impurities arise from the Si dopant cell, possibly in the form of a Si-impurity

compound formed from an interaction between the Si and some gaseous species either in the UHV ambient or during air exposure.

The electrical properties of the epilayers are considered to be influenced by two, competing, phenomena related to the arsenic flux. The first influences the site occupancy, and hence the electrical behaviour of the Si dopant in the GaAs host crystal. This process tends to produce less compensated material as the As_4 :Ga flux ratio is increased. The second concerns the production of electrically active defects or defect impurity complexes through interactions involving excess As_4 on the growing surface. This process tends to degrade the electrical properties of the GaAs:Si material as the As_4 :Ga flux ratio is increased.

CHAPTER 5

Fabrication of Microwave Mixer Diodes5.1 Introduction

The fabrication and evaluation of electronic devices represents, perhaps, the ultimate test of any material produced by the MBE technique. During this project cooperation with the General Electric Company (Hirst Research Centre) enabled a collaborative program to be instigated on the deposition of thin GaAs epilayers for fabrication into Mott barrier diodes for use in mm wave beam lead mixer diodes. At the time of writing this thesis the device evaluation programme was still continuing although sufficient progress had been made to include this final chapter. Commercial secrecy has necessitated the omission of various details.

The Mott diode is an n/n^+ (epilayer-substrate) or an $n/n^+/n^+$ (epilayer-buffer layer-substrate) structure with an ohmic contact to the n^+ substrate and a rectifying (Schottky) contact to the epilayer. In a Mott barrier diode, as opposed to a Schottky barrier diode, the epitaxial layer is fully depleted at zero bias. The advantages of the Mott diode and its conduction processes are discussed elsewhere (McColl and Millea 1973, Sze 1969). For optimum device operation the n -epilayer (the active layer) should remain depleted throughout the operating cycle of the diode, i.e. the active GaAs layer must have a thickness less than the zero bias depletion width. For GaAs the zero bias depletion width for a carrier concentration of 10^{17} cm^{-3} is $0.09 \mu\text{m}$ increasing to $0.3 \mu\text{m}$ for 10^{16} cm^{-3} . The existence of an undepleted region introduces a series resistance and as a consequence device performance is less efficient. Furthermore, unless the n/n^+ transition is abrupt another source of series resistance can be introduced (McColl and Millea 1973). The MBE technique has several advantages in this area since it offers the means of producing large areas with good surface morphology and with controllable thicknesses $\sim 0.05 \mu\text{m}$ and abrupt n/n^+ interfaces. Promising results have previously been obtained for microwave and mm-wave mixer diodes prepared by MBE (Ballamy and Cho 1976, Schneider et al. 1977).

5.2 Experimental

MBE GaAs:Si layers were prepared as described in Chapter 4 and consequently all the material fabricated into devices was compensated n-type GaAs. The structures prepared were of two forms: (i) n/n⁺ epilayer-substrate and (ii) n/n⁺/n⁺ epilayer-buffer layer-substrate. The substrates were n⁺ Te doped (100) GaAs ($n \sim 2 \times 10^{18} \text{ cm}^{-3}$) of nominal thickness 0.5 mm, as supplied by MCP Ltd (Wembley). All the buffer layers were doped to $n \sim 2 \times 10^{18} \text{ cm}^{-3}$ and were 0.25 μm in thickness. The active layers had free carrier concentrations of either $1 \times 10^{17} \text{ cm}^{-3}$ or $2 \times 10^{16} \text{ cm}^{-3}$ with thicknesses of 0.1 μm or 0.05 μm . A selection of the above possible combinations was deposited. The epilayers were processed into devices under the supervision of Dr. M.J. Sisson at the Hirst Research Centre. The processing steps in the device production are outlined below:

- (1) The indium was removed from the back of the slice using an HCl etch and a lapping technique.
- (2) The substrate was lapped down to a thickness of 100 μm .
- (3) The back ohmic contact was evaporated onto the substrate.
- (4) Using the standard photolithography technique 5 μm - 10 μm diameter windows were opened in a pre-deposited SiO₂ mask covering the n-epilayer.
- (5) Mott barriers were formed on the GaAs by the evaporation of Ti/Au onto these windows and using overlay defining masks.

These devices were then either tested on the slice using probe methods or as discrete devices when packaged in ceramic microwave encapsulations using bonded Au contact wires.

5.3 Results

The initial measurements made include the reverse bias voltage (V_B), the forward bias (turn-on) voltage (V_F), the series resistance (R_S) and the capacitance of the structure (C_T). These measurements enable the identification of slices suitable for further processing and testing. Table 2 below shows the results from several diodes fabricated from a single n/n⁺/n⁺ structure with $n = 2 \times 10^{16} \text{ cm}^{-3}$ and $d = 0.1 \mu\text{m}$. The dot sizes were 6-7 μm in diameter.

Table 2 Characteristics of typical Mott barrier diodes

V_B (volts)		V_F (volts)		R_S (ohms)	C_T (pF)
1 μ A	10 μ A	1 μ A	1 mA		
4.4	4.8	0.62	0.68	2	0.183
4.2	4.8	0.64	0.70	2	0.185
3.2	4.2	0.66	0.72	2.5	0.151
3.4	4.6	0.68	0.72	2	0.146
4.6	5.4	0.64	0.72	2	0.129

Examination of the capacitance of several diodes showed that $1/C^2$ was virtually insensitive to applied voltage indicating that the active layers were fully depleted. Preliminary results from AEI Semiconductors (Lincoln) for several diodes operating at 9.375 GHz (i.e. X band) gave overall noise figures of 6-7 dB.

5.4 Discussion

It is too early to come to any firm conclusions except to note that MBE has enabled the production of device structures with a substantially reduced series resistance (2Ω compared to about 5Ω for standard devices). This reduction, which results from the relative thinness of the MBE layers, is considered to be a significant improvement and should lead to improved device performances. The quoted noise figures compare favourably with standard AEI production diodes especially since the impedance of the test circuit had not been optimized to match the impedance of these MBE diodes. Results from higher frequency operation are required before these diodes can be critically compared with other mixer diodes.

CONCLUDING REMARKS

The preceding chapters of this thesis have clearly shown that the MBE growth conditions contain important parameters which influence the optical and electrical properties of deposited (100) GaAs and InAs epilayers. The situation arises primarily due to the influence of the MBE growth conditions upon the incorporation of various impurities whether they be present unintentionally (i.e. system impurities) or present in the form of intentional dopants. The overall conclusion must be that the MBE system-material combination must be systematically and critically evaluated before the highest quality layers can be obtained. However, it should be noted, firstly, that the majority carrier transport properties are principally relevant to majority carrier devices (e.g. FETs) and the production of minority carrier devices may require different and perhaps more exacting growth conditions. For example, the production of the best quality MBE AlGaAs-GaAs DH lasers requires a growth temperature of 620-650°C (Tsang 1979, 1980, Tsang et al. 1980) this is a quite severe restriction on the growth conditions which would never have been arrived at from mere Hall measurements. Secondly, and perhaps more importantly, the MBE growth technique relies heavily on certain areas of high technology which are continually being improved. The production of the UHV environment and the preparation of pure, UHV compatible materials for the components of MBE systems are two vital areas of associated technology. As has been shown in this thesis the properties of MBE III-V compounds can be critically linked with the construction of the parent MBE system. Consequently the experimental results and the science which is extracted from the data, although valid, is in a sense also system dependant. Improvements in MBE systems through both technological advances and the results of explorative studies similar to those reported herein will undoubtedly lead to a better understanding of the production of MBE III-V compounds and thus the production of better quality MBE material.

FURTHER WORK

The work discussed in this thesis was itself a continuation of an earlier study on the growth of MBE (100) InAs (Meggitt 1979). Following the completion of this present project and some exploratory work (concerning $\text{In}_x\text{Ga}_{1-x}\text{As}$) the MBE system is being thoroughly updated, using the experience gained from this and earlier work, to be used for a detailed analysis of the preparation and properties of MBE (100) $\text{In}_x\text{Ga}_{1-x}\text{As}$. The ternary compound being of interest for both microwave (J.J. Harris, private communication 1980) and opto-electronic (Miller et al. 1978) applications and this project will be undertaken in close collaboration with PRL (Redhill). The new MBE system is to be fitted with another substrate heater, a complete BN source assembly, a high vacuum system isolation valve and sample load lock. The latter will ensure that the system can be maintained under UHV conditions continually. Using this arrangement the source cells and the substrate heater can be kept at an outgassing temperature all the time. It is considered that these developments will, in total, lead to an improvement in the quality of both doped and undoped material through a reduction in system impurities. However, the continued use of the oil diffusion pump does represent a potential source of contamination. The use of an ion-pump for several depositions would produce interesting data since it would enable a fair comparison between material prepared using the two different types of pump to be made.

It is intended that studies similar to those reported herein will be undertaken on the ternary compound. The electrical properties will be examined for systematic variations due to changes in alloy composition, growth rate, growth temperature and $\text{As}_4:\text{In} + \text{Ga}$ flux ratio. Furthermore it is expected that the heteroepitaxial $\text{In}_x\text{Ga}_{1-x}\text{As}/\text{GaAs}$ layers will exhibit variations in transport properties with depth and it would be interesting to compare these results with those obtained from the heteroepitaxial growth of $\text{In}_x\text{Ga}_{1-x}\text{As}/\text{InP}$ or indeed with that one case ($\text{In}_{.53}\text{Ga}_{.47}\text{As}$) where perfect lattice matching exists with InP. Such a study would require some initial work on the cleaning of InP substrates and possibly the growth of (100) InP buffer layers.

van der Meer

ACKNOWLEDGEMENTS

I would like to thank the Department of Physics, City of London Polytechnic, for the provision of a Research Assistantship and Dr. J. Goddard, Head of Department, for providing the facilities for this research. I am truly indebted to Drs. E.H.C. Parker (City of London Polytechnic) and J.J. Harris (Philips Research Laboratories) for their supervision and criticism throughout this work. Thanks are also due to Dr. R.M. King (CLP) for helpful discussions and G.J.C. Burton and A. Aldridge (CLP) for excellent technical assistance.

This work has only been possible through the considerable effort of the following people who I trust will accept this brief acknowledgement: R. Elam, P. Driscoll, W. Hugkulstone, E. Beck, G.A. Curtis, R.S. Blakemore, M.G. Dowsett, W.J.O. Boyle, R.A. Kubiak, S.R.L. McGlashan, B.T. Meggitt, and P. Cook (all of CLP), R.F.C. Farrow and G.R. Jones (RSRE, Malvern), W. Liley (The Polytechnic, Hatfield), G.B. Scott, J.S. Roberts, J.H. Neave, C.T. Foxon and B.A. Joyce (all of PRL, Redhill), I. Dorrity, M.J. Sisson and F.J. Hilsden (all of GEC Hirst Research Centre, Wembley) and D. Williams (Vacuum Generators Ltd, Hastings).

REFERENCES

- Arthur, J.R., 1968 J. Appl. Phys. 39, 4032
- Arthur, J.R. and LePore, J.J., 1969 J. Vac. Sci. Technol. 6, 545
- Ashen D.J., Dean, P., Hurle, D.T., Mullin J.B. and White A.M., 1975, J. Phys. Chem. Solids 36, 1041
- Balagurov, L.A., Borkovskaya, O.Y., Dmitruk, N.L., Maeva O.I. and Omel'yanovskii, E.M., 1976 Sov. Phys. Semicond. 10, 659
- Baliga B.J. and Ghandi, S.K., 1974 J. Electrochem. Soc. 121, 1646
- Ballamy W.C. and Cho, A.Y., 1976 IEEE Trans. Elect. Dev. ED23, 481
- Bass S.J., 1979 J. Crystal Growth 47, 613
- Bauer, E. 1969 in "Techniques of Metals Research" ed. R. Bunshan 3, 501
- Bean J.C. and Dingle R., 1979 Appl. Phys. Lett. 35, 925
- Bean J.C. and Poate J.M., 1980 Appl. Phys. Lett. 36, 59
- Benninghoven A., 1975 Surf. Sci. 53, 569
- Binet M., 1975 Electron. Lett. 11, 580
- Boyle, W.J.O., Parker E.H.C., Dowsett M.G. and King R.M., 1977 private communication, to be published
- Brozel M.R., Clegg J.B. and Newman R.C., 1978 J. Phys. D 11, 1331
- Calawa A.R., 1978 Appl. Phys. Lett. 33, 1020
- Carson K.R., Wierum F.A. and Rudee M.L., 1970 J. Vac. Sci. Technol. 7, 347
- Chang C., 1974 in "Characterization of Solid Surfaces" ed. P. Kane and G. Larrabee (Plenum Press, New York) p.509
- Chang C., Ludeke R., Chang L.L. and Esaki L., 1977 Appl. Phys. Lett. 31 759
- Chang L.L. and Esaki L., 1979 Prog. Crystal Growth Charact. 2, 3
- Chang L.L., Kawai N., Sai-Halasz G.A., Ludeke R. and Esaki L., 1979a Appl. Phys. Lett. 35, 939
- Chang L.L. and Ludeke R., 1975 in "Epitaxial Growth" Part A. Ed. J. Matthews (Academic Press, New York) p.37
- Chang L.L., Sai-Halasz G.A. Nawai N.J. and Esaki L., 1979b J. Vac. Sci Technol. 16, 1504
- Chang L.L., Segmüller A. and Esaki L., 1976 Appl. Phys. Lett. 28, 39
- Cheung D.T., Andrews A.M. and Gertner E.R., 1977 Appl. Phys. Lett. 30, 587

- Cho A.Y., 1969 Surf. Sci. 17, 494
- Cho A.Y., 1970a J. Appl. Phys. 41, 2780
- Cho A.Y., 1970b J. Appl. Phys. 41, 782
- Cho A.Y., 1971a J. Appl. Phys. 42, 2074
- Cho A.Y., 1971b J. Vac. Sci. Technol. 8, S31
- Cho A.Y., 1975 J. Appl. Phys. 46, 1733
- Cho A.Y., 1977 Jap. J. Appl. Phys. 16 Suppl. 16-1, 435
- Cho A.Y., 1978 Presented as 1st Int. Sym. on MBE, Paris, unpublished
- Cho A.Y., 1979 J. Vac. Sci. Technol. 16, 275
- Cho A.Y. and Arthur J.R., 1975 Prog. Solid Stat Chem. 10, 157
- Cho A.Y., Casey Jr H.C. and Foy P.W., 1977 Appl. Phys. Lett. 30, 397
- Cho A.Y. and Chen Y.S., 1970 Solid State Commun 8, 377
- Cho A.Y. and Hayashi I., 1971a J. Appl. Phys. 42, 4422
- Cho A.Y. and Hayashi I., 1971b Solid State Electron. 14, 125
- Cho A.Y. and Hayashi I., 1971c Metall. Trans. 2, 777
- Cho A.Y. and Panish M.B., 1972 J. Appl. Phys. 43, 5118
- Cho A.Y., Panish M.B. and Hayashi I., 1971 Proc. Sym. GaAs and Rel. Compounds 1970, Inst. of Phys. p.18
- Cho A.Y. and Reinhardt F.K., 1974 J. Appl. Phys. 45, 1812
- Cho A.Y. and Stokowski S.E., 1971 Solid State Commun. 9, 565
- Chopra K.L., 1969 in "Thin Film Phenomena" (McGraw Hill, New York)
- Chu W.K., Mayer J.W., Nicolet M.A., Buck T.M., Amsel G. and Eisen F., 1973 Thin Solid Films 17, 1
- Collins D., 1979 Appl. Phys. Lett. 35, 67
- Covington D.W. and Hicklin W.H., 1978 Electron. Lett. 14, 752
- Covington D.W. and Meeks E.L., 1979 J. Vac. Sci. Technol. 16, 847
- Cronin G.R., Conrad R.W. and Borello S.R., 1966 J. Electrochem. Soc. 113, 1336
- Dashevskii M.Y. Ivleva V.S., Krol L.Y., Kurilenko I.N., Litvak-Gorskaya L.B., Mitrofanova R.S. and Fridlyand E.Y., 1971 Sov. Phys. Semicond. 5, 757
- Davey J.E. and Pankey T., 1968 J. Appl. Phys. 39, 1941
- Dawson D.L., 1972 Prog. Solid State Chem. 7, 117

- Decker G.E., 1977 J. Vac. Sci. Technol. 14, 640
- Delhomme B.J., Blanchet R.C. and Urgell J.J., 1978 Presented at 1st Int. Sym. on MBE, Paris, and private communication
- Dingle R., 1977 J. Vac. Sci. Technol. 14, 1006
- Dingle R., Störmer H.L., Gossard A.C. and Wiegmann W., 1978 Appl. Phys. Lett. 33, 665
- Esaki L. and Tsu R., 1970 IBM J. Res. Develop. 14, 61
- Farnsworth H.E., Schlier R.E., George T.H. and Burger R.M., 1958 J. Appl. Phys. 29, 1150
- Farrow R.F.C., 1977 J. Phys. D. 10, L135
- Farrow R.F.C., 1977a in "Crystal Growth and Materials" Ed. E. Kaldis and H. Scheel (N. Holland, Amsterdam) Vol.1, p.237
- Foxon C.T., 1973 Acta. Electron. 16, 323
- Foxon C.T., 1978 Acta. Electron. 21, 139
- Foxon C.T., Boudry M.R. and Joyce B.A., 1974 Surf. Sci. 44, 69
- Foxon C.T., Harvey J.A. and Joyce B.A., 1973 J. Phys. Chem. Solids. 34, 1693
- Foxon C.T. and Joyce B.A., 1975 Surf. Sci. 50, 434
- Foxon C.T. and Joyce B.A., 1977 Surf. Sci. 64, 293
- Foxon C.T. and Joyce B.A., 1978 J. Crystal Growth 44, 75
- Foxon C.T. and Joyce B.A., 1980 to be published, presented at Anglo-French MBE Conf., Nov. 1979, Paris.
- Fuller C.S. and Allison H.W., 1962 J. Electrochem. Soc. 109, 880
- Grange J.D. and Parker E.H.C., 1979 Phys. Bull. 30, 20
- Günther K.G., 1958 Z. Naturforsch 13a, 1081
- Heckingbottom R., Todd C.J. and Davies G.J., 1979 J. Electrochem. Soc. 126, 1210
- Heckingbottom R., Todd C.J. and Davies G.J., 1980 J. Electrochem. Soc. 127, 444
- Hirose M., Fischer A. and Ploog K., 1978 Phys. Stat. Sol (a) 45, K175
- Holloway H. and Walpole J.N., 1979 Prog. Crystal Growth Charact. 2, 49
- Holloway S. and Beeby J.L., 1978 J. Phys. C. 11, L247
- Honig R.E. and Kramer D.A., 1969 RCA Rev. 30, 285
- Iida S. and Ito K., 1971 J. Electrochem. Soc. 118, 768
- Ilegems M. 1977 J. Appl. Phys. 48, 1278

- Ilegems M. and Dingle R., 1975 Gallium Arsenide and Related Compounds, 1974. Inst. Phys. Conf. Ser. 24, 1
- Ilegems M. Dingle R. and Rupp Jr. L.W., 1975 J. Appl. Phys. 46, 3059
- Jensen E.W., 1973 Solid State Technol. Aug. p.49
- Jona F. 1965 IBM J. Res. Devel. 9, 375
- Joyce B.A., 1979 Surf. Sci. 86, 92
- Joyce B.A. and Foxon C.T., 1975 J. Crystal Growth 31, 122
- Joyce B.A. and Foxon C.T., 1977a Inst. Phys. Conf. Ser. 32, 17
- Joyce B.A. and Foxon C.T., 1977b Jap. J. Appl. Phys. 16 Suppl. 16-1, 17
- Kressel H., 1974 J. Electron. Mater. 3, 747
- Kroemer H., Chien W.Y., Casey Jr. H.C. and Cho A.Y., 1978 Appl Phys. Lett. 33, 749
- Kroger F.A., 1974 in "The Chemistry of Imperfect Crystals" (N. Holland, Amsterdam)
- Kunig H.E., 1970 J. Vac. Sci. Technol. 7, 100
- Lang D.V., 1974 J. Appl. Phys. 45, 3023
- Lang D.V., Cho A.Y., Gossard A.C., Ilegems M. and Wiegmann W., 1976 J. Appl. Phys. 47, 2558
- Laurence G., Simondet F. and Saget P., 1979 Appl. Phys. 19, 63
- Lee T.P., Holden W.S. and Cho A.Y., 1978 Appl. Phys. Lett. 32, 415
- Lum W.Y., Wieder H.H., Koschel W.H., Bishop S.G. and McCombe B.D., 1977 Appl. Phys. Lett. 30, 1
- Luscher P.E., 1977 Solid State Technol. 20, 43
- Many A., Goldstein Y. and Grover W.B., 1971 in "Semiconductor Surfaces" (N. Holland, Amsterdam) p.154
- Masud N. and Pendry J.B., 1976 J. Phys. C. 9, 814
- McColl M. and Millea M.F., 1973 Proc. IEEE 51, 499
- McFee J.H., Miller B.I. and Bachmann K.J., 1977 J. Electrochem. Soc. 124, 259
- McGlashan S.R.L., King R.M. and Parker E.H.C., 1979 J. Vac. Sci. Technol. 16, 1174
- Meggitt, B.T., 1979 PhD thesis, CNA
- Meggitt B.T., Parker E.H.C. and King R.M., 1978 Appl. Phys. Lett. 33, 528
- Meggitt B.T., Parker E.H.C., King R.M. and Grange J.D., 1980 J. Crystal Growth, to be published

- Menadue J.P., 1972 Acta. Cryst. A28, 1
- Miller B.I., McFee J.H., Martin R.J. and Tien P.K., 1978 Appl. Phys. Lett. 33, 44
- Mil'vidskii M.G. and Solv'eva E.V., 1979 Sov. Phys. Semicond. 13, 325
- Mizuno O., Watanabe H. and Shinoda D., 1975 Jap. J. Appl. Phys. 14, 184
- Moazed K.L., 1966 in "The Use of Thin Films in Physical Investigations" Ed. J. Anderson (Academic Press, London) p.203
- Morkoc H. and Cho A.Y., 1979 J. Appl. Phys. 50, 6413
- Murotani T., Shimano T. and Mitsui S., 1978 J. Crystal Growth 45, 302
- Neave J.H., Blood P. and Joyce B.A., 1980 Appl. Phys. Lett. 36, 311
- Neave J.H. and Joyce B.A., 1978a J. Crystal Growth 43, 204
- Neave J.H. and Joyce B.A., 1978b J. Crystal Growth 44, 387
- Nogai H. and Noguchi Y., 1978 Appl. Phys. Lett. 32, 234
- Nagata S. and Tanaka T., 1977 J. Appl. Phys. 48, 940
- Olsen G.H., 1975 J. Crystal Growth 31, 223
- Otsubo M., Oda T., Mitsui S. and Miki H., 1977 J. Electrochem. Soc. 124, 1907
- Palm L., Bruch H., Bachem K.H. and Balk P., 1979 J. Electron. Mater. 8, 555
- Parker E.H.C. and Williams D., 1976 Thin Solid Films 35, 373
- van der Pauw L.J., 1958 Philips Res. Rep. 13, 1
- Petritz R.L., 1958 Phys. Rev. 110, 1254
- Phillips J.C., 1973 Surf. Sci. 40, 459
- Ploog K., 1979a in "Crystals - Growth, Properties and Applications" Ed. L. Boschke (Springer-Verlag, Heidelberg).
- Ploog K., 1979b J. Vac. Sci. Technol. 16, 838
- Ploog K. and Fischer A., 1977 Appl. Phys. 13, 111
- Ploog K. and Fischer A., 1978 J. Vac. Sci. Technol. 15, 255
- Prutton M. 1975 in "Surface Physics" (Clarendon Press, Oxford)
- Ramsey N.F., 1956 in "Molecular Beams" (Clarendon Press, Oxford)
- Read W.T., 1954 Phil. Mag. 45, 775
- Redhead P.A., Hobson J.P. and Kornelson E.V., 1968 in "The Physical Basis of Ultrahigh Vacuum" (Chapman and Hall)
- Rode D.L., 1971 Phys. Rev. B3, 3287

- Rode D.L., 1975 in "Semiconductors and Semimetals" Eds. R.K. Willardson and A.C. Beer Vol.10 Ch.1.
- Rode D.L. and Knight S., 1971 Phys. Rev. B3, 2534
- Schneider M.V. Linke R.A. and Cho A.Y., 1977 Appl. Phys. Lett. 31, 219
- Schröter W., 1979 Inst. Phys. Conf. Ser. 46, 114
- Schwartz B., 1975 CRC Crit. Rev. Solid State Sciences, Nov. p.609
- Scott G.B. and Roberts J.S., 1979 Inst. Phys. Conf. Ser. 45, 181
- Shen L.Y.L., 1978 J. Vac. Sci. Technol. 15, 10
- Shimano T., Murotani T., Nakatani M., Otsubo M. and Mitsui S., 1979 Surf. Sci. 86, 126
- Shiota I., Motoya K., Ohmi T., Miyamoto N. and Nishizawa J., 1977 J. Electrochem. Soc. 124, 155
- Sites J.R. and Weider H.H., 1975 CRC Crit. Rev. Solid State Sciences 5, 385
- Sloope B.W. and Tiller C.O., 1965 J. Appl. Phys. 36, 3174
- Sloope B.W. and Tiller C.O., 1966 J. Appl. Phys. 37, 887
- Sloope B.W. and Tiller C.O., 1967 J. Appl. Phys. 38, 140
- Smith D.L. and Pickhardt V.Y., 1975 J. Appl. Phys. 46, 2366
- Spitzer W.G. and Allred W., 1968 J. Appl. Phys. 39, 4999
- Sze S.M., 1969 in "The Physics of Semiconductor Devices" (J. Wiley and Son)
- Trifonova E.P. and Hitova L., 1980 Thin Solid Films 65, 61
- Tsang W.M., Cameron D.C. and Duncan W., 1979 Appl Phys. Lett. 34, 413
- Tsang W.T., 1979 Appl. Phys. Lett. 34, 473
- Tsang W.T., 1980 Appl. Phys. Lett. 36, 11
- Tsang W.T. and Cho A.Y., 1978 Appl. Phys. Lett. 32, 491
- Tsang W.T., Reinhardt F.K. and Ditzenberger J.A., 1980 Appl. Phys. Lett. 36, 118
- Tuck B., 1975 J. Mater. Sci. 10, 321
- van Vechten J.A., 1975 J. Electrochem. Soc. 122, 423
- van Vechten J.A., 1977 J. Vac. Sci. Technol. 14, 992
- Wagner N.K., 1976 Thin Solid Films 38, 353
- Wallace C.A. and Ward R.C.C., 1975 J. Appl. Crystallogr. 8, 255

- Wataze M., Mitsui Y., Shimano, T., Nakatani M. and Mitsui S., 1978
Electron. Lett. 14, 759
- Wieder H.H., 1970 in "Intermetallic Semiconducting Films" Vol.10
(Pergamon Press)
- Wieder H.H., 1974 Appl. Phys. Lett. 25, 206
- Wieder H.H., 1977 Thin Solid Films 41, 185
- Wood E.A., 1964 J. Appl. Phys. 35, 1306
- Wood C.E.C., 1976 Appl. Phys. Lett. 29, 746
- Wood C.E.C., 1978 Appl. Phys. Lett. 33, 770
- Wood C.E.C. and Joyce B.A., 1978 J. Appl. Phys. 49, 4854
- Wood C.E.C., Woodcock J. and Harris J.J., 1979 Inst. Phys. Conf. Ser.
45, 28
- Yano M. Nogami M., Matsushima Y. and Kimata M., 1977 Jap. J. Appl.
Phys. 16, 2131
- Yano M., Suzuki Y., Ishii T., Matsushima Y. and Kimata M., 1978
Jap. J. Appl. Phys. 17, 2091
- Yao T., Makita Y. and Maekawa S., 1979 Appl. Phys. Lett. 35, 97
- Zehner D.M., White C.W. and Ownby G.W., 1980 Appl. Phys. Lett. 36, 56
- Zemel J.N., 1975 in "Surface Physics of Phosphors and Semiconductors"
Eds. C.G. Scott and C.E. Read (Academic Press, London) p.536

Relationship of MBE growth parameters with the electrical properties of thin (100) InAs epilayers

JD Grange, EHC Parker and RM King

Cass Semiconductor and Surface Research, Department of Physics, Sir John Cass School of Science and Technology, City of London Polytechnic, 31 Jewry Street, London EC3N 2EY

Received 1 February 1979, in final form 15 March 1979

Abstract. A study of the electrical properties of InAs heteroepitaxial layers grown on (100) GaAs and their dependence upon growth parameters has been undertaken. InAs films 1 μm thick were grown by molecular beam deposition at a substrate temperature of 370°C. Layers with residual n-type carrier concentrations in the range 5×10^{16} – $2 \times 10^{18} \text{ cm}^{-3}$ at room temperature were obtained. These mobile carriers arise from both bulk dopants and interface effects. It has been observed that the electrical properties of the InAs epilayers are critically dependent upon the incident indium and arsenic fluxes. High values of In and As₄ fluxes produced residual bulk n-type doping levels in the 10^{18} cm^{-3} range and caused additional scattering. The lowest carrier concentrations and highest mobilities were obtained for the lowest value of indium flux used ($1 \times 10^{14} \text{ atoms cm}^{-2} \text{ s}^{-1}$) and with the smallest arsenic flux consistent with the deposition of stoichiometric layers. Depth profile measurements on the best films indicated that the residual carriers primarily arose from donor centres situated at the film–substrate interface. The material remote from this interface had bulk-like mobilities and near-intrinsic carrier concentrations. The use of a 0.1 μm GaAs buffer layer isolated the films from a further source of donor centres. The presence of gaseous oxygen during film growth has been found to degrade film electrical properties. No effects were observed when hydrogen was present.

1. Introduction

Molecular beam epitaxy (MBE) (Cho and Arthur 1975) has been developed from surface studies on GaAs (Cho 1969, 1970b, 1971) to include the deposition of various epitaxial layers (Arthur and LePore 1969, Matsushima *et al* 1976, Chang *et al* 1977, Yano *et al* 1977) and the fabrication of microwave (Cho *et al* 1974, 1977b, Wood 1976) and electro-optic devices (Cho *et al* 1976, 1977a). There is little reported work, however, on the relationship between the MBE growth conditions and the electrical properties of the deposited layers, a knowledge of which would lead to more controlled and reproducible device performance. Cho (1970b, 1971, 1976) has examined how the Ga:As₂ flux ratio and substrate temperature influence the formation of surface reconstructions observed on (001) GaAs during molecular beam deposition. A detailed study of the structure and stoichiometry of (100) GaAs surfaces during molecular beam epitaxy has been reported by Neave and Joyce (1978). Gonda *et al* (1975) and Gonda and Matsushima (1976) have examined the effect of substrate temperature on the crystalline state of GaAs and on the relative amounts of As and P incorporated into GaAsP, though no electrical properties

were reported. There have been several papers concerning impurity incorporation into GaAs and the different dopant behaviour obtained under Ga- and As-rich conditions (Cho and Hayashi 1971a, Cho and Panish 1972, Ilegems and Dingle 1975). Wood and Joyce (1978) have studied tin-doping effects in GaAs films grown by MBE. Previous work on the growth of InAs by MBE (Yano *et al* 1977, Meggitt *et al* 1978) showed that improved electrical properties were obtained with thicker layers and layers grown at higher temperatures.

Here, as part of a detailed investigation of the MBE technique, we report the results of a systematic study into the relationship of MBE growth parameters to the electrical properties of thin heteroepitaxial (100) InAs layers grown at 370 °C. It is of interest to investigate the origin of the degradation of the electrical properties of MBE layers that occurs at low growth temperatures and for this reason such a low deposition temperature was chosen for this study. Kinetic studies (Foxon and Joyce 1978) and MEED studies (Meggitt 1979) indicate that stoichiometric, single-crystal InAs is obtained down to substrate temperatures of at least 225 °C. Furthermore, the reduction of growth temperatures will reduce inter-layer diffusion, facilitate the incorporation of elements with high vapour pressures and also help to define the fundamental limits to MBE growth.

2. Experimental details

Layers of InAs 1 μm thick were deposited by MBE on to high-resistivity GaAs buffer layers which had been predeposited at 530 °C to a thickness of 0.1 μm on to Cr-doped semi-insulating (100) GaAs substrates. MBE growth took place in a stainless steel diffusion-pumped chamber where base pressures of $\sim 10^{-10}$ Torr were obtained. Elemental sources of indium, gallium and arsenic were evaporated from spectroscopically pure graphite effusion cells. The source materials were all of 6–9 s purity and the β -form, air-stable, arsenic was used throughout since it has been found to give layers with improved electrical characteristics. The effusion rates from the group III cells were determined absolutely to $\pm 10\%$ by depositing indium and gallium on to thin aluminium foils which had been cleaned and placed in the vacuum system. The fluxes were then calculated from the change in weight of the aluminium foils. Repeated calibration depositions, SEM measurements on both step and cleaved edges of films, and quartz crystal monitoring showed that the effusion rates were reproducible to within $\pm 5\%$. The As_4 flux was monitored using the ionisation gauge reading within the growth chamber and calibrated from the onset of indium-rich growth, as discussed in §3. The substrates were etched in a $15\text{H}_2\text{SO}_4:1\text{H}_2\text{O}_2:1\text{H}_2\text{O}$ solution and heated in vacuum to 580 °C for 20 min in an arsenic flux. The electrical properties of the films were examined *ex situ* with the van der Pauw technique (van der Pauw 1958). The reproducibility of the measured properties from run to run was in general better than $\pm 10\%$, the exception being for samples with carrier concentrations $> 10^{18} \text{ cm}^{-3}$. The samples showed a variation of electrical properties of $< 10\%$ across a 4 cm long substrate. Electron channelling patterns (Meggitt *et al* 1978) have indicated that the layers are well-oriented (100) single-crystal structures. Further evidence for their (100) single-crystal nature has been found using inclined beam Laue and back-reflection x-ray techniques. The electrical and structural properties of thin (100) InAs layers grown in this system have been reported previously (Meggitt *et al* 1978).

Using the apparatus and procedure outlined above, InAs epilayers were grown with $\text{As}_4:\text{In}$ flux ratios varying from $< 0.5:1$ to $> 50:1$ using indium fluxes of $5.6 \times 10^{14} \text{ atoms cm}^{-2} \text{ s}^{-1}$ and $1.0 \times 10^{14} \text{ atoms cm}^{-2} \text{ s}^{-1}$. These fluxes correspond to growth rates of

$\sim 1.1 \mu\text{m}$
and hydro

3. Results

For a given
was found
the layers
concentra
during de

The
pressure
point wa
(figure 1)
took on
obtained
minimum
electrical
grown u
(plate).
scale the
have the

The
 As_2 due

$\sim 1.1 \mu\text{m h}^{-1}$ and $0.2 \mu\text{m h}^{-1}$. A gas leak-in facility on the MBE system allowed oxygen and hydrogen to be present as a background ambient during film growth.

3. Results

For a given indium flux the measured carrier concentration n ($= 1/R_{He}$) of the epilayers was found to depend upon the arsenic flux used during each growth. As shown in figure 1, the layers produced with a high arsenic flux were found to have a higher measured carrier concentration. This dependence of epilayer carrier concentration on arsenic flux used during deposition is shown in figure 1 for the two indium fluxes used.

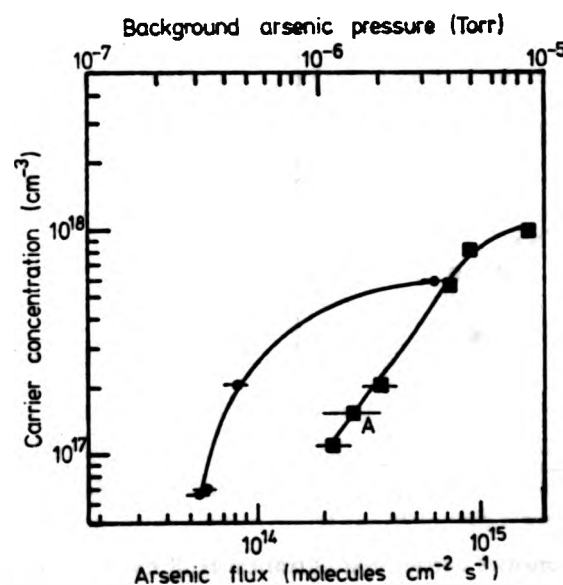


Figure 1. The room temperature carrier concentration of InAs epilayers plotted against arsenic flux used during deposition. ■ $F_{In} = 5.6 \times 10^{14}$ atoms $\text{cm}^{-2} \text{s}^{-1}$; ● $F_{In} = 1.0 \times 10^{14}$ atoms $\text{cm}^{-2} \text{s}^{-1}$.

The point labelled A was obtained with an increased arsenic background-to-beam pressure by not using any liquid nitrogen trapping in the growth chamber. The plotting point was then obtained by filling the shrouds at the termination of growth. The layers (figure 1) were mirror-like in appearance, but for $\text{As}_4:\text{In}$ flux ratios > 4 , many layers took on a milky appearance. For an $\text{As}_4:\text{In}$ flux ratio > 75 , epitaxial InAs was not obtained at this growth temperature. Any further reduction in the arsenic flux from the minimum values shown resulted in indium-rich growth and an obvious degradation of electrical properties as well as surface morphology. SEM micrographs of InAs layers grown under indium-rich, optimum and arsenic-rich conditions are shown in figure 2 (plate). The onset of indium-rich growth at the two deposition rates has been used to scale the arsenic fluxes since, using the kinetic approach (Foxon and Joyce 1978), we have that the minimum arsenic flux required for stoichiometric growth is given by

$$F_{As_4} \approx \frac{1}{2} F_{In}.$$

The above expression is only approximate, since at 370°C an InAs layer is losing As_2 due to thermal decomposition. This loss of $\text{As}_2 \sim 3 \times 10^{12}$ molecules $\text{cm}^{-2} \text{s}^{-1}$ is

constant irrespective of the incident indium flux. The incident As_4 flux thus has to compensate for this loss as well as satisfy the arriving indium atoms. Assuming an equality in the above equation introduces a small error in calibrating the arsenic fluxes. Thus, by knowing the indium fluxes and identifying the point of the onset of indium-rich growth, a calibration of the As_4 beam flux against the ionisation gauge reading in the chamber is possible. This method assumes that there is a linear relationship between the ionisation gauge reading and the As_4 beam pressure and also that the effect of the liquid nitrogen trapping in the system is the same from run to run.

The mobility-carrier concentration plot of figure 3 shows the mobility degradation due to the presence of excess arsenic during growth, and also illustrates the presence of an independent source of doping and scattering associated with the indium arrival rate

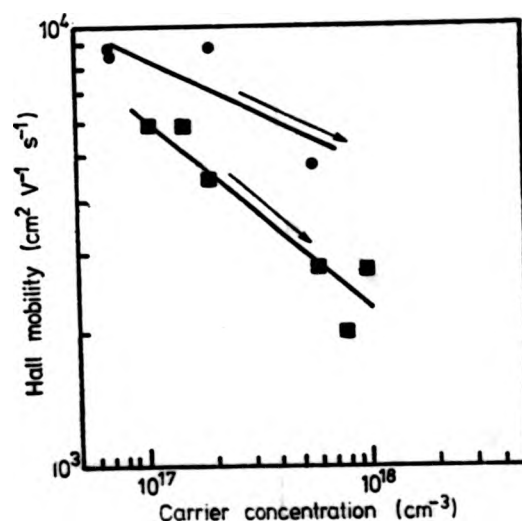


Figure 3. Room temperature carrier concentration/Hall mobility plot for the epilayers deposited using the two different indium fluxes. Arrows indicate directions of increasing As_4 flux: symbols as in figure 1.

(i.e. the growth rate). The measured values of carrier mobility for a given carrier concentration of all the epilayers are lower than those of bulk InAs. Harman *et al* (1956) have made measurements of the transport properties of bulk InAs. They reported a room temperature mobility of $30\,000\text{ cm}^2\text{ V}^{-1}\text{ s}^{-1}$ for a donor concentration of $1.7 \times 10^{16}\text{ cm}^{-3}$ decreasing to $10\,000\text{ cm}^2\text{ V}^{-1}\text{ s}^{-1}$ as the donor concentration increased to $3 \times 10^{18}\text{ cm}^{-3}$.

Further experiments were performed using the optimum arsenic flux for an In flux of $5.6 \times 10^{14}\text{ atoms cm}^{-2}\text{ s}^{-1}$ with growth taking place in oxygen and hydrogen ambients of 5×10^{-7} Torr. The effect of the oxygen was to degrade severely the measured film properties ($n > 10^{18}\text{ cm}^{-3}$; $\mu < 10^3\text{ cm}^2\text{ V}^{-1}\text{ s}^{-1}$). No effect has been observed, however, using a hydrogen ambient.

Figure 4 is a depth profile of epilayers deposited under optimum conditions with an In flux of $1.0 \times 10^{14}\text{ atoms cm}^{-2}\text{ s}^{-1}$. Two layers were deposited simultaneously, one on a $0.1\text{ }\mu\text{m}$ GaAs buffer layer and the other deposited directly on to the Cr-doped substrate. This was effected on the same substrate by employing a molybdenum mask to shield half of the substrate from the impinging Ga beam. The depth profile was obtained by step etching in a $1\text{H}_2\text{SO}_4:1\text{H}_2\text{O}_2:100\text{H}_2\text{O}$ solution and taking sequential van der Pauw measurements

4. Discussion

4.1. Effect of As_4 flux

Figures 1, 2 and 3 show the effect of As_4 flux on the morphology and carrier concentration of the Ga-As₄-Ga epilayers (Joyce 1975, 1976). It is seen that as the As_4 flux increases, the surface becomes smoother and the carrier concentration increases. This is due to the incorporation of arsenic into the GaAs surface, otherwise the surface would be a non-zero stoichiometry. MEED examination of the epilayers grown under optimum conditions shows that they are right up to the stages of indium-rich growth. This is due to an indium-stabilized surface which is necessary for electrical activation. The presence of indium on the surface (Joyce and Foster 1976) is thought to be the reason why thin films can be grown under optimum conditions.

We conclude that the optimum arsenic flux is exceeded when the As_4 flux is exceeded (figure 1) was 1.5×10^{-6} Torr, produced during deposition whereupon the sample are cooled to 1.5×10^{-6} Torr since the kinetic

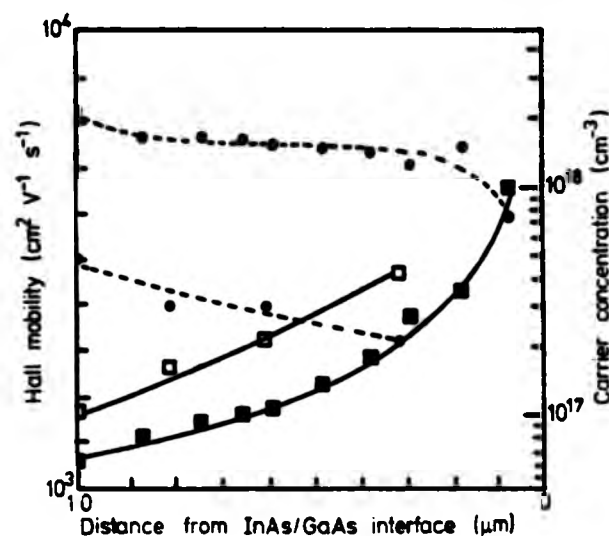


Figure 4. Variation of carrier concentration and mobility with depth for two of the epilayers deposited under optimum conditions at the lower indium flux. ●, mobility of buffered layer; ○, mobility of unbuffered layer; ■, carrier concentration of buffered layer; □, carrier concentration of unbuffered layer. Broken (for the mobilities) and solid (for the carrier concentrations) curves are best fits to the experimental data.

4. Discussion

4.1. Effect of arsenic flux

Figures 1, 2 and 3 clearly show the degradation of electrical properties and surface morphology due to increasing the arsenic flux for a given indium flux. Kinetic studies of the Ga-As₄-GaAs (100) and In-As₄-InAs (100) systems have been reported (Foxon and Joyce 1975, 1978). The interpretation of these studies has been that for arsenic incorporation into GaAs or InAs epilayers there must be free gallium or indium at the growing surface, otherwise arsenic desorption occurs. Kinetic studies do not, however, preclude a non-zero sticking coefficient for As₄ on GaAs and InAs stoichiometric layers. *In situ* MEED examination on separate layers has shown that all the layers reported here were grown under As-stabilised conditions. Arsenic-stabilised conditions were maintained right up to the onset of indium precipitation, which may be indicative that at the initial stages of indium-rich growth the surface coverage of indium is not sufficient to generate an indium-stabilised reconstruction over the whole surface. None of the epilayers used for electrical analysis were examined by electron diffraction prior to electrical characterisation. The possibility of electron-beam-induced effects has previously been conjectured (Joyce and Foxon 1977) and it is known that local electron beam irradiation of PbTe thin films can modify the measured transport properties (McGlashan *et al* 1979).

We conclude therefore that optimum electrical properties are obtained with the smallest arsenic flux consistent with the deposition of stoichiometric layers. Once this critical flux is exceeded, the electrical properties are degraded. The experimental point labelled A (figure 1) was obtained with an artificially high background arsenic pressure of 6×10^{-6} Torr, produced by not using liquid nitrogen trapping in the system. The arsenic flux used during deposition was then obtained by filling the trapping at the termination of growth, whereupon the system pressure fell to $\sim 1.5 \times 10^{-6}$ Torr. The electrical properties of this sample are commensurate with those expected if an arsenic background pressure of 1.5×10^{-6} Torr had been used throughout the deposition. This result is rather surprising, since the kinetic theory of gases shows that a background pressure of 6×10^{-6} Torr

corresponds to an As_4 flux at the substrate of 7×10^{14} molecules $\text{cm}^{-2} \text{s}^{-1}$. This is nearly three times the estimated beam flux. This large background As_4 flux, apparently, does not influence the growing InAs film in the same manner as does the incident As_4 beam flux. We consider that the most likely explanation is that the ionisation gauge, which is calibrated for nitrogen, gave an artificially high arsenic pressure reading and the background As_4 arrival rate was really small compared with the beam flux. The authors are not aware of any work which has obtained an ionisation gauge sensitivity factor for As_4 pressure measurements, but a factor of 10 variation in this parameter has been reported for different gases (AEI publication 2032-69).

If the background pressure readings were indeed correct then it seems that there is something in the mechanism of InAs film growth by MBE which enables a differentiation between the As_4 molecules arriving direct from the source and those which arrive after one or more collisions with the chamber walls. As_4 molecules coming from the background would presumably be thermally equilibrated with the walls of the chamber ($\sim 20^\circ\text{C}$) and also have a different distribution of incident directions to those arriving at nearly normal incidence directly from the arsenic source at 260°C . It is far from clear how either of these properties could affect the probability of incorporation into the growing film.

Whether the degradation is due to arsenic incorporation or an increase in the defect content of the epilayer because of excess arsenic impinging on the growing surface or due to some impurity mechanism is as yet unknown. High arsenic concentrations have been observed to produce compensation effects in InAs grown by VPE (Cronin *et al* 1966). The increase in As_4 :In flux ratio may be expected to produce In vacancies in the InAs which themselves may produce the increase in n-type doping. A further explanation is that monatomic arsenic is being incorporated in the indium sublattice or as interstitials and there acts as an n-type dopant. It is also possible that with a substrate temperature of 370°C some of the As_4 molecules do not dissociate, and As_4 inclusions occur within the epilayer. It was found that annealing the InAs samples either in sealed ampoules or in the UHV chamber at 530°C under an arsenic flux did not produce any improvement in the electrical properties. The severe mobility degradations found for high arsenic fluxes does not suggest that we were observing an increase in ionised impurity scattering associated with a simple substitutional impurity.

Depth profiling data (to be discussed in §4.5) indicates that the layers deposited under high As_4 fluxes are uniformly doped throughout the epilayer, and hence that the observed dependence of the carrier concentration on the As_4 flux must be a bulk phenomenon and not a problem related to the initial vacuum cleaning or the nucleation stage of film growth.

Transitions between energy levels observed in photoluminescence measurements on MBE grown GaAs (Cho and Hayashi 1971b) have been tentatively linked to Ga vacancies formed by growth under As-stabilised conditions. Ilegems and Dingle (1975) however argue for an impurity-vacancy complex giving a dopant behaviour for manganese in GaAs dependent upon growth conditions. (100) GaAs layers grown in our system (JD Grange 1978, unpublished results) gave very similar electrical properties and freeze-out behaviour to that reported by Ilegems and Dingle and this is indicative of the presence of a system impurity. The p-type doping was found to increase with increasing As_4 :Ga flux ratio. The p-type doping was found to be a minimum for growth taking place under Ga-rich conditions ($p(300\text{K}) = 1 \times 10^{15} \text{cm}^{-3}$). Subsequent photoluminescence measurements have confirmed the presence of manganese in our GaAs epilayers with an activation energy of 112 meV. Carbon has also been detected. The Mn_{Ga} photoluminescence peak was found to increase as the arsenic coverage per unit time used

during deposition peaks when that under epilayers and epilayers built in the InAs during deposition increase in acceptor in an acceptor

4.2. Effect

The indium figure 3 the carrier concentration 5.6×10^{14} electrical properties and although the concentration in all cases the background best electrical was influenced defects, surface Application that, at low higher flux increased (111) CaF affected by deposited

The growth available

4.3. Gas

The improvement be due to Some super artificially ties presumably however, limits $2 \times$ arsenic-C

Using of MBE electrical 5×10^{-7}

during deposition increased. This peak was small compared with the carbon and exciton peaks when growth took place under Ga-rich conditions. The conclusion is, therefore, that under Ga-rich conditions very little manganese is incorporated into the GaAs epilayers as an optically or electrically active impurity. It may still be present in the epilayers but in some inactive form. We must assume that some manganese was present in the InAs layers but the level of its electrical activity may depend upon the As_4 flux used during deposition. It is unlikely that the manganese was responsible for the observed increase in n-type doping as the As_4 :In flux ratio was increased, since Mn is a known acceptor in GaAs and InSb (Dashevskii *et al* 1971) and therefore might be expected to be an acceptor in InAs.

4.2. Effect of indium arrival rate

The indium arrival rate controls the growth rate of the sample and it can be seen from figure 3 that the layers deposited with an In flux of 1.0×10^{14} atoms $cm^{-2} s^{-1}$ have lower carrier concentrations and higher mobilities than those deposited using an In flux of 5.6×10^{14} atoms $cm^{-2} s^{-1}$. Since all samples were $1 \mu m$ thick, the films with the best electrical properties were exposed to the background ambient for over five times as long, and although the measured background pressure was lower for the slower growth rate, the concentrations of impurity species (CO and H_2O predominantly) were roughly equal in all cases. We thus conclude that the residual doping in these epilayers was not due to the background UHV ambient. The fact that the lowest growth rate gave samples with the best electrical properties is confirmation that the nucleation/condensation rate of InAs was influencing film properties. The use of too high a growth rate could introduce point defects, stacking faults and dislocations originating at the film-substrate interface. Application of the theory of heterogeneous nucleation to epitaxy (Moazed 1966) implies that, at low flux rates, preferred epitaxial sites will act as nucleation centres, whereas for higher fluxes random nucleation may occur. The increase of epitaxial temperature with increased growth rate has been observed by Cho (1970a) in the MBE growth of GaP on (111) CaF_2 . The electrical properties of InP have been noted (McFee *et al* 1977) to be affected by the growth rate. The effect of the growth rate on the properties of vacuum-deposited Ge is well documented (Sloope and Tiller 1965, 1966, 1967).

The growth rate is often fixed by the thickness of the layer(s) required and the time available for deposition, and as such is not always an arbitrary parameter.

4.3. Gaseous effects

The improvement in electrical properties found by using the β -arsenic was considered to be due to inadequate outgassing of the α -arsenic source which oxidises on air exposure. Some supportive evidence for this has been obtained from the growth of layers under artificially high oxygen levels (5×10^{-7} Torr). The observed degradation in film properties presumably resulted from oxygen incorporation in the InAs lattice. There has, however, been no correlation between carrier concentrations and base pressure (in the limits 2×10^{-10} Torr to 2×10^{-9} Torr), though it is possible that either an indium or arsenic- O_2 interaction is responsible for the residual doping.

Using an ambient of hydrogen has been reported to improve the electrical properties of MBE GaAs (Calawa 1978) but we have not obtained evidence for an effect on the electrical properties of the InAs when deposition took place with a hydrogen ambient of 5×10^{-7} Torr.

4.4. Buffer layer

It has been reported (Meggitt *et al* 1978) that the surface morphology of InAs epilayers was improved if deposited on a 0.1–0.5 μm high-resistivity GaAs buffer layer. This observation has been repeated on many layers, though occasionally the buffered and unbuffered layers had comparable smoothness.

Over twenty layers were deposited, at 370°C, with different As₄:In ratios in the manner described earlier using a buffer layer of 0.1 μm on only half of the substrate. For many of the layers there was little or no appreciable difference in the electrical properties of the buffered and unbuffered layers. But for the layers grown at the slower rate under optimum conditions (i.e. $n < 1 \times 10^{17} \text{ cm}^{-3}$) a reproducible difference did exist. We believe that the effect is present on all the epilayers but is only observed when the effective bulk doping is reduced below $\sim 1 \times 10^{17} \text{ cm}^{-3}$.

Table 1 shows that the best layers were deposited on a GaAs buffer layer.

Table 1. Effects on epilayer deposition of a GaAs buffer layer.

Film no.		Room temperature	
		n (cm^{-3})	μ ($\text{cm}^2 \text{ V}^{-1} \text{ s}^{-1}$)
42	Buffered	6.4×10^{16}	8300
	Unbuffered	9.7×10^{16}	5000
40	Buffered	6.2×10^{16}	8600
	Unbuffered	1.2×10^{17}	4900

The implication of this is that the buffer layer is responsible for isolating the InAs epilayer from a source of donor centres on the GaAs substrate which could originate from impurities present on the vacuum-annealed substrate or diffuse out from the substrate bulk.

4.5. Depth profile data

Depth profiles have been obtained for high ($n \sim 10^{18} \text{ cm}^{-3}$) and low doped ($n \lesssim 10^{17} \text{ cm}^{-3}$) InAs epilayers. These profiles indicate that two separate doping processes are occurring in these samples. One is a bulk effect, the other is associated with the film–substrate interface. The increase in doping observed due to high impinging arsenic and indium fluxes is considered to lead to bulk doping of the epilayers. A 5.5 μm epilayer deposited under a high arsenic flux at the faster growth rate was measured as having a room temperature carrier concentration of $2 \times 10^{18} \text{ cm}^{-3}$ and a mobility of $1000 \text{ cm}^2 \text{ V}^{-1} \text{ s}^{-1}$. Depth profiling of this sample (both buffered and unbuffered portions) indicated uniform transport properties right up to the interface, though no measurements were obtained on a layer thinner than 0.3 μm . Such a profile is indicative of uniform bulk doping. Completely different carrier concentration profiles are obtained on the lowest doped samples. There is an approximately constant mobility up to within $\sim 0.1 \mu\text{m}$ of the interface, yet at the same time the carrier concentration varies by over an order of magnitude (figure 4). Such a profile does, however, imply that the number of charge carriers per unit area was independent of the remaining epilayer thickness. It is the profile obtained from a low-doped sample which will now be considered in more detail.

The
equation
accumu
proper
The

where
band
density
and d
An
applied
InAs s
has be
depth.
analys

using
 $\Delta N, \mu$

the morphology of InAs epilayers
activity GaAs buffer layer. This
occasionally the buffered and

ferent As₄:In ratios in the man-
only half of the substrate. For
ference in the electrical properties
grown at the slower rate under
e difference did exist. We believe
observed when the effective bulk

a GaAs buffer layer.

s buffer layer.

(V⁻¹ s⁻¹)

nsible for isolating the InAs epi-
rate which could originate from
diffuse out from the substrate

and low doped ($n \lesssim 10^{17} \text{ cm}^{-3}$)
growing processes are occurring in
with the film-substrate interface.
g arsenic and indium fluxes is
5 μm epilayer deposited under a
as having a room temperature
of $1000 \text{ cm}^2 \text{ V}^{-1} \text{ s}^{-1}$. Depth pro-
ns) indicated uniform transport
ments were obtained on a layer
form bulk doping. Completely
e lowest doped samples. There
1 μm of the interface, yet at the
er of magnitude (figure 4). Such
carriers per unit area was inde-
ofile obtained from a low-doped

The obtained depth profiles are striking since they can be accurately fitted to the equations (Zemel 1975) relating band bending, caused by an inversion, depletion or an accumulation layer at a semiconductor interface or surface, to the measured transport properties.

The Hall coefficient R_H and conductivity σ can be expressed:

$$\sigma d = \sigma_0 d + e \Delta N \mu_{NS} + e \Delta P \mu_{PS} \quad (1)$$

$$R_H \sigma^2 d = R_{H0} \sigma_0^2 d - e \Delta N \mu^2_{NS} + e \Delta P \mu^2_{PS} \quad (2)$$

where R_{H0} is the Hall coefficient at flat band conditions, σ_0 is the conductivity at flat band conditions, ΔN is the surface charge density (electrons), ΔP is the surface charge density (holes), μ_{PS} is the surface mobility (holes), μ_{NS} is the surface mobility (electrons), and d is the layer thickness.

An equally good fit can be obtained using the two-layer model (Petritz 1958) as applied by Wieder (1974, 1977) and Sites and Wieder (1975) to thicker heteroepitaxial InAs samples. The variation of carrier concentration and mobility with depth (figure 4) has been replotted (figure 5) as the variation of Hall coefficient and conductivity with depth. This is because it is more convenient to treat these quantities in a theoretical analysis. The fit of experimental points to the theoretical curve (figure 5) was made by

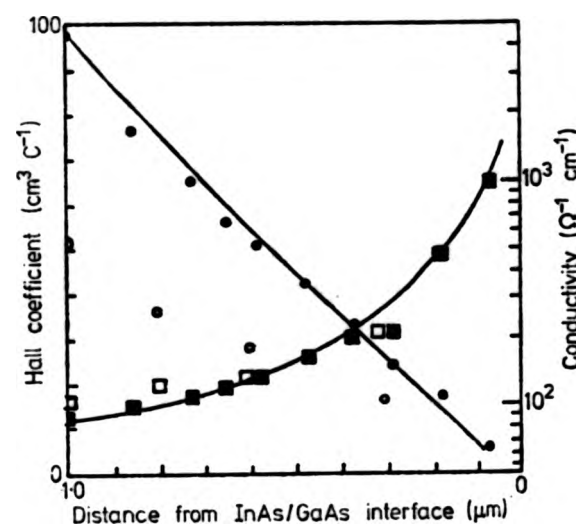


Figure 5. Variation of the measured Hall coefficient and conductivity with depth for the epilayers of figure 4. ■, conductivity of buffered layer; □, conductivity of unbuffered layer; ●, Hall coefficient of buffered layer; ○, Hall coefficient of unbuffered layer. Solid curves are calculated variations with the parameters given in the text and using equation (1) and (2).

using our experimental data with equations (1) and (2) to obtain the unknown quantities ΔN , μ_{NS} , σ_0 and R_{H0} (we have assumed $\Delta N \mu_{NS} \gg \Delta P \mu_{PS}$). This gives

$$\sigma_0 = 10 (\Omega \text{ cm})^{-1}$$

$$R_{H0} = 2988 \text{ cm}^3 \text{ C}^{-1}$$

$$\Delta N = 8.7 \times 10^{12} \text{ cm}^{-2}$$

$$\mu_{NS} = 5342 \text{ cm}^2 \text{ V}^{-1} \text{ s}^{-1}$$

from which we obtain:

$$n_{\text{bulk}} = 2.1 \pm 0.7 \times 10^{15} \text{ cm}^{-3}$$

$$\mu_{\text{bulk}} = 3.0 \pm 0.5 \times 10^4 \text{ cm}^2 \text{ V}^{-1} \text{ s}^{-1}$$

for the material remote from the space charge region.

This compares with the directly measured values of $n = 6.4 \times 10^{16} \text{ cm}^{-3}$ and $\mu = 8300 \text{ cm}^2 \text{ V}^{-1} \text{ s}^{-1}$. The implication of the analysis is that the measured electrical properties of the epilayer were dominated by a strong accumulation region at the film-substrate interface and that the material remote from the interfacial space charge region is comparable to the best obtained by any method of preparation. Using the expressions of Many *et al* (1971), the derived value of ΔN implies band bending of $\approx 11 kT$ units ($T = 300 \text{ K}$), assuming that the bulk Fermi level is near its intrinsic position. The band gap of InAs = $14 kT$ units, thus at the interface the Fermi level is well into the conduction band. Equations (1) and (2) take no account of any quantum effects and obviously Fermi-Dirac statistics are applicable. The existence of a positive interface charge density in p(GaAs)-N($\text{Al}_x\text{Ga}_{1-x}\text{As}$) heterojunctions produced by MBE also has been recently proposed (Kroemer *et al* 1978).

The two-layer model used by Wieder (1974) was supported by data obtained by an examination of the variation of R_H and ρ with magnetic field. The presence of a non-uniform doping profile is expected to give rise to circulating Hall currents (Petritz 1958) and be evident in the dependence of the Hall coefficient and the resistivity on the applied magnetic field. The variation of $\Delta\rho/\rho_0$ (viz. the magnetoresistance effect) observed with these thin MBE samples is consistent with the application of the two-layer model. However, we have observed little variation of R_H with field over the range of magnetic field used ($B < 0.5 \text{ T}$).

Baliga and Ghandi (1974) reported that the carrier concentration of various thin InAs layers ($0.2\text{--}1.0 \mu\text{m}$) produced by vPE was inversely proportional to the layer thickness. They interpreted their results in terms of a continuously varying defect density in the epilayers, decreasing away from the film-substrate interface. In isolation, our results on the variation of measured carrier concentration with depth support this theory. However, we note that the mobility (especially on the buffered layer) is constant up to $0.1 \mu\text{m}$ of the epilayer-substrate interface, yet the carrier concentration has apparently increased by over an order of magnitude. We believe that, by itself, the n versus d profile is not open to unambiguous interpretation. It is possible that the lattice mismatch at the interface is responsible for generating defects in the InAs layer but an interface space charge model finds more experimental support than a theory based on the variation of defect density with epitaxial layer thickness.

The authors do have reservations arising from the use of the acid etch to thin down layers. The etch rate has been observed to vary from $0.03 \mu\text{m min}^{-1}$ to $0.1 \mu\text{m min}^{-1}$ on different samples. Samples grown on buffer layers have always etched slower than those deposited directly on to the substrate. This may be due to more structural defects present in the unbuffered layers. It would seem likely that the etch rate did increase towards the interface because of an increasing defect density caused by the large lattice mismatch ($\sim 7\%$) between InAs and GaAs. The effects of the relief, or non-relief, of lattice mismatch have been discussed by Olsen (1975). Attempts have been made using SEM measurements and x-ray analysis to ascertain whether the etch rate is uniform both over the whole sample area and with depth. Measurements obtained have not been conclusive regarding the variation of etch rate with depth throughout the entire film although they did indicate

that the etch rate was established through the etch pits or was possible due to

5. Conclusion

The As_4 :In film showing the electrical properties of an excessive As_4 high indium film. The data obtained from the bulk of the film is a simplistic approximation of a strong accumulation region which dominates the deposited material (s^{-1}) and low isolated the etch rate is clearly required as a factor in obtaining

Acknowledgments

The authors are grateful to the Science Research Council, G.R. Jones, W. Liley (The University of Liverpool) and J.J. Harris (P.O. Box 147, Chester)

References

- Arthur J R and Baliga B J and Calawa A R 1974
- Chang C, Luo C and Cho A Y 1969
- 1970a *J. Appl. Phys.*
- 1970b *J. Appl. Phys.*
- 1971 *J. Appl. Phys.*
- 1976 *J. Appl. Phys.*
- Cho A Y and Baliga B J 1974
- Cho A Y, Casperson W A and Cho A Y, DiLuzio G 1974 *48* 346
- Cho A Y, Dixon R and Cho A Y, DuBois R 1971b *J. Appl. Phys.*
- Cho A Y and Baliga B J 1974

that the etch rate is constant to at least within 0.2 μm of the interface. Also it has been established that the etch rate is the same over the sample area (16 mm^2), with too few etch pits or hillocks to affect the measurements. $C-V$ profiling of samples was not possible due to a very large leakage current across the diode.

5. Conclusions

The As_4 :In flux ratio and the value of the indium flux are important parameters influencing the electrical properties of the InAs layers grown by MBE at 370°C. The use of an excessive As_4 flux produced residual n-type carrier concentrations above 10^{18}cm^{-3} , and high indium flux rates gave additional doping and mobility degradations. The electrical data obtained can be interpreted in terms of the incorporation of excess arsenic into the bulk of the epilayers and thus suggests that the kinetic model of MBE growth is a too simplistic approach. Depth profile measurements on the lowest doped epilayers indicate a strong accumulation region ($\Delta N \sim 8 \times 10^{12} \text{cm}^{-2}$) at the epilayer-substrate interface which dominated the measured electrical properties of these 1 μm thick films. The deposited material remote from this interface had near bulk mobility ($\sim 30\,000 \text{cm}^2 \text{V}^{-1} \text{s}^{-1}$) and low residual carrier concentration ($\sim 2 \times 10^{15} \text{cm}^{-3}$). A 0.1 μm buffer layer isolated the epilayers from some further source of donor centres. Although further work is clearly required, it appears that the low substrate temperature used was not a limiting factor in obtaining bulk-like InAs by MBE techniques.

Acknowledgments

The authors are indebted to G B Scott (PRL, Redhill) for the photoluminescence measurements, G R Jones (RSRE Malvern) for the inclined beam Laue x-ray measurements, and W Liley (The Polytechnic, Hatfield) for SEM measurements. We would also like to thank J J Harris (PRL, Redhill) for his help during the course of this work.

References

- Arthur J R and LePore J J 1969 *J. Vac. Sci. Technol.* 6 545
- Baliga B J and Ghandi S K 1974 *J. Electrochem. Soc.* 121 1646
- Calawa A R 1978 *Appl. Phys. Lett.* 33 1020
- Chang C, Ludeke R, Chang L L and Esaki L 1977 *Appl. Phys. Lett.* 31 759
- Cho A Y 1969 *Surface Sci.* 17 494
- 1970a *J. Appl. Phys.* 41 782
- 1970b *J. Appl. Phys.* 41 2780
- 1971 *J. Appl. Phys.* 42 2074
- 1976 *J. Appl. Phys.* 47 2841
- Cho A Y and Arthur J R 1975 *Prog. Solid St. Chem.* 10 157
- Cho A Y, Casey Jr H C and Foy P W 1977a *Appl. Phys. Lett.* 30 397
- Cho A Y, DiLorenzo J V, Hewitt B S, Niehaus W C, Schlosser W O and Radice C 1977b *J. Appl. Phys.* 48 346
- Cho A Y, Dixon R W, Casey Jr H C and Hartman R L 1976 *Appl. Phys. Lett.* 28 501
- Cho A Y, Dunn C N, Kuvus R L and Shroeder W E 1974 *Appl. Phys. Lett.* 25 224
- Cho A Y and Hayashi I 1971a *J. Appl. Phys.* 42 4422
- 1971b *Solid St. Electron.* 14 125
- Cho A Y and Panish M B 1972 *J. Appl. Phys.* 43 5118

- Cronin GR, Conrad RW and Borrello SR 1966 *J. Electrochem. Soc.* **113** 1336
 Dashevskii MY, Ivleva VS, Krol LY, Kurilenko IN, Litvak-Gorskaya LB, Mitrofanova RS and Fridlyand EY 1971 *Sov. Phys.—Semicond.* **5** 757
 Foxon CT and Joyce BA 1975 *Surface Sci.* **50** 434
 — 1978 *J. Cryst. Growth* **44** 75
 Gonda S and Matsushima Y 1976 *J. Appl. Phys.* **47** 4198
 Gonda S, Matsushima Y, Makita Y and Mukai S 1975 *Japan. J. Appl. Phys.* **14** 935
 Harman TC, Goering HL and Beer AC 1956 *Phys. Rev.* **104** 1562
 Ilegems M and Dingle R 1975 *Gallium Arsenide and Related Compounds, 1974. Inst. Phys. Conf. Ser. No. 24* p 1
 Joyce BA and Foxon CT 1977 *Solid State Devices, 1976. Inst. Phys. Conf. Ser. No. 32* p 17
 Kroemer H, Chien WY, Casey Jr HC and Cho AY 1978 *Appl. Phys. Lett.* **33** 749
 Many A, Goldstein Y and Grover WB 1971 *Semiconductor Surfaces* (Amsterdam: North Holland) p 154
 McFee JH, Miller BI and Bachmann KJ 1977 *J. Electrochem. Soc.* **124** 259
 McGlashan SRL, King RM and Parker EHC 1979 presented at 6th P.C.S.I. Asilomar (USA) January/February *J. Vac. Sci. Technol.* to be published July/August
 Matsushima Y, Hirofuji Y, Gonda S, Mukai S and Kimata M 1976 *Japan. J. Appl. Phys.* **15** 2321
 Meggitt BT 1979 *PhD Thesis CNAA*
 Meggitt BT, Parker EHC and King RM 1978 *Appl. Phys. Lett.* **33** 528
 Moazed KL 1966 *The Use of Thin Films in Physical Investigations* ed. JC Anderson (London: Academic Press) p 203
 Neave JH and Joyce BA 1978 *J. Cryst. Growth* **44** 387
 Olsen GH 1975 *J. Cryst. Growth* **31** 223
 van der Pauw LJ 1958 *Philips Res. Rep.* **13** 1
 Petritz RL 1958 *Phys. Rev.* **110** 1254
 Sites JR and Weider HH 1975 *CRC Crit. Rev. Solid St. Sci.* **5** 385
 Sloope BW and Tiller CO 1965 *J. Appl. Phys.* **36** 3174
 — 1966 *J. Appl. Phys.* **37** 887
 — 1967 *J. Appl. Phys.* **38** 140
 Wieder HH 1974 *Appl. Phys. Lett.* **25** 206
 — 1977 *Thin Solid Films* **41** 185
 Wood CEC 1976 *Appl. Phys. Lett.* **29** 746
 Wood CEC and Joyce BA 1978 *J. Appl. Phys.* **49** 4854
 Yano M, Nogami M, Matsushima Y and Kimata M 1977 *Japan. J. Appl. Phys.* **16** 2131
 Zemel JN 1975 *Surface Physics of Phosphors and Semiconductors* eds CG Scott and CE Reed (London: Academic Press) p 536

(b)



Figure 2.
 ratios. M
 surface, A
 conditions
 rich cond

Soc. 113 1336

Gorskaya L B, Mitrofanova R S and

Appl. Phys. 14 935

ounds, 1974. Inst. Phys. Conf. Ser. No.

s. Conf. Ser. No. 32 p 17

Phys. Lett. 33 749

es (Amsterdam: North Holland) p 154

oc. 124 259

6th P.C.S.I. Asilomar (USA) January/

76 Japan. J. Appl. Phys. 15 2321

33 528

ed. J C Anderson (London: Academic

5

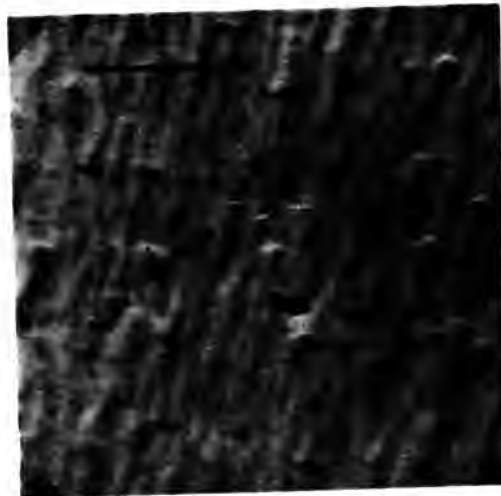
J. Appl. Phys. 16 2131

eds C G Scott and C E Reed (London:

(a)



(b)



(c)

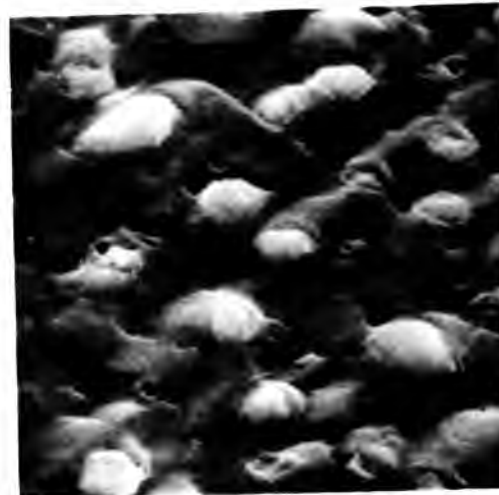


Figure 2. SEM micrographs of $1\ \mu\text{m}$ InAs epilayers deposited with different $\text{As}_4:\text{In}$ flux ratios. Marker length is $2\ \mu\text{m}$ in all cases. (a) Edge region of an indium precipitated surface, $\text{As}_4:\text{In}$ flux ratio $< 0.5:1$. (b) Surface of an epilayer deposited under optimum conditions, $\text{As}_4:\text{In}$ flux ratio $0.5:1$. (c) Surface of an epilayer deposited under arsenic-rich conditions, $\text{As}_4:\text{In}$ flux ratio $25:1$.

**TIGHTLY
BOUND
COPY**

DEVICE FABRICATION FOR THE FUTURE?

J D Grange
and
E H C Parker

Molecular beam epitaxy has recently been developed from surface physics experiments to a device fabrication technology. The technique, its applications and potential are outlined in this article

Molecular beam epitaxy (MBE) describes the growth of elemental, compound and alloy films on crystalline surfaces from directed, thermal energy molecular beams under ultrahigh vacuum conditions (pressures $< 10^{-9}$ Torr). In this process, an underlying single crystal substrate influences the film growth to produce an 'orientated overgrowth', a process known as epitaxy. The deposited film generally has the same crystallographic orientation as the substrate but not necessarily the same chemical composition.

Semiconductor materials and devices represent the major application of the technique, and MBE is now used in the commercial production of microwave devices (mixer diodes) and for the fabrication of electro-optic devices such as solid state lasers. Device performances are comparable with those produced by better established techniques.

Considerable attention has been devoted to the MBE technique since its development at the Bell Telephone Laboratories, USA, at the beginning of the decade, much of the pioneering work being done then and now by A Y Cho. Coupled with the development of MBE has been an upsurge of interest in ultrahigh vacuum technology and associated surface analytical techniques (*Physics Bulletin* April 1976 p165).

Near perfect surfaces

MBE offers a means of producing, and then studying, near perfect surfaces. Previous studies were limited to those which could be obtained by cleaving in a vacuum, though electronic devices are not usually prepared on surfaces which can be obtained by cleavage. For example, MBE is being used in a study of the 'intrinsic' electronic properties of (100) GaAs and InP surfaces

and their interfaces with other semiconductors and metals, with a view to understanding the factors limiting the performance of various microwave devices.

Many materials have been deposited as thin films ($< 10 \mu\text{m}$) by MBE, but III-V compounds in general and GaAs in particular have received most attention. This is because of the immediate commercial benefit of GaAs with its superior high frequency properties compared to silicon. Furthermore, the growth kinetics of III-V compounds by MBE are more fully understood from the work of J R Arthur at Bell Telephone Laboratories, and C T Foxon and B A Joyce at Philips Research Laboratories (UK), on the interaction between gallium and arsenic molecular beams with single crystal gallium arsenide substrates. Film formation by MBE involves processes operating far from thermodynamic equilibrium. The growth of the layer is controlled by surface kinetics and lifetimes of the molecular species at the growing film interface. Despite this apparent imbalance, II-VI and IV-VI compound growth, particularly the lead and tin chalcogenides, is exciting considerable interest. In fact the growth of IV-VI compounds has developed as far as the fabrication of high performance arrays for photodiodes for the detection of infrared radiation, and $\text{Pb}_x\text{Sn}_{1-x}\text{Te}$ double heterostructure lasers have been made.

Early work

Simple vacuum evaporation of polycrystalline films has been achieved in

medium to high vacua ($\sim 10^{-7}$ Torr) for some time. The evaporation was, however, not congruent for many compounds at temperatures sufficiently high for practical mass transfer. Noncongruent evaporation describes the preferential evaporation of one of the constituents of a compound on heating (e.g. above $\sim 620^\circ\text{C}$ As, preferentially evaporates from GaAs). Thus the production of stoichiometric films by vacuum deposition was difficult in the early years, and the problem was not well understood until studies of reaction kinetics between surfaces and molecular beams were undertaken. The three temperature technique of K G Günther (1958) was one of the early examples which could be acknowledged as the forerunner of MBE. Günther obtained homogeneous, though polycrystalline, films of InAs and InSb on a variety of substrates by the evaporation of the elements from quartz crucibles. Indeed, it was with a modified three temperature technique that J E Davey and T Pankey (Naval Research Laboratory, USA) reported in 1968 the first homoepitaxial growth of GaAs by vacuum deposition. In contrast to the III-V compounds, the Pb and Sn chalcogenides exhibit predominantly congruent evaporation and this led to the vacuum sublimation of these compounds for the deposition of polycrystalline photoconductors as early as the 1940s.

Major differences between the early work and MBE are that in the latter, epitaxial single crystal films are grown on clean single crystal substrates. The importance of cleanliness for obtaining good epitaxial films only became evident when surface analytical instruments were incorporated into the growth chamber. The presence of contaminants inhibited epitaxy in the early work and films produced were

polycrystalline. It is possible to arrange that in MBE all the molecules taking part in the film growth arrive at the substrate in the molecular beam, and not from some background ambient.

Modern systems

Modern MBE systems pumped by ion, turbomolecular or diffusion pumps can reach an ultimate pressure of 10^{-11} – 10^{-10} Torr. Careful system design can ensure that pressures in the 10^{-10} Torr range are maintained during film growth. An impurity background pressure of 10^{-8} Torr corresponds to an arrival rate of about 1 monolayer/s and, even allowing for the possibility of low sticking coefficients for these impurities, it is clear that pure films will not be obtained. Residual active impurity concentrations of less than 10^{16} cm $^{-3}$, however, have been achieved in MBE systems.

Figure 1 shows the top view of a typical single chamber MBE system which would be used for research purposes. More sophisticated multichamber systems allow the growth chamber to be kept under vacuum while the substrate is loaded and then transferred into it via an interlock system. Such systems give fast turn round times and also allow the separation of the surface analytical instruments from the growth area so that the risk of contamination of either the film during growth or of these very sensitive instruments by the molecular beams is minimised. Systems differ greatly in automation and complexity: Nobel Laureate L Esaki (IBM Research Center, USA) has a fully automated, computer controlled system, whereas the authors have a simple but effective system (figure 2) which is manually controlled. The molecular beams are produced in small ovens or effusion cells made of high purity graphite or pyrolytic boron nitride. These cells are resistively heated using molybdenum or tantalum heater wires and temperatures are monitored by thermocouples in good thermal contact with the cells. The effusion of molecules from the cells can be examined on the basis of the kinetic theory by a method due to M Knudsen (1909). For almost true Knudsen sources (sources with an extremely thin aperture) good agreement has been found between the theoretically predicted and experimentally observed fluxes. In practice the sources used in most MBE systems are not true Knudsen sources and a comprehensive theoretical analysis of effusion rates is difficult. In general the effusion cells are calibrated and then some flux monitor, e.g. a quadrupole mass spectrometer, used to check the beam fluxes during growth. This same instrument would be used for residual gas analysis.

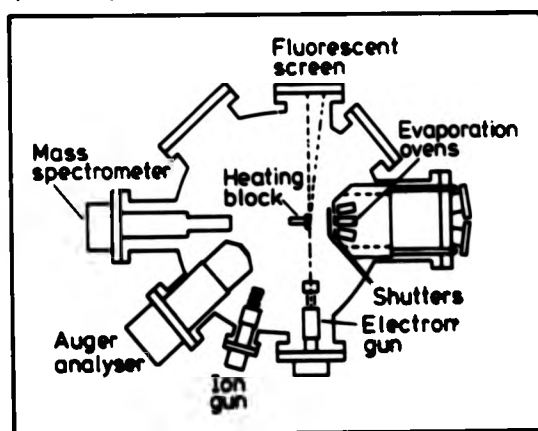
The growth of ternary and quaternary alloys (e.g. GaInAsP) and structures incorporating them is obtained by the insertion of the required number of effusion cells. Figure 3 shows a cluster of seven such cells. They are individually shuttered, providing abrupt termination of growth or incorporation of a given species. In this way alternating layers of various materials are possible, even on an atomic scale. These multilayered structures have been ex-

tensively studied by the group at the IBM Research Center. Electrical properties of alternating GaAs–GaAlAs structures with repeat spacings less than 10^{-8} m and layers as thin as 10^{-9} m have been examined for quantum electronic effects. No other growth technique can achieve such control in growing multilayered structures. The cells

Figure 1 Cross-section of a typical MBE system

Figure 2 MBE system at the authors' laboratory

Figure 3 Photograph of effusion cells for the production of molecular beams (courtesy of Vacuum Generators Ltd)



are enclosed by radiation shielding to prevent heat loss and the entire assembly is contained in a liquid nitrogen cooled shroud, to minimise any outgassing into the vacuum chamber which may lead to impurity incorporation in the growing film. System design is often dependent on the material to be grown. For example, early attempts to grow Al $_x$ Ga $_{1-x}$ As layers suitable for electro-optic devices proved difficult because of the reactive nature of the materials' surface. Background species containing oxygen in the growth chamber have much higher sticking coefficients on this material than on GaAs and their incorporation into structures resulted in poor device performance due to low photoluminescence and poor optical transmission. This led to the use of pyrolytic boron nitride, with its low outgassing rate, as the cell material. Large amounts of metallic gettering and liquid nitrogen trapping keep the concentration of oxygen containing species to a minimum.

Analytical equipment

Attached to the system shown in figure 1 are two of the various surface analytical techniques used in MBE growth. These are Auger electron spectroscopy (AES) and reflection high energy electron diffraction (RHEED). Surface compositions and contaminants are examined by AES. However, secondary ion mass spectrometry (SIMS) is likely to find increasing application in MBE due to its higher sensitivity, provision of chemical information and freedom from electron beam induced effects. RHEED is used primarily to ensure that flat single crystal growth is taking place, as is evident by the elongation and eventual streaking of the diffraction patterns seen on the phosphor screen. The technique is also used to study the many reconstructed surface structures seen on GaAs and related compounds. Reconstruction is a reordering of the outermost layer of atoms at the surface of a crystal, often leading to a surface layer in which the atoms are spaced farther apart than in the bulk. The effect, which is particularly pronounced in covalently bonded crystals such as the III–Vs where the bonds are highly directional, gives rise to extra diffraction lines in the RHEED patterns. These analytical facilities are useful in the early stages of setting up an MBE system and for establishing and optimising the growth conditions.

Substrate preparation is important in MBE, and AES and RHEED have played an important role in the development of substrate cleaning procedures. Submonolayers of carbon have been found to have a drastic effect on film nucleation and growth. Various cleaning methods have been devised which produce clean (contamination < 0.05 monolayer), near stoichiometric, single crystal surfaces. A common technique is chemical etching followed by heat treatment in UHV, which is sometimes supplemented by ion cleaning and annealing cycles. Surface analysis techniques would, however, not be required in routine production runs and much of the work in the authors' laboratory is carried out without recourse to any such facilities.

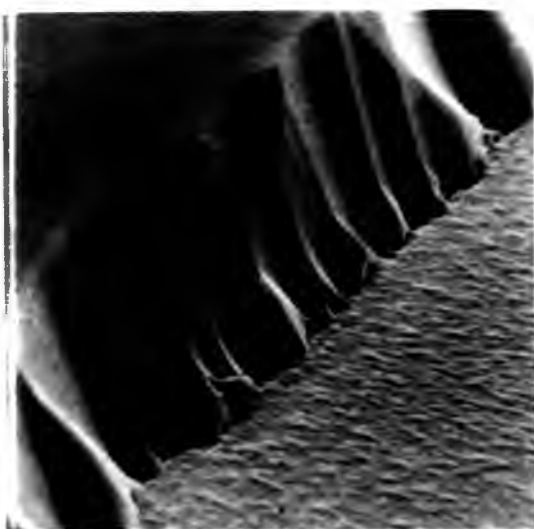


Figure 4 Scanning electron micrograph of edge of a 1.4 μm InAs film grown by MBE

A recurrent problem in MBE is that good epitaxial films of a given material require a suitable substrate. Choice of substrate is governed by the extent of any lattice mismatch between it and the deposited film, which may cause strain in the latter and hence crystal defects and a degradation of electrical properties. Providing this mismatch is not too large, the problem can be overcome by 'grading' the growth: the film composition is varied during deposition to avoid lattice mismatch during the initial stages. Any interdiffusion of atoms which may occur between the film and the substrate has to be considered. In fact the substrate should act merely as an orientation platform for growth and not interfere with any of the properties of the deposited film.

In most MBE work growth rates are 0.1–1 μm h⁻¹ and substrate temperatures depend on the material deposited. In general MBE offers lower growth temperatures than any other technique, a factor which may be important if diffusion effects are significant. Figure 4 shows a scanning electron micrograph of the edge of a 1.4 μm InAs film grown in the authors' laboratory. The growth temperature was 530 °C compared with 750 °C for other techniques. In recent work this temperature has been reduced to 300 °C by a careful control of growth parameters. MBE is interesting for device applications: as well as producing smooth thin layers, its slow growth rates allow a good control over growth profiles and layer thicknesses. Yet at the same time MBE can produce abrupt interfaces and hence abrupt doping profiles. There are a number of devices for which growth control is absolutely vital and it is in these areas that MBE has been successfully applied. Two broad classifications of this type of device are those intended for microwave operation (FETS, varactors, IMPATT and mixer diodes) and those designed for electro-optic functions (injection lasers, LEDs, optical waveguides and optical couplers). Whilst it would require a separate article to describe comprehensively the device applications of MBE, an insight into the technique's potential can be gained from examining two devices, the varactor and the injection laser.

The varactor or variable capacitor is

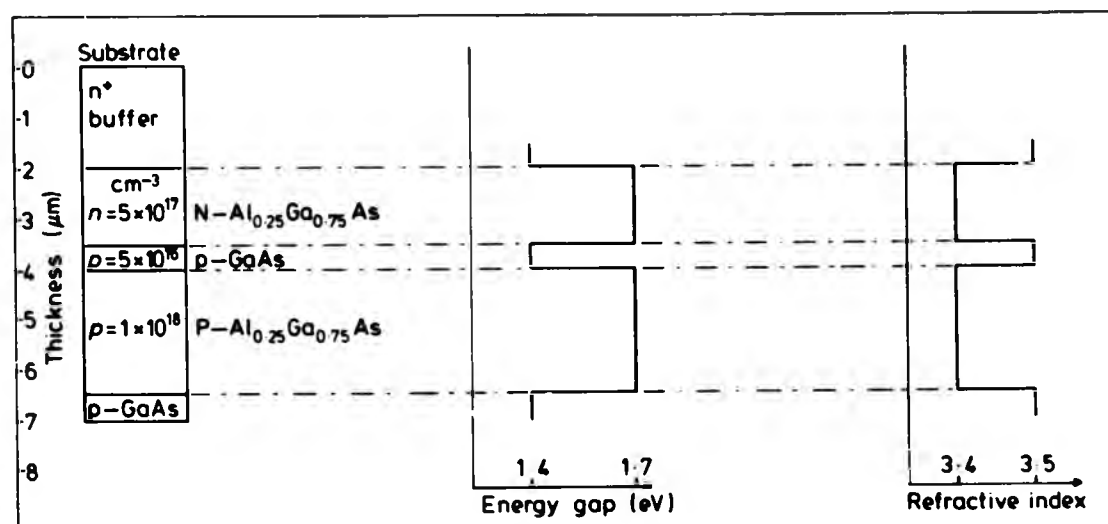


Figure 5 Schematic diagram of an injection laser showing the variation of energy gap and refractive index across the structure

usually a Schottky-barrier diode with a special doping profile, such that a large change in diode capacitance (due to widening of the depletion layer) can be effected by a small change in reverse bias. Schottky-barrier diodes differ from other diodes in that the junction is formed by a metal and a semiconductor material. In this application, it is the ability of MBE to constantly vary the carrier concentration with depth over a distance of 1 μm which makes it such a suitable technique. In work with tuned circuits it may be desirable to have the resonant frequency of the circuit proportional to the applied bias voltage. A detailed analysis of the problem shows that if the carrier concentration in the semiconductor is proportional to $d^{-3/2}$, where d is the distance from the junction, then the resonant frequency will be proportional to the applied bias voltage. The required doping profile is achieved by altering the temperature of (and hence the flux from) the effusion oven which is supplying the dopant.

The solid state injection laser is a more complex multilayered structure which requires the growth of flat, thin layers with abrupt changes in both chemical composition and doping levels. A simple example is shown in figure 5 along with the variation of energy gap and refractive index across the structure. Although excellent lasers are produced by other techniques the stringent requirements of such a device make it an obvious application for MBE. The operating structure is in effect a forward biased p-n junction, formed using doped Al_xGa_{1-x}As, with a thin layer of low carrier concentration GaAs sandwiched between the two layers. Electrons and holes are injected into the central GaAs, known as the active layer, where they provide a population inversion which leads to a lasing action upon electron-hole recombination. The wavelength of the laser light is characteristic of the energy gap of the active GaAs region and not the surrounding AlGaAs cladding. Also, because of the different refractive indices, the structure acts as a waveguide which promotes greater efficiency.

Conclusions

With the increasing complexity of electronic devices, existing growth technologies are

unable to provide materials with the required electronic specifications. This stems from their inability to accurately position material within the device structure. MBE is one of the newer techniques of device fabrication which is currently being assessed by the electronics industry, particularly in Japan and the USA. It allows a much closer control of the fluxes reaching the substrate and of the compositional and doping profiles in the final device structure. Furthermore the growth parameters are easy to monitor and regulate electrically, making this technique highly suitable for automatic production. MBE is compatible with the techniques of surface and bulk analysis which mostly rely on vacuum technology. These may be applied directly on the chamber to investigate production yield problems. MBE will possibly be used to fabricate fully integrated optical systems. Using moving masks, it has been shown recently that the technique has the exciting capability to produce 'written' structures with the molecular beams. Strips of ternary compounds as narrow as 10 μm have been written with longitudinal compositional variations. The potential market for electro-optical communication systems is vast and MBE seems set to play a pivotal role in this area. MBE also allows new materials with tailored band structures to be researched and complex multilayered devices to be fabricated and tested. The indications are, therefore, that MBE will be intimately involved in the development and realisation of future generations of electronic devices ■

Acknowledgments

The help of past and present members of the Semiconductor and Surface Research Group is gratefully acknowledged.

Thanks are especially due to Mr W Hugkulstone for help in preparation of the figures.

Further reading

Cho A Y and Arthur J R 1975 *Progress in Solid State Chemistry* G A Somorjai and J O McCaldin (eds) (Pergamon) 10, 157

J D Grange and E H C Parker, D Phil, M Inst P are in the Physics Department at the Sir John Cass School of Science and Technology, City of London Polytechnic

Attention is drawn to the fact that the copyright of this thesis rests with its author.

This copy of the thesis has been supplied on condition that anyone who consults it is understood to recognise that its copyright rests with its author and that no quotation from the thesis and no information derived from it may be published without the author's prior written consent.

I

D 37709'81

END